

GENETIC AND BIOCHEMICAL ANALYSIS OF THE ENDORIBONUCLEASE E/G FAMILY IN
RNA METABOLISM IN *ESCHERICHIA COLI* K-12

by

DAE HWAN CHUNG

(Under the Direction of Sidney R. Kushner)

ABSTRACT

Degradation of mRNA and maturation of stable RNAs provide important mechanisms for controlling gene expression at post-transcriptional level. In *Escherichia coli*, the RNase E/G endoribonuclease family plays a central role in the initiation of both processes. This dissertation research was an attempt to broaden our understanding of physiological roles and functional relationships of RNase E and RNase G by using a combination of genetic and biochemical analysis.

The *rng-219* and *rng-248* alleles, comprising single amino acid substitutions within the predicted RNase H domain of RNase G, are able to support cell viability in the total absence of RNase E when present at physiologically relevant protein levels. These observations suggest that the difference in biological activities between the two enzymes is governed by their RNase H domains to some extent.

The *in vivo* characterization of *rneΔ1018/rng-219* and *rneΔ1018/rng-248* double mutants allowed critical examination of the distinct physiological roles of RNase E and RNase G in *E. coli* RNA metabolism. The degradation of certain mRNAs and the processing of some tRNA precursors are absolutely dependent on RNase E activity. In contrast, 9S rRNA processing is effectively restored by the altered RNase G proteins in the absence of RNase E.

We also examined the biochemical properties of purified RNase E, RNase G and Rng-219 proteins. The purified RNase G and Rng-219 proteins cleave structured RNA substrates, such as 9S rRNA and tRNAs, at identical sites as RNase E. Although, both RNase E/G prefer RNA substrates with 5'-monophosphate termini, the presence of a 5'-triphosphate affects the efficiency of RNase E much more than RNase G. A surprising result is the greater catalytic activity of RNase G and Rng-219 proteins in the presence of Mn^{2+} than Mg^{2+} .

INDEX WORDS: RNase E, RNase G, mRNA degradation, 9S rRNA processing, tRNA precursor, *Escherichia coli*

GENETIC AND BIOCHEMICAL ANALYSIS OF THE ENDORIBONUCLEASE E/G FAMILY IN
RNA METABOLISM IN *ESCHERICHIA COLI* K-12

by

DAE HWAN CHUNG

B. S., Ajou University, SOUTH KOREA, 1997

M. S., University of Philippines, Philippines, 1999

A Dissertation Submitted to the Graduate Faculty of The University of Georgia in Partial
Fulfillment of the Requirements for the Degree

DOCTOR OF PHILOSOPHY

ATHENS, GEORGIA

2008

© 2008

DAE HWAN CHUNG

All Rights Reserved

GENETIC AND BIOCHEMICAL ANALYSIS OF THE ENDORIBONUCLEASE E/G FAMILY IN
RNA METABOLISM IN *ESCHERICHIA COLI* K-12

by

DAE HWAN CHUNG

Major Professor: Sidney R. Kushner

Committee: Anna Glasgow Karls
Michael McEachern
Michael Terns
Richard Meagher

Electronic Version Approved:

Maureen Grasso
Dean of the Graduate School
The University of Georgia
August 2008

DEDICATION

To my parents, sisters, wife, and my son.

ACKNOWLEDGEMENTS

I would like to express my heartfelt gratitude to my major advisor Dr. Sidney R. Kushner, for providing insightful advice with constant encouragement, strong support, and great patience. I want to thank the other members of my advisory committee, Dr. Anna Glasgow-Karls, Dr. Michael McEachern, Dr. Michael Terns, and Dr. Richard Meagher, for their help in directing my research and providing constructive criticism. I also wish to thank all the past and present members of the Kushner lab for all their help. A special thank to Dr. Bijoy Mohanty and Dr. Tariq Perwez, for their answering millions questions, fruitful guiding, and enthusiastic encouragement.

I appreciate many kind and friendly fellow graduate students, visitors, postdoctoral researchers, staffs and faculty members in the department of Genetics. I would like to thank my wife, YOON KYUNG OH, for taking care of me, and my lovely son, ALEXANDER CHUNG, for being great joy and inspiration for us. Finally, in a very inadequate manner, I wish to thank my dear father, mother, and sisters. Their love, support and understanding are the primary power leading my every success.

TABLE OF CONTENTS

	Page
ACKNOWLEDGEMENTS	v
CHAPTER	
1 Introduction and Literature Review	1
2 Single amino acid changes in the predicted RNase H domain of <i>E. coli</i> RNase G lead to the complementation of RNase E deletion mutants	54
3 Biochemical analysis of RNase G reveals significant overlap in substrate specificity and cleavage site selection with its essential homologue, RNase E	108
4 Conclusion.....	172
APPENDICES	
A Single amino acid changes in the predicted RNase H domain of <i>E. coli</i> RNase G lead to complementation of RNase E mutants	181

CHAPTER I

Introduction and Literature Review

INTRODUCTION

Ribonucleases involved in mRNA degradation and RNA maturation (or processing) play important roles in many aspects of RNA metabolism. For example, messenger RNA (mRNA) degradation is a fundamental aspect of the control of gene expression in *Escherichia coli* by helping regulate the steady-state level of transcripts. The inherent instability of mRNAs (1,2) and the wide variation of their half-lives from a few seconds to more than 30 minutes (3-5) is thought to play an important role in cellular adaptation to a variety of growth conditions and environmental changes (6-9). mRNA instability is principally caused by the activity of several endo- and exoribonucleases involved in their degradation, although certain important structural features of mRNA molecules can also affect their stability (10-14).

In contrast, stable RNAs, primarily ribosomal RNAs (rRNAs) and transfer RNAs (tRNAs), are typically synthesized as parts of functionally inactive large precursor molecules that must be subsequently processed to their mature forms. Maturation of rRNAs and tRNAs in bacteria is initiated by separating individual RNA units from larger precursor RNAs by endonucleolytic cleavages. These larger precursor RNA molecules include individual rRNAs and tRNAs within the seven ribosomal RNA operons, tRNAs associated with mRNAs in multifunctional transcripts, tRNAs existing as a monocistronic transcripts, or tRNAs present in polycistronic precursors (15,16). Endonucleolytic cleavage events release smaller precursors that are matured into 16S, 23S, and 5S rRNAs, and tRNAs. The final processing steps are carried out by a combination of additional endonucleolytic and 3'→5' exonucleolytic cleavage reactions (16-19).

In *E. coli*, mRNA degradation, tRNA and rRNA maturation start with endonucleolytic cleavages followed by exonucleolytic processing of the fragments. There is significant overlap among the endoribonucleases involved in the decay of mRNAs and the processing of structural RNAs (rRNAs and tRNAs). Many of the endoribonucleases (RNase E, RNase G, RNase III, RNase P, and perhaps others) involved in mRNA degradation also participate in the maturation

of stable RNAs (15,16,20-22). In contrast, the exoribonucleases involved in mRNA degradation are different from those in RNA maturation. In mRNA degradation, RNase II, PNPase (polynucleotide phosphorylase), RNase R, and oligoribonuclease are used to degrade the decay intermediates (23-28). Interestingly, the exoribonucleolytic trimming of 3' ends in the maturation of the stable RNAs is accomplished by a combination of RNase PH, RNase D, RNase BN, RNase T and RNase II (18,29-32).

This review summarizes the salient features of the *E. coli* ribonucleases involved in mRNA degradation and stable RNA maturation, and in particular, the RNase E/G endoribonuclease family which are involved in numerous post-transcriptional mechanisms in bacteria.

RIBONUCLEASES

Close to twenty RNases have already been identified in *Escherichia coli* (16). The ribonucleases involved in RNA metabolism in *E. coli* fall into two major classes according to their mode of action. Endoribonucleases cleave RNAs internally by cleaving either side of the phosphodiester linkage depending on the reaction mechanism, while exoribonucleases digest RNAs from the ends.

Exoribonucleases involved in *E. coli* RNA metabolism

Exoribonucleases digest RNA molecules one nucleotide at a time from either 3' or 5' terminus. Currently, eight 3' to 5' exoribonucleases have been characterized in *E. coli* (Table 1.1) (15,19). No evidence of a 5' to 3' exoribonuclease activity has yet been found in *E. coli*. Six of the exoribonucleases release nucleoside 5' monophosphates by hydrolytic cleavages (RNase II, RNase BN, RNase D, RNase R, RNase T, and oligoribonuclease). The remaining

two, generate nucleoside diphosphates by employing a phosphorolytic mechanism (polynucleotide phosphorylase, and RNase PH).

A. RIBONUCLEASE II (RNase II)

RNase II is encoded by the *rnb* gene, which is located at 29 minutes on the *E. coli* genetic map (33,34). The gene contains two functional promoters and is transcribed as a monocistronic mRNA (35). The protein contains 644 amino acids with a calculated molecular mass of 72.5 kDa and is not associated with other macromolecular components (36,37).

Recent studies have shown that the post-translational levels of RNase II are partly regulated by a protein called Gmr (Gene modulating RNase II) (38).

RNase II is a Mg^{2+} and K^+ dependent hydrolytic 3'→5' exoribonuclease, specific for single-stranded RNA, releasing ribonucleoside 5' monophosphates (37,39). It exhibits high processivity, but is sensitive to RNA secondary structure. *In vitro* studies employing a synthetic RNA substrate suggest that the catalytic activity of RNase II is significantly impeded as it approaches within ~10 unpaired residues of a double-stranded region (37,40). Although RNase II can degrade relatively short single-stranded RNAs, its activity is limited to substrates longer than 3-5 nucleotides (41,42).

RNase II is responsible for 90% of the exonucleolytic activity in crude extracts of *E. coli* (43). The primary physiological role of RNase II appears to be the degradation of mRNA, and it is essential for cell viability in the absence of PNPase (polynucleotide phosphorylase) (23). However, RNase II can paradoxically act to protect some mRNAs and antisense RNAs from further degradation by blocking the access of other 3'→5' exonucleases where it rapidly degrades poly (A) tails and remains bound to the substrate (44-48). In the absence of other exoribonucleases, RNase II also functions in the maturation of tRNAs and other small, stable RNAs (18,19).

B. POLYNUCLEOTIDE PHOSPHORYLASE (PNPase)

Polynucleotide phosphorylase (PNPase) is a homotrimer of a 711 amino acid polypeptide encoded by the *pnp* gene. It maps at 71.3 min on the *E. coli* chromosome and lies downstream of the *rpsO* gene as a part of a dicistronic operon (49,50). PNPase catalyzes three reactions *in vitro*: the processive 3' to 5' phosphorolytic degradation of single-stranded RNA releasing nucleoside diphosphates; the synthesis of RNA using nucleoside diphosphates as substrates; and, an exchange reaction between free phosphate and the β -phosphate of ribonucleoside diphosphates (51-53). *In vivo*, PNPase is the 3'→5' exoribonuclease involved in processive phosphorolytic degradation of poly(A) tails, mRNAs and certain defective tRNAs (23,48,54,55). PNPase also functions as a second poly(A) polymerase activity in *E. coli* by adding heteropolymeric 3' tails (56).

In *E. coli*, PNPase is found mostly in the cytoplasm (57) with a major fraction being a constituent of the degradosome, a multiprotein complex formed by RNase E (which provides the scaffold to the entire structure), enolase, RhlB (an RNA helicase) and PNPase (58-60). While PNPase is inhibited by secondary structures (40), the presence of an RNA helicase in the degradosome (61,62), as well as the activity of poly(A) polymerase (46), enables PNPase to eventually proceed to degrade mRNAs containing secondary structures such as Rho independent transcription terminators.

During *E. coli* cell growth at low temperatures, PNPase plays an important role in cold shock adaptation. The level of PNPase is increased by about seven-fold after cold shock (63) and the enzyme is required to repress the production of cold shock proteins at the end of the acclimation phase by selective degradation of CSP (cold shock protein) mRNAs at 15°C (64). However, PNPase does not seem to be essential to *E. coli* viability under normal growth conditions, unless either RNase II or RNase R, the other main exoribonucleases in the cell, are also defective (23,42,65,66). Strains carrying a mutations in both the *pnp* and the *rph* gene

(encoding the exoribonuclease RNase PH) show extreme cold sensitivity at 31°C and are unable to assemble 50S ribosomes at this temperature (67). These results imply that PNPase contains a high degree of functional overlap in specific processes with other *E. coli* exoribonucleases.

C. OLIOGORIBONUCLEASE (ORNase)

Escherichia coli oligoribonuclease (ORNase) was initially identified as an RNase specific for short oligoribonucleotides (24,68). ORNase is encoded by *orn* gene, which maps at 94 minutes on the *E. coli* chromosome. It is the smallest among the eight known *E. coli* exoribonucleases with a reported molecular weight of 20.7 kDa (34,69). Its ability to digest RNA oligonucleotides 5 nt and shorter is required to complete the RNA degradation process (24), since these small molecules are not substrates for PNPase, RNase II and RNase R (42,53). In a conditional *orn* mutant, small fragments (2-5 nt in length) derived from mRNAs accumulate to high levels. Oligoribonuclease is the only exoribonuclease that is by itself essential for cell viability (24).

D. RIBONUCLEASE T (RNase T)

Escherichia coli RNase T, encoded by the *rnt* gene, maps at 37.2 min on the *E. coli* chromosome and encodes a 23.5 kDa polypeptide that is active as an α_2 dimer form both *in vivo* and *in vitro* (70,71). This enzyme appears to be the unique exoribonuclease in *E. coli* that is capable of efficiently removing residues close to a duplex structure without unwinding the double helix. Thus, RNase T plays an important role for the 3' end maturation of many stable RNAs (29). Its exoribonuclease activity is essential for generating the mature 3' ends of 5S

and 23S rRNAs (72,73) and tRNA 3' end processing (18). Interestingly, RNase T also displays strong DNA exonuclease activity (74,75).

E. RIBONUCLEASE (RNase D)

Escherichia coli RNase D with a molecular mass of 42.7 kDa is encoded by the *rnd* gene, maps at 40.6 minutes on the *E. coli* chromosome (76,77). The enzyme is a 3'→5' hydrolytic exoribonuclease that displays a high degree of specificity for certain tRNA-related molecules. *In vitro*, RNase D is active on denatured tRNA molecules and on tRNAs containing additional residues following the mature 3' terminus (76,78). Subsequent *in vivo* studies have shown that RNase D participates in the 3' end maturation of tRNAs (19), but strains lacking RNase D do not exhibit any noticeable growth defects (79). RNase D does become essential for cell viability when other exoribonucleases, such as RNase II, BN, T, and PH, are eliminated. This property of RNase D suggests that it can function as a backup enzyme when the primary nucleases employed for tRNA maturation are missing (18,29,30).

F. RIBONUCLEASE R (RNase R)

RNase R, encoded by *rnr*, was originally discovered as a residual hydrolytic exoribonuclease activity in strains lacking RNase II (39,80). While RNase II accounts for more than 90% of the poly(A) RNA degrading activity in crude cell extracts, RNase R contributes only residual activity against this substrate. RNase R shares structural properties, including ~60% of sequence similarity with RNase II (65,81). *In vitro* studies by Deutscher's group strongly suggest that RNase R is the only known *E. coli* exoribonuclease that is able to degrade RNA with secondary structures without the aid of a helicase activity (42).

RNase R mutants have no growth phenotype in rich medium. However, a double mutant strain missing of both RNase R and PNPase activity is inviable (65). Fragments of 16S and 23S rRNA accumulate at high levels in a temperature-sensitive double mutant (66). RNase R also plays a role in the degradation of defective stable RNAs (55) and structured regions of mRNAs, such as REP (repeated extragenic palindrome) elements (28).

G. RIBONUCLEASE PH (RNase PH)

RNase PH, encoded by *rph*, is the member of the PDX exoribonuclease family, which catalyzes a Pi-dependent degradation of RNA leading to the release of nucleoside diphosphates rather than monophosphates (82,83). This enzyme is involved in 3' end maturation of tRNAs and other small, stable RNAs in *E. coli*. (19,84,85). Like PNPase, the other phosphorolytic exoribonuclease in *E. coli*, RNase PH is also able to carry out a synthetic reaction in which nucleoside diphosphates are substrates for the addition of nucleotides onto the 3' termini of a variety of RNAs (86). *rph* single mutants grow normally and exhibit no defect in tRNA maturation. However, RNase T⁻ RNase PH⁻ double-mutant strains exhibit a significant growth defect and high accumulation of tRNA precursors (18,87). Furthermore, the RNase PH⁻ PNPase⁻ double mutant is cold-sensitive and shows a defect in 50S ribosomal subunit assembly (67).

H. RIBONUCLEASE BN (RNase BN)

RNase BN has been renamed as RNase Z, which is an endoribonuclease. It will be discussed in more detail in the section on RNase Z.

Endoribonucleases involved in mRNA degradation and stable RNA maturation other than RNase E/G endoribonuclease family

Endoribonucleases are hydrolytic enzymes which cleave internal phosphodiester linkages within ribonucleic acids. The biochemical behaviors and functional roles of five well-characterized endoribonucleases in *E. coli* are presented below. These are RNases I, III, P, LS, and Z (Table 1.2).

A. RIBONUCLEASE III (RNase III)

RNase III was discovered in 1967 as the third RNase activity of *E. coli* (88). It is the only known double-stranded RNA (dsRNA) specific endoribonuclease in *E. coli* (89,90). *E. coli* RNase III, encoded by the *rnc* gene, is active as a homodimer of two identical polypeptides of 226 amino acids with a calculated molecular mass of 25.6 kDa (91,92). The bacterial RNase III proteins, including *E. coli* RNase III and *Aquifex aeolicus* RNase III, are composed of an N-terminal endonuclease domain (endoND) and a C-terminal dsRNA-binding domain (dsRBD) (93-95). This enzyme can alter gene expression either by cleaving dsRNA or by binding to RNAs without subsequent cleavage (96). As a processing enzyme, RNase III cleaves regions of 11 or more base pairs of RNA–RNA duplex structure, creating 5'- phosphate and 3' hydroxyl termini with an overhang of 2 nucleotides length (15,93,97). It also acts as a regulatory protein that binds and stabilizes certain substrates, thus suppressing the expression of some genes (98,99).

The primary functional role of RNase III is the maturation of the ribosomal RNAs. The enzyme cleaves in the double-stranded regions bracketing the 16S and 23S rRNAs in the primary 30S transcript of the rRNA operons, providing shorter intermediates for further processing (17,100). The inactivation of RNase III activity in *E. coli* leads to accumulation of the

incompletely processed 23S and some 30S rRNA species but only exhibits a mild effect on cell growth (101,102). RNase III is also involved in the maturation or degradation of some tRNAs and mRNAs (15,90,93). Although the half-lives of total pulse-labeled RNA were not significantly affected in an RNase III mutant, degradation of some mRNAs is initiated by RNase III cleavages (103,104). The direct involvement of RNase III in mRNA degradation was observed for several mRNAs, including *rnc* (105), *pnp* (106), *dicB* (107), and *metY* (108).

B. RIBONUCLEASE I/I* (RNase I/RNase I*)

RNase I is a nonspecific endoribonuclease that mainly resides in the periplasmic space of *E. coli* (109,110). Unlike other *E. coli* ribonucleases, it does not require a divalent cation for cleavage activity and generates cleavage products with 3'-phosphates (111). The physiological role of RNase I remains unclear. RNase I deficient strains show no obvious phenotype and no major metabolic defect (110,112). However, a number of studies have suggested that RNase I may be involved in stable RNA degradation under certain stress conditions (113-115). Furthermore, the identification and characterization of RNase I*, an isoform of RNase I found in the bacterial inner membrane, has suggested that RNase I might play some role in the terminal step in mRNA degradation (116).

C. RIBONUCLEASE P (RNase P)

RNase P is an essential endoribonuclease, which was initially discovered in attempts to elucidate the biosynthesis of tRNA precursors in *E. coli* (117). It is a ribonucleoprotein complex and has been found in all three domains of life (Archaea, Bacteria and Eukarya) as well as in mitochondria and chloroplasts (118,119). *E. coli* RNase P consists of a catalytic RNA subunit (MI RNA) 377 nt in length and a small basic protein subunit (C5 protein) 13.8 kDa in mass

(120,121). The activity of RNase P generates cleavage products with 5'-phosphate and 3'-OH termini in a reaction that requires Mg^{2+} , but other cations can also be utilized (122). *In vitro*, the MI RNA can slowly cleave tRNA precursors in the absence of C5 protein. However, the addition of C5 protein significantly increases the efficiency of cleavage under physiological conditions and the C5 protein subunit is required for RNase P activity and cell viability *in vivo* (123,124).

RNase P catalyses the hydrolytic removal of the 5' leader sequences from tRNA precursors to produce the mature 5' terminus. This cleavage reaction is essential to generate functional tRNA molecules (118,125). It is also involved in maturation of the 5' end of p4.5S RNA, several small RNAs, and in the processing of a limited number of polycistronic mRNAs (126,127) and tRNAs (128,129). A global survey of RNase P function identified cleavage sites within the intercistronic regions of the *tna*, *secG*, *rbs*, and *his* operons, indicating that RNase P plays a very limited role in mRNA turnover (127).

D. RIBONUCLEASE LS (RNase LS)

RNase LS (Late-gene Silencing in bacteriophage T4) is encoded by *rnIA* (formerly named *yfiN*), which maps at 59.6 min on the *E. coli* chromosome (130,131). It preferentially cleaves RNA 3' to pyrimidines with broad sequence specificity (132,133). The primary physical role of *E. coli* RNase LS seems to be as an antagonist of bacteriophage T4 (134). RNase LS also plays some role in *E. coli* mRNA decay. The examination of the chemical decay of individual transcripts in RNase LS mutant allele revealed that the decay rate of *rpsO* and *bla* was decreased compare to wild type (131). In addition, the involvement of RNase LS in the degradation of stable RNA, a 307 nucleotide fragment possessing an internal sequence of 23S rRNA, has been suggested (131).

E. RIBONUCLEASE Z (RNase Z)

RNase Z is required for the maturation of the 3'-end of tRNA precursors lacking a chromosomally encoded CCA determinant in eukaryotic cells and *Bacillus subtilis* (135,136). Genes encoding RNase Z homologues have been found in eukaryotes, archaea, and about half of the sequenced eubacterial genomes (137,138). *E. coli* RNase Z is encoded by *rnz/elaC*, mapping at 51.3 min on the *E. coli* chromosome (139,140). However, no obvious function was initially ascribed to *E. coli* RNase Z, since all of the 86 tRNAs in *E. coli* contain chromosomally encoded a CCA triplet and are not substrates for RNase Z (137,141). However, recent study has clearly demonstrated that this enzyme is involved in mRNA decay as an endonuclease and has no appreciable activity on *E. coli* tRNA precursors under physiological conditions (140).

Ezraty *et al.* (2005) have claimed that the *E. coli elaC* gene encodes RNase BN, a previously characterized 3' to 5' exonuclease involved in 3' end maturation of tRNAs (87,142). They observed only limited exonucleolytic cleavage activity under conditions of high Co^{2+} (0.2 mM) and microgram levels of protein (141). In contrast, RNase Z-specific endonucleolytic cleavages were observed at nanogram amounts of protein. Additionally, optimal RNase BN reaction conditions completely abolished the endonucleolytic activity of RNase Z on the *trnD-Leu2* transcript (140). These results suggest that the functional role of *E. coli* RNase Z under physiological conditions is in mRNA degradation as an endoribonuclease.

The RNase E/G endoribonuclease family

The RNase E/G endoribonuclease family plays central role in both RNA degradation and processing in *E. coli* (26,143-145). Proteins in this endoribonuclease family contain an evolutionarily conserved amino terminal domain which contains an S1 RNA binding domain, which is a highly distributed and ancient single-stranded RNA-binding motif (146-148). Genes

encoding RNase E/G-like proteins have been found in many bacteria, cyanobacteria, red and green algae, plastid genomes and the nuclear genomes of several higher plants (149-151).

A. RIBONUCLEASE E (RNase E)

RNase E (*rne*) is an essential endoribonuclease in *E. coli* that was initially discovered as an rRNA processing enzyme required for converting 9S rRNA precursors into 126-residue pre-5S rRNA (152,153). This multifunctional enzyme was independently identified as *ams-1* (altered mRNA stability), a thermo-labile mutation that led to increased chemical half-life of total RNA at elevated temperatures (154,155). The subsequent cloning and sequencing of the *ams* gene as well as *ams-1* and *rne-3071* mutants revealed that *ams* and *rne* encode the same protein (156-159). The *ams-1* allele has been renamed *rne-1* to more accurately reflect its biochemical function. *E. coli* RNase E is a 1061 amino acid protein with a calculated molecular weight of 118 kDa, but which migrates on SDS-PAGE gels with an apparent size of 180 kDa (Fig. 1.1) (58,160,161).

Various studies have demonstrated that RNase E plays a significant role in many aspects of RNA metabolism in *E. coli*. It has been shown to be involved in the maturation of tRNAs (162-164), the processing of 16S rRNA precursors (165,166), the maturation of the M1 subunit of RNase P (164,167), the regulation of DNA synthesis by ColE1-type plasmids (168), the tmRNA mediated control of mRNA quality (169), the decay of small noncoding regulatory RNAs (170,171), and in the degradation of many, if not most mRNAs (155,172-175). In addition, RNase E activity is essential to maintain a proper cellular ratio of the FtsZ and FtsA proteins, which are involved in cell division process in *E. coli* (176,177).

RNase E has been shown to be composed of at least three functionally and structurally distinct domains (Fig. 1.1). The N-terminal half of the protein contains the highly conserved catalytic domain, which is associated with endonucleolytic activity and appears to be sufficient

for cell viability (164,174,178,179). The X-ray crystallographic structure of RNase E revealed that the N-terminal 529-amino acid segment forms a catalytically active homotetramer held together by a pair of Zn ions (180,181). The catalytic core of each RNase E protomer contains five subdomains; an RNase H domain, a S1 RNA binding domain, a 5' sensor region, a DNase 1 domain, and a Zn²⁺ link (180). Mutations in the S1 RNA binding domain such as *rne-1* (at residue 66) and *rne-3071* (at residue 68) alleles result in thermolabile RNase E activity (Fig. 1.1) (146). A truncated RNase E protein, which consists of only the first 395 amino acids and lacks the Zn²⁺ link region, is sufficient to maintain the cell viability (179). This result indicates that tetrameric quaternary structure is not essential for the core enzymatic function of RNase E.

A central region of the RNase E protein contains an arginine-rich RNA-binding site (ARRBS), which is located between amino acid residues 597 and 684 (Fig. 1.1) (182). This segment of the protein contains proline-rich regions that have been shown to be responsible for the slower-than-expected migration when analyzed by SDS/PAGE (178). Although this region has a strong RNA binding activity *in vitro*, it does not show any noticeable effect on endonucleolytic cleavage activity of RNase E *in vivo* (178,182). The deletion of the ARRBS from the RNase E protein yields strains that exhibit almost identical growth properties and only a slight defect on mRNA decay compared with the full length protein (164,174).

The rest of the C-terminal region is an exceptionally long stretch of unstructured protein, highly divergent across bacterial species that serves as a scaffold for the formation of a multi-component complex called the degradosome (Fig. 1.1) (60,147,183-185). Extensive biochemical and immunological experiments have revealed that RNase E based degradosome contains the 3'→5' phosphorolytic exoribonuclease polynucleotide phosphorylase (PNPase), a DEAD-box ATP-dependent RNA helicase (RhIB), and the glycolytic pathway enzyme enolase (Fig. 1.1) (58-60,186-188). RNase E is also co-purified and co-precipitated with other associated proteins, present in substoichiometric amounts relative to major components, including

polyphosphate kinase (PPK), which catalyzes the reversible polymerization of polyphosphate from ADP, and the chaperon proteins DnaK and GroEL (187,189,190). RNase E is also able to form variable ribonucleoprotein complexes with Hfq/small RNAs in the absence of PNPase, RhlB, and enolase, through its C-terminal scaffold region. This RNase E-Hfq complex, distinct from the RNA degradosome, appears to be necessary for the degradation of mRNAs targeted by small RNAs (191).

The physical association of an endoribonuclease (RNase E), an exoribonuclease (PNPase), and an RNA helicase (RhlB) in a single multiprotein complex makes the degradosome ideally suited for breakdown of specific transcripts (175). In degradosome-dependent mRNA decay, RhlB is required to unwind structured RNA molecules so that they become suitable substrates for the associated ribonucleases (RNase E and PNPase) (59). In addition, endonucleolytic cleavage activity of RNase E can remove 3' stem-loops and release RNA fragments containing single-stranded 3' ends, providing substrates for PNPase (188). The role of enolase, an enzyme that catalyses the reversible dehydration of 2-phosphoglycerate to phosphoenolpyruvate, in the degradosome is still unclear (183). Recently, enolase was proposed to play a regulatory role in the degradation of *ptsG* mRNA in response to phosphosugar stress (192).

In *E. coli*, the degradosome assembly is not essential for cell growth, rRNA processing, and normal mRNA decay (174,193,194). However, it is required to sense intracellular poly (A) level (195). In addition, the degradosome has been shown to be important for degradation of mRNA fragments containing REP (repeated extragenic palindrome) elements and untranslated mRNAs (196,197).

A recent study, based on *in vivo* fluorescence tagging of proteins, shows that the major components of the RNA degradosome are co-localized as helical filamentous structures that coil around the length of the cell (198). The authors indicated that the RNA degradosome exists

as a cytoskeletal structure in *E. coli*, thereby compartmentalizing RNA degradative and processing activities within the cell (198,199).

Variants of the RNA degradosome complex have been found in other bacteria such as *Streptomyces coelicolor* and *Rhodobacter capsulatus*, although PNPase was not identified in the complex found in *R. capsulatus* (149,200). The widespread existence of degradosome-like multiprotein complexes among phylogenetically distant organisms indicates that the physical and functional associations of ribonucleases, helicases, and cofactors ensure a tight control of mRNA processing and decay that cannot be efficiently achieved by free enzymes (145,201).

RNase E cleaves a single-stranded RNA with a preference for A/U-rich sequences, and generates products with a free 3'-hydroxyl group and a 5'-monophosphate (202-204). It requires either Mn^{2+} or Mg^{2+} and a monovalent cation such as Na^+ , K^+ , or NH_4^+ for catalytic activity (153). In addition, RNase E seems to be a 5' end-dependent endoribonuclease (205,206), although under certain circumstances, the enzyme can cleave at internal sites without any interaction with the 5'-terminus (207). Subsequently, biochemical characterization of RNase E has revealed that it preferentially cleaves substrates with a 5'-monophosphate over those with a 5'-OH or triphosphate group (205,208,209) and degrades the substrates processively or quasi-processively in the 3' to 5' scanning mode (210).

The crystal structure of the homotetrameric catalytic domain of RNase E in complex with 5'-monophosphate RNA substrate provides a molecular explanation for the basis of 5'-end selectivity and a plausible catalytic mechanism for this enzyme (180). A number of specific interactions were observed between the 5'-terminal phosphate and residues of a 5'-sensor pocket, which appears too small to entirely accommodate 5' ends that are tri-phosphorylated or double-stranded RNA (180,211). A 'mouse-trap'-like mechanism of RNase E has been proposed whereby binding of the 5'-monophosphate by the 5'-sensor pocket induces the

neighboring S1 domain to clamp down on the RNA downstream, increasing the catalytic power of the enzyme (180,209).

RNase E autoregulates its own synthesis by controlling the degradation rate of its mRNA (*rne*), such that its half-life varies inversely with cellular RNase E activity (212,213). Feedback inhibition of *rne* gene expression is, in part, mediated in *cis* by a 351 nucleotide 5' untranslated region (UTR), which contains an evolutionarily well-conserved RNA stem-loop structures (214,215). The C-terminal region of RNase E has also been implicated in the autoregulation of the protein level (174,215). In addition, the synthesis of RNase E is also affected by the cellular poly(A) levels and composition of growth medium (9,195). Furthermore, two recently discovered protein inhibitors of RNase E, RraA and RraB (Regulators of ribonuclease activity A and B), inhibit RNase E endonucleolytic activity and appear to interact with the non-catalytic region of RNase E (216,217). Thus, the cellular level and activity of RNase E in *E. coli* is tightly controlled at many different levels.

B. RIBONUCLEASE G (RNase G)

Escherichia coli RNase G was originally identified as the product of the *cafA* gene (cytoplasmic axial filament), overproduction of which causes significant morphological changes, including the formation of anucleated chained cells containing long axial filaments and mini cells. These findings suggested that CafA might have a role in chromosome segregation and cell division (218). Interestingly, the elongated cell phenotype associated with the over-expression of CafA protein was also observed when RNase E was inactivated by temperature elevation in strains carrying an *rne* temperature-sensitive mutation (i.e. *rne-3071* and *rne-1*) (154,219,220). Subsequently, CafA has been demonstrated to have endoribonucleolytic activity both *in vivo* (165,166,211,221) and *in vitro* (215,222). Accordingly, it has been renamed RNase G (*cafA* to *rng*) to more accurately reflect its biochemical properties.

RNase G has been shown to be an endoribonuclease involved in maturation of the 5' terminus of 16S rRNA in *E. coli* (165,166). A strain carrying the *rng::cat* mutation accumulates a precursor form of 16S rRNA, called 16.3S rRNA, which contains 66 extra 5' nucleotides and a mature 3'-terminus (165,166). In addition, it is also involved in the degradation of the *adhE* and *eno* mRNAs (223,224). Microarray analysis of the *E. coli* transcriptome revealed that the steady-state level of only 18 mRNAs was significantly affected (at least 1.5 fold increase) by the inactivation of RNase G (225). These results suggest that RNase G has a very limited role in mRNA degradation in *E. coli*. Two independent research groups isolated and characterized novel RNase G mutants that were defective in degradation of *adhE* and *eno* mRNA transcripts, while the maturation of 16.3S rRNA appears to be normal in cells containing these mutants (211,223). These findings suggest that substrate recognition or catalysis of RNase G is quite different on rRNA and mRNA molecules.

A series of *in vitro* and *in vivo* studies of RNase G have demonstrated that its rate of cleavage of RNA is dependent on the nature of 5'-end of the substrates (211,215,222). It cleaves RNA molecules at single-stranded sites within A/U rich regions, and has a preference for 5'-monophosphorylated substrates rather than 5'-triphosphorylated or 5'-hydroxylated ones (215,222). In contrast, the 3'-phosphorylation status did not affect the cleavage activity of RNase G at all (222). The RNA binding studies and Michaelis–Menten analysis of RNase G demonstrated that the presence of a 5' monophosphate enhanced the binding of RNase G to RNA substrates (211).

RNase G, encoded by the *rng/cafA* gene located at 73 min on the *E. coli* genetic map (226), is 489 amino acids in length with a predicted molecular mass of 55 kDa (Fig. 1.1) (227). Velocity sedimentation and oxidative cross-linking analysis employing purified RNase G protein indicated that RNase G exists principally as dimers in equilibrium with a small pool of monomers, tetramers and higher multimers (227). Dimerization is necessary for full catalytic activation of

RNase G (227). The prevention of dimer formation by multiple mutations in serine residues, which are involved in inter- and intramolecular interaction (227), or by employing protein chimeras, which contain Maltose binding protein (MBP) domain at amino terminus (222), results in a partial loss of its activity and a shift in the distribution of RNase G multimers toward the monomeric form.

C. Structural and functional relationship between RNase E and RNase G

The best characterized members of RNase E/G endoribonuclease family are *Escherichia coli* RNase E and RNase G, polypeptides of 1061 and 489 amino acids, respectively (Fig. 1.1) (148,165,228). The RNase E/G-like proteins have been classified into four subgroups based on the position and sequences of their putative catalytic domains, and the presence or absence of auxiliary regions containing 'scaffold' sequences (149). According to this classification, *E. coli* RNase E is a Type I enzyme, which contains the catalytic domain near the N-terminal end and the 'scaffold' is in the C-terminal half. In contrast, *E. coli* RNase G resembles type IV enzymes, which contain only the highly conserved catalytic domain and have sizes ranging from 375 to 515 amino acids in length (149).

There is 49.5% sequence similarity and 34.1% sequence identity between the N-terminal domain of RNase E (residues 1-489) and the entire length of RNase G (146,178). While RNase G shares a high degree of homology with the N-terminal domain of RNase E, the highly conserved region associated with endonucleolytic activity, it completely lacks an Arginine rich binding site and a C-terminal domain, which is largely unstructured and poorly conserved across the bacterial species (Fig. 1.1) (60,178,188). More extensive sequence similarity between the two proteins is found in two regions, residues 39-61 and 317-351 of RNase G (Fig. 1.1) (146,229). The high similarity region 1 (HSR 1, residues 39-61) contains a consensus motif for nucleotide binding and is a part of the S1 RNA binding domain (180,230). Two independently

isolated *rne* temperature-sensitive mutations, *rne-1* and *rne-3071* alleles, are mapped within this region (146). The HSR 2 (residues 317-351) appears to be part of the DNase I-like domain which contains the catalytic site of this endoribonuclease family (178,180).

In view of the sequence similarity and structural homology of RNase G to the catalytic domain of RNase E, it is not surprising that these two enzymes have a number of common *in vitro* properties. Both enzymes have a propensity to cleave the AU-rich single-stranded segments and a preference for substrates with a 5' monophosphate over a 5' triphosphate or 5' hydroxyl ones (204,205,215,222). Furthermore, *in vitro* analysis of RNase E/G homologues from both Gram-Negative and Gram-Positive bacteria strongly suggests that the 5'-end dependence is apparently a common feature of this endoribonuclease family, and may be an ancient and evolutionally conserved mechanism (231,232). However, their precise substrate specificities and scanning mode of enzymatic action in cleavage site selection are not identical. A purified RNase G preparation was able to cleave two RNase E substrates *in vitro* (RNA I and the 5' UTR of *ompA*) at sites somewhat different from those recognized by RNase E, and it exhibited slower cleavage rate than purified RNase E. In addition, it cleaved a 9S rRNA precursor only at high enzyme levels (222). In contrast, RNase E degrades substrates quasi-processively in a 3' to 5' scanning mode, whereas RNase G exhibits a nondirectional and distributive mode of action on the cleavage of the same substrates (210). Moreover, RNase G appears to cleave more promiscuously within a given sequence *in vitro* than does RNase E (222). The formation of either RNase E or RNase G multimers (predominantly tetramers and dimers, respectively) is required for the full functioning of these enzymes (180,209,227,233).

Some functional homology between RNase E and RNase G was also suggested, albeit only partially (229,234). The conditional lethality associated with the *rne-1* allele was partially suppressed by the introduction of the wild-type *rng* allele on a high copy number plasmid. On

the other hand, introduction of the *rng:cat* mutation into the *rne-1* mutant strain exacerbated its temperature sensitivity (234,235).

Although RNase E and RNase G share considerable sequence homology, catalytic properties and some functional overlap, RNase G has very limited biological functions. Unlike RNase E, which is an essential endoribonuclease and plays central roles in RNA degradation and processing (155,162-164,236), RNase G is dispensable and its inactivation does not result in any discernable effect on cell growth under normal physiological conditions (165,166,234). Both RNase G and RNase E are required for a two step, sequential maturation of the 5' terminus of 16S rRNA. However, RNase G is responsible for generating the mature 5' end of 16S rRNA (165,166,237). Recent *in vivo* studies demonstrated that although RNase G inefficiently participates in mRNA degradation and 9S rRNA processing, RNase G does not involved in either tRNA maturation or M1 RNA processing (225,235,238).

The limited physiological role of RNase G in *E. coli* is possibly explained by observations that its cellular concentration is < 4% that of RNase E (225). Therefore, RNase E is the primary source of total cellular RNase E/G activity in normal physiological conditions, and is an essential endoribonuclease in *E. coli*. In fact, over-expression of the wild type RNase G did not rescue an *rne* mutant phenotype in *E. coli* (215,234,235,238). In contrast, high level expression of altered forms of RNase G, which contain either six additional amino acids at its N-terminus or six histidine residues at C-terminus, resulted in apparent complementation the RNase E deficiency (177,225,238).

My dissertation research has attempted to broaden our understanding of physiological roles and functional relationships of RNase E/G endoribonuclease family in RNA metabolism in *Escherichia coli*. Although extensive studies have been performed over the past 30 years to obtain a better understanding of the biological functions and biochemical mechanisms of RNase E, these studies have had major limitations. In particular, these investigations employed either

temperature sensitive or various kinds of truncation mutation proteins, in which strains retained residual RNase E activity. Furthermore, what specific features of the two proteins are responsible for the differences in the biological activities between RNase E and its homolog RNase G, still remains as an unanswered question.

In this dissertation, isolation and characterization of altered RNase G proteins (Rng-219 and Rng-248), which are able to support cell viability in the total absence of RNase E when present at levels comparable to normal physiological amount of RNase E, has provided a unique opportunity to investigate more carefully important questions outlined. As described in Chapter 2, our molecular genetics and computer modeling analysis data suggest that the RNase H domain region in two proteins is responsible for at least some of differences between their *in vivo* biological activities. Additionally, *in vivo* analysis of the *rng-219* and *rng-248* alleles in the complete absence of RNase E has provided interesting new insights into the distinct roles of RNase E and RNase G in tRNA maturation, mRNA decay and 9S rRNA processing. Purification and biochemical characterizations of Rne, Rng and Rne-219 proteins are presented in Chapter 3. These data show that *in vitro* the RNase E and RNase G actually have surprisingly similar substrate specificities and that RNase G is much more active in the presence of Mn^{2+} than Mg^{2+} .

REFERENCES

1. Brenner, S., Jacob, F. and Meselson, M. (1961) An unstable intermediate carrying information from genes to ribosomes for protein synthesis. *Nature*, **190**, 576-581.
2. Gros, F., Hiatt, H., Gilbert, W., Kurland, C.B., Risebrough, R.W. and Watson, J.D. (1961) Unstable ribonucleic acid revealed by pulse labelling of *Escherichia coli*. *Nature*, **190**, 581-585.
3. Pedersen, S., Reeh, S. and Friesen, J.D. (1978) Functional mRNA half-lives in *E. coli*.

- Mol. Gen. Genet.*, **166**, 329-336.
4. Bäga, M., Gäransson, M., Normark, S. and Uhlin, B.E. (1988) Processed mRNA with differential stability in the regulation of *E. coli* pilin gene expression. *Cell*, **52**, 197-206.
 5. Goldenberg, D., Azar, I. and Oppenheim, A.B. (1996) Differential mRNA stability of the *cspA* gene in the cold-shock response of *Escherichia coli*. *Mol. Microbiol.*, **19**, 241-248.
 6. Nilsson, G., Belasco, J.G., Cohen, S.N. and von Gabain, A. (1984) Growth-rate dependent regulation of mRNA stability in *Escherichia coli*. *Nature*, **312**, 75-77.
 7. Resnekov, O., Rutberg, L. and von Gabain, A. (1990) Changes in the stability of specific mRNA species in response to growth stage in *Bacillus subtilis*. *Proc. Natl. Acad. Sci. USA*, **87**, 8355-8359.
 8. Klug, G. (1991) Endonucleolytic degradation of *puf* mRNA in *Rhodobacter capsulatus* is influenced by oxygen. *Proc. Natl. Acad. Sci. USA*, **88**, 1765-1769.
 9. Le Derout, J., Regnier, P. and Hajnsdorf, E. (2002) Both temperature and medium composition regulate RNase E processing efficiency of the *rpsO* mRNA coding for ribosomal protein of S15 of *Escherichia coli*. *J. Mol. Biol.*, **319**, 341-349.
 10. Belasco, J.G., Nilsson, G., von Gabain, A. and Cohen, S.N. (1986) The stability of *E. coli* gene transcripts is dependent on determinants localized to specific mRNA segments. *Cell*, **46**, 245-251.
 11. Mackie, G.A. (1987) Posttranscriptional regulation of ribosomal protein S20 and stability of S20 mRNA species. *J. Bacteriol.*, **169**, 2697-2701.
 12. Plamann, M.D. and Stauffer, G.V. (1990) *E. coli glyA* mRNA decay: The role of 3' secondary Structure and the effects of the *pnp* and *rnb* mutations. *Mol. Gen. Genet.*, **220**, 301-306.
 13. Emory, S.A., Bouvet, P. and Belasco, J.G. (1992) A 5'-terminal stem-loop Structure can stabilize mRNA in *Escherichia coli*. *Genes Dev.*, **6**, 135-148.

14. Diwa, A. and Belasco, J.G. (2002) Critical features of a conserved RNA stem-loop important for feedback regulation of RNase E synthesis. *J. Biol. Chem.*, **277**, 20415-20422.
15. Nicholson, A.W. (1999) Function, mechanism and regulation of bacterial ribonucleases. *FEMS Microbiol. Rev.*, **23**, 371-390.
16. Deutscher, M.P. (2006) Degradation of RNA in bacteria: comparison of mRNA and stable RNA. *Nucleic Acids Res.*, **34**, 659-666.
17. Srivastava, A.K. and Schlessinger, D. (1990) Mechanisms and regulation of bacterial ribosomal RNA processing. *Annu. Rev. Microbiol.*, **44**, 105-129.
18. Li, Z. and Deutscher, M.P. (1996) Maturation pathways for *E.coli* tRNA precursors: a random multienzyme process *in vivo*. *Cell*, **86**, 503-512.
19. Li, Z., Pandit, S. and Deutscher, M.P. (1998) 3' Exoribonucleolytic trimming is a common feature of the maturation of small, stable RNAs in *Escherichia coli*. *Proc. Natl. Acad. Sci. USA*, **95**, 2856-2861.
20. Kushner, S.R. (1996) In Neidhardt, F. C., Curtiss III, R., Ingraham, J. L., Lin, E. C. C., Low, J., K.B., Magasanik, B., Reznikoff, W. S., Riley, M., Schaechter, M. and Umberger, H. E. (eds.), *Escherichia coli and Salmonella: Cellular and Molecular Biology, Second Edition*. ASM Press, Washington, DC, Vol. 1, pp. 849-860.
21. Condon, C. (2007) Maturation and degradation of RNA in bacteria. *Curr. Opin. Microbiol.*, **10**, 271-278.
22. Worrall, J.A.R. and Luisi, B.F. (2007) Information available at cut rates: Structure and mechanism of ribonucleases. *Curr. Opin. Struct. Biol.*, **17**, 128-137.
23. Donovan, W.P. and Kushner, S.R. (1986) Polynucleotide phosphorylase and ribonuclease II are required for cell viability and mRNA turnover in *Escherichia coli* K-12. *Proc. Natl. Acad. Sci. USA*, **83**, 120-124.

24. Ghosh, S. and Deutscher, M.P. (1999) Oligoribonuclease is an essential component of the mRNA decay pathway. *Proc. Natl. Acad. Sci. USA*, **96**, 4372-4377.
25. Steege, D.A. (2000) Emerging features of mRNA decay in bacteria. *RNA*, **6**, 1079-1090.
26. Kushner, S.R. (2002) mRNA decay in *Escherichia coli* comes of age. *J. Bacteriol.*, **184**, 4658-4665.
27. Mohanty, B.K. and Kushner, S.R. (2003) Genomic analysis in *Escherichia coli* demonstrates differential roles for polynucleotide phosphorylase and RNase II in mRNA abundance and decay. *Mol. Microbiol.*, **50**, 645-658.
28. Cheng, Z.-F. and Deutscher, M.P. (2005) An important role for RNase R in mRNA decay. *Mol. Cell*, **17**, 313-318.
29. Kelly, K.O. and Deutscher, M.P. (1992) The presence of only one of five exoribonucleases is sufficient to support the growth of *Escherichia coli*. *J. Bacteriol.*, **174**, 6682-6684.
30. Reuven, N.B. and Deutscher, M.P. (1993) Multiple exoribonucleases are required for the 3' processing of *Escherichia coli* tRNA precursors *in vivo*. *FASEB J.*, **7**, 143-148.
31. Callahan, C. and Deutscher, M.P. (1996) Identification and characterization of the *Escherichia coli rbn* gene encoding the tRNA processing enzyme RNase BN. *J. Bacteriol.*, **178**, 7329-7332.
32. Zuo, Y. and Deutscher, M.P. (2002) The physiological role of RNase T can be explained by its unusual substrate specificity. *J. Biol. Chem.*, **277**, 29654-29661.
33. Zilhao, R., Cairrao, F., Régnier, P. and Arraiano, C.M. (1995) Precise physical mapping of the *Escherichia coli rnb* gene, encoding ribonuclease II. *Mol. Gen. Genet.*, **248**, 242-246.
34. Rudd, K.E. (1998) Linkage map of *Escherichia coli* K-12, Edition 10: the physical map. *Microbiol. Molec. Biol. Rev.*, **62**, 985-1019.

35. Zilhao, R., Plumbridge, J., Hajnsdorf, E., Régnier, P. and Arraiano, C.M. (1996) *Escherichia coli* RNase II: Characterization of the promoters involved in the transcription of *rnb*. *Microbiol.*, **142**, 367-375.
36. Deutscher, M.P., Marlor, C.W. and Zaniewski, R. (1984) Ribonuclease T: new exoribonuclease possibly involved in end-turnover of tRNA. *Proc. Natl. Acad. Sci. USA*, **81**, 4290-4293.
37. Coburn, G.A. and Mackie, A.G. (1996) Overexpression, purification and properties of *Escherichia coli* ribonuclease II. *J. Biol. Chem.*, **271**, 1048-1053.
38. Cairrao, F., Chora, A., Zilhao, R., Carpousis, A.J. and Arraiano, C.M. (2001) RNase II levels change according to the growth conditions: characterization of *gmr*, a new *Escherichia coli* gene involved in the modulation of RNase II. *Mol. Microbiol.*, **39**, 1550-1561.
39. Gupta, R.S., Kasai, T. and Schlessinger, D. (1977) Purification and some novel properties of *Escherichia coli* RNase II. *J. Biol. Chem.*, **252**, 8945-8949.
40. Spickler, C. and Mackie, G.A. (2000) Action of RNase II and polynucleotide phosphorylase against RNAs containing stem-loops of defined Structure. *J. Bacteriol.*, **182**, 2422-2427.
41. Cannistraro, V.J. and Kennell, D. (1999) The reaction mechanism of ribonuclease II and its interaction with nucleic acid secondary structures. *Biochim. Biophys. Acta*, **1433**, 170-187.
42. Cheng, Z.F. and Deutscher, M.P. (2002) Purification and characterization of the *Escherichia coli* exoribonuclease RNase R. Comparison with RNase II. *J. Biol. Chem.*, **277**, 21624-21649.
43. Deutscher, M.P. and Reuven, N.B. (1991) Enzymatic basis for hydrolytic versus phosphorolytic mRNA degradation in *Escherichia coli* and *Bacillus subtilis*. *Proc. Natl.*

- Acad. Sci. USA*, **88**, 3277-3280.
44. Hajnsdorf, E., Steier, O., Coscoy, L., Teyssset, L. and Régnier, P. (1994) Roles of RNase E, RNase II and PNPase in the degradation of the *rpsO* transcripts of *Escherichia coli*: stabilizing function of RNase II and evidence for efficient degradation in an *ams pnp rnb* mutant. *EMBO J.*, **13**, 3368-3377.
 45. Cruz, A.A., Marujo, P.E., Newbury, S.F. and Arraiano, C.M. (1996) RNase E can inhibit the decay of some degradation intermediates: Degradation of *Desulfovibrio vulgaris* cytochrome c-3 mRNA in *E. coli*. *Biochimie*, **78**, 227-235.
 46. Coburn, G.A. and Mackie, G.A. (1998) Reconstitution of the degradation of the mRNA for ribosomal protein S20 with purified enzymes. *J. Mol. Biol.*, **279**, 1061-1074.
 47. Marujo, P.E., Hajnsdorf, E., Le Derout, J., Andrade, R., Arraiano, C.M. and Regnier, P. (2000) RNase II removes the oligo(A) tails that destabilize the *rpsO* mRNA of *Escherichia coli*. *RNA*, **6**, 1185-1193.
 48. Mohanty, B.K. and Kushner, S.R. (2000) Polynucleotide phosphorylase, RNase II and RNase E play different roles in the *in vivo* modulation of polyadenylation in *Escherichia coli*. *Mol. Microbiol.*, **36**, 982-994.
 49. Portier, C. (1975) Quaternary Structure of polynucleotide phosphorylase from *Escherichia coli*: Evidence of a complex between two types of polypeptide chains. *Eur. J. Biochem.*, **55**, 573-582.
 50. Regnier, P., Grunberg-Manago, M. and Portier, C. (1987) Nucleotide sequence of the *pnp* gene of *Escherichia coli* encoding polynucleotide phosphorylase. *J. Biol. Chem.*, **262**, 63-68.
 51. Thang, M.N., Guschlbauer, W., Zachau, H.G. and Grunberg-Manago, M. (1967) Degradation of transfer ribonucleic acid by polynucleotide phosphorylase. I. Mechanism of phosphorylisis and Structure of tRNA. *J. Mol. Biol.*, **26**, 403-421.

52. Godefroy, T., Cohn, M. and M., G. (1970) Kinetics of polymerization and phosphorolysis reactions of *E. coli* polynucleotide phosphorylase. Role of oligonucleotides in polymerization. *Eur. J. Biochem.*, **12**, 236-249.
53. Littauer, U.Z. and Soreq, H. (1982) In Boyer, P. D. (ed.), *The Enzymes*. Academic Press, New York, Vol. 15, pp. 517-553.
54. O'Hara, E.B., Chekanova, J.A., Ingle, C.A., Kushner, Z.R., Peters, E. and Kushner, S.R. (1995) Polyadenylation helps regulate mRNA decay in *Escherichia coli*. *Proc. Natl. Acad. Sci. USA*, **92**, 1807-1811.
55. Li, Z., Reimers, S., Pandit, S. and Deutscher, M.P. (2002) RNA quality control: degradation of defective transfer RNA. *EMBO J.*, **21**, 1132-1138.
56. Mohanty, B.K. and Kushner, S.R. (2000) Polynucleotide phosphorylase functions both as a 3' - 5' exonuclease and a poly(A) polymerase in *Escherichia coli*. *Proc. Natl. Acad. Sci. USA*, **97**, 11966-11971.
57. Liou, G.-G., Jane, W.-N., Cohen, S.N., Lin, N.-S. and Lin-Chao, S. (2001) RNA degradosomes exist *in vivo* in *Escherichia coli* as multicomponent complexes associated with the cytoplasmic membrane via the N-terminal region of ribonuclease E. *Proc. Natl. Acad. Sci. USA*, **98**, 63-68.
58. Carpousis, A.J., Van Houwe, G., Ehretsmann, C. and Krisch, H.M. (1994) Copurification of *E. coli* RNAase E and PNPase: Evidence for a specific association between two enzymes important in RNA processing and degradation. *Cell*, **76**, 889-900.
59. Py, B., Higgins, C.F., Krisch, H.M. and Carpousis, A.J. (1996) A DEAD-box RNA helicase in the *Escherichia coli* RNA degradosome. *Nature*, **381**, 169-172.
60. Vanzo, N.F., Li, Y.S., Py, B., Blum, E., Higgins, C.F., Raynal, L.C., Krisch, H.M. and Carpousis, A.J. (1998) Ribonuclease E organizes the protein interactions in the *Escherichia coli* RNA degradosome. *Genes Dev.*, **12**, 2770-2781.

61. Liou, G.-G., Chang, H.-Y., Lin, C.-S. and Lin-Chao, S. (2002) DEAD box RhlB RNA helicase physically associates with exoribonuclease PNPase to degrade double-stranded RNA independent of the degradosome-assembling region of RNase E. *J. Biol. Chem.*, **277**, 41157-41162.
62. Lin, P.-H. and Lin-Chao, S. (2005) RhlB helicase rather than enolase is the B-subunit of the *Escherichia coli* polynucleotide phosphorylase (PNPase)-exoribonucleolytic complex. *Proc. Natl. Acad. Sci. USA*, **102**, 16590-16595.
63. Jones, P.G., VanBogelen, R.A. and Neidhardt, F.C. (1987) Induction of proteins in response to low temperature in *Escherichia coli*. *J. Bacteriol.* , **169**, 2092-2095.
64. Yamanaka, K. and Inouye, M. (2001) Selective mRNA degradation by polynucleotide phosphorylase in cold shock adaptation in *Escherichia coli*. *J. Bacteriol.*, **183**, 2808-2816.
65. Cheng, Z.F., Zuo, Y., Li, Z., Rudd, K.E. and Deutscher, M.P. (1998) The *vacB* gene required for virulence in *Shigella flexneri* and *Escherichia coli* encodes the exoribonuclease RNase R. *J. Biol. Chem.*, **273**, 14077-14080.
66. Cheng, Z.F. and Deutscher, M.P. (2003) Quality control of ribosomal RNA mediated by polynucleotide phosphorylase and RNase R. *Proc. Natl. Acad. Sci. USA*, **100**, 6388-6393.
67. Zhou, Z. and Deutscher, M.P. (1997) An essential function for the phosphate-dependent exoribonucleases RNase PH and polynucleotide phosphorylase. *J. Bacteriol.*, **179**, 4391-4395.
68. Niyogi, S.K. and Datta, A.K. (1975) A novel oligoribonuclease of *Escherichia coli* I. Isolation and properties. *J. Biol. Chem.*, **250**, 7307-7312.
69. Zhang, X., Zhu, L. and Deutscher, M.P. (1998) Oligoribonuclease is encoded by a highly conserved gene in the 3'-5' exonuclease superfamily. *J. Bacteriol.*, **180**, 2779-2781.
70. Deutscher, M.P., Marlor, C.W. and Zaniewski, R. (1985) RNase T is responsible for the

- end-turnover of tRNA in *Escherichia coli*. *Proc. Natl. Acad. Sci. USA*, **82**, 6427-6430.
71. Huang, S. and Deutscher, M.P. (1992) Sequence and transcriptional analysis of the *Escherichia coli rnt* gene encoding RNase T. *J. Biol. Chem.*, **267**, 25609-25613.
 72. Li, Z. and Deutscher, M.P. (1995) The tRNA processing enzyme RNase T is essential for maturation of 5S RNA. *Proc. Natl. Acad. Sci. USA*, **92**, 6883-6886.
 73. Li, Z., Pandit, S. and Deutscher, M.P. (1999) Maturation of 23S ribosomal RNA requires the exoribonuclease RNase T. *RNA*, **5**, 139-146.
 74. Viswanathan, M., Lanjuin, A. and Lovett, S.T. (1999) Identification of RNase T as a high-copy suppressor of the UV sensitivity associated with single-strand DNA exonuclease deficiency in *Escherichia coli*. *Genetics*, **151**, 929-934.
 75. Zuo, Y. and Deutscher, M.P. (1999) The DNase activity of RNase T and its application to DNA cloning. *Nucleic Acids Res.*, **27**, 4077-4082.
 76. Cudny, H., Zaniewski, R. and Deutscher, M.P. (1981) *Escherichia coli* RNase D. Catalytic properties and substrate specificity. *J. Biol. Chem.*, **256**, 5633-5637.
 77. Zhang, J. and Deutscher, M.P. (1988) *Escherichia coli* RNase D: sequencing of the *rnd* structural gene and purification of the overexpressed protein. *Nucleic Acids Res.*, **16**, 6265-6278.
 78. Ghosh, R.K. and Deutscher, M.P. (1978) Identification of an *Escherichia coli* nuclease acting on structurally altered transfer RNA molecules. *J. Biol. Chem.*, **253**, 997-1000.
 79. Blouin, R.T., Zaniewski, R. and Deutscher, M.P. (1983) Ribonuclease D is not essential for the normal growth of *Escherichia coli* or bacteriophage T4 or for the biosynthesis of a T4 suppressor tRNA. *J. Biol. Chem.*, **258**, 1423-1426.
 80. Kasai, T., Gupta, R.S. and Schlessinger, D. (1977) Exoribonucleases in wild type *Escherichia coli* and RNase II-deficient mutants. *J. Biol. Chem.*, **252**, 8950-8956.
 81. Deutscher, M.P. (1993) Promiscuous exoribonucleases of *Escherichia coli*. *J. Bacteriol.*,

- 175**, 4577-4583.
82. Cudny, H. and Deutscher, M.P. (1988) 3' Processing of tRNA precursors in ribonuclease-deficient *Escherichia coli*. *J. Biol. Chem.*, **263**, 1518-1523.
 83. Kelly, K.O. and Deutscher, M.P. (1992) Characterization of *Escherichia coli* RNase PH. *J. Biol. Chem.*, **267**, 17153-17158.
 84. Deutscher, M.P., Marshall, G.T. and Cudny, H. (1988) RNase PH: A new phosphate-dependent nuclease distinct from polynucleotide phosphorylase. *Proc. Natl. Acad. Sci. USA*, **85**, 4710-4714.
 85. Li, Z. and Deutscher, M.P. (1994) The role of individual exoribonucleases in processing at the 3' end of *Escherichia coli* tRNA precursors. *J. Biol. Chem.*, **269**, 6064-6071.
 86. Ost, K.A. and Deutscher, M.P. (1990) RNase PH catalyzes a synthetic reaction, the addition of nucleotides to the 3' end of RNA. *Biochimie*, **72**, 813-818.
 87. Kelly, K.O., Reuven, N.B., Li, Z. and Deutscher, M.P. (1992) RNase PH is essential for tRNA processing and viability in RNase-deficient *Escherichia coli* cells. *J. Biol. Chem.*, **267**, 16015-16018.
 88. Robertson, H.D., Webster, R.E. and Zinder, N.D. (1967) A nuclease specific for double-stranded RNA. *Virology*, **12**, 718-719.
 89. Robertson, H.D., Webster, R.E. and Zinder, N.D. (1968) Purification and properties of ribonuclease III from *Escherichia coli*. *J. Biol. Chem.*, **243**, 82-91.
 90. Conrad, C. and Rauhut, R. (2002) Ribonuclease III: new sense from nuisance. *Int. J. Biochem. Cell Biol.*, **34**, 116-129.
 91. March, P.E., Ahnn, J. and Inouye, M. (1985) The DNA sequence of the gene (*rnc*) encoding ribonuclease III of *Escherichia coli*. *Nucleic Acids Res.*, **13**, 4677-4685.
 92. Nashimoto, H. and Uchida, H. (1985) DNA sequencing of the *Escherichia coli* ribonuclease III gene and its mutations. *Mol. Gen. Genet.*, **201**, 25-29.

93. Court, D. (1993) In Belasco, J. and Brawerman, G. (eds.), *Control of messenger RNA stability*. Academic Press, New York, pp. 71-117.
94. Li, H. and Nicholson, A.W. (1996) Defining the enzyme binding domain of a ribonuclease III processing signal. Ethylation interference and hydroxyl radical footprinting using catalytically inactive RNase III mutants. *EMBO J.*, **15**, 1421-1433.
95. Blaszczyk, J., Tropea, J.E., Bubunencko, M., Routzahn, K.M., Waugh, D.S., Court, D.L. and Ji, X.H. (2001) Crystallographic and modeling studies of RNase III suggest a mechanism for double-stranded RNA cleavage. *Structure (Cambridge)*, **9**, 1225-1236.
96. Gan, J., Tropea, J.E., Austin, B.P., Court, D.L., Waugh, D.S. and Ji, X. (2006) Structural Insight into the Mechanism of Double-Stranded RNA Processing by Ribonuclease III. *Cell*, **124**, 355-366.
97. Robertson, H.D. (1982) *Escherichia coli* ribonuclease III cleavage sites. *Cell*, **30**, 669-672.
98. Dasgupta, S., Fernandez, L., Kameyama, L., Inada, T., Nakamura, Y., Pappas, A. and Court, D.L. (1998) Genetic uncoupling of the dsRNA-binding and RNA cleavage activities of the *Escherichia coli* endoribonuclease RNase III--the effect of dsRNA binding on gene expression. *Mol. Microbiol.*, **28**, 629-640.
99. Calin-Jageman, I. and Nicholson, A.W. (2003) RNA Structure-dependent uncoupling of substrate recognition and cleavage by *Escherichia coli* ribonuclease III. *Nucleic Acids Res.*, **31**, 2381-2392.
100. Bram, R.J., Young, R.A. and Steitz, J.A. (1980) The ribonuclease III site flanking 23S sequences in the 30S ribosomal precursor RNA of *Escherichia coli*. *Cell*, **19**, 393-401.
101. King, T.C., Sirdeshmukh, R. and Schlessinger, D. (1984) RNase III cleavage is obligate for maturation but not for function of *Escherichia coli* pre-23S rRNA. *Proc. Natl. Acad. Sci. USA*, **81**, 185-188.

102. Babitzke, P., Granger, L. and Kushner, S.R. (1993) Analysis of mRNA decay and rRNA processing in *Escherichia coli* multiple mutants carrying a deletion in RNase III. *J. Bacteriol.*, **175**, 229-239.
103. Grunberg-Manago, M. (1999) Messenger RNA stability and its role in control of gene expression in bacteria and phages. *Annu. Rev. Gen.*, **33**, 193-227.
104. Wilson, H.R., Yu, D., Peters, H.K., 3rd, Zhou, J.G. and Court, D.L. (2002) The global regulator RNase III modulates translation repression by the transcription elongation factor N. *EMBO J.*, **21**, 4154-4161.
105. Bardwell, J.C.A., Regnier, P., Chen, S.-M., Nakamura, Y., Grunberg-Manago, M. and Court, D.L. (1989) Autoregulation of RNase III operon by mRNA processing. *EMBO J.* , **8**, 3401-3407.
106. Portier, C., Dondon, L., Grunberg-Manago, M. and Regnier, P. (1987) The first step in the functional inactivation of the *Escherichia coli* polynucleotide phosphorylase messenger is ribonuclease III processing at the 5' end. *EMBO J.*, **6**, 2165-2170.
107. Faubladiere, M., Cam, K. and Bouche, J.P. (1990) *Escherichia coli* cell division inhibitor *dicF*-RNA of the *dicB* operon. *J. Mol. Biol.*, **32**, 461-471.
108. Regnier, P. and Grunberg-Manago, M. (1989) Cleavage by RNase III in the transcripts of the *metY-nus-infB* operon of *Escherichia coli* releases the tRNA and initiates the decay of the downstream mRNA. *J. Mol. Biol.*, **210**, 293-302.
109. Neu, H.C. and Heppel, L.A. (1964) Some observations on the "latent" ribonuclease of *Escherichia coli*. *Biochemistry*, **51**, 1267-1274.
110. Zhu, L., Gangopadhyay, T., Padmandabha, K.P. and Deutscher, M.P. (1990) *Escherichia coli rna* gene encoding RNase I: Cloning, overexpression, subcellular distribution of the enzyme, and use of an *rna* deletion to identify additional RNases. *J. Bacteriol.*, **172**, 3146-3151.

111. Meador III, J., Cannon, B., Cannistraro, V.J. and Kennell, D. (1990) Purification and characterization of *Escherichia coli* RNase I. Comparisons with RNase M. *Eur. J. Biochem.*, **187**, 549-553.
112. Gesteland, R.F. (1966) Isolation and characterization of ribonuclease I mutants of *Escherichia coli*. *J. Mol. Biol.*, **16**, 67-84.
113. Beppu, T. and Arima, K. (1969) Induction by mercuric ion of extensive degradation of cellular ribonucleic acid in *Escherichia coli*. *J. Bacteriol.*, **98**, 888-897.
114. Kaplan, R. and Apirion, D. (1974) The involvement of ribonuclease I, ribonuclease II, and polynucleotide phosphorylase in the degradation of stable ribonucleic acid during carbon starvation in *E. coli*. *J. Biol. Chem.*, **249**, 149-151.
115. Ito, R. and Ohnishi, Y. (1983) The roles of RNA polymerase and RNAase I in stable RNA degradation in *Escherichia coli* carrying the *srnB+* gene. *Biochim. Biophys. Acta*, **739**, 27-34.
116. Cannistraro, V.J. and Kennell, D. (1991) RNase I*, a form of RNase I, and mRNA degradation in *Escherichia coli*. *J. Bacteriol.*, **173**, 4653-4659.
117. Robertson, H.D., Altman, S. and Smith, J.D. (1972) Purification and Properties of a Specific *Escherichia coli* Ribonuclease which Cleaves a Tyrosine Transfer Ribonucleic Acid Precursor. *J. Biol. Chem.*, **247**, 5243-5251.
118. Frank, D.N. and Pace, N.R. (1998) Ribonuclease P: unity and diversity in a tRNA processing ribozyme. *Annu. Rev. Biochem.*, **67**, 153-180.
119. Schon, A. (1999) Ribonuclease P: the diversity of a ubiquitous RNA processing enzyme. *FEMS Microbiol. Rev.*, **23**, 391-406.
120. Guerrier-Takada, C., Gardiner, K., Marsh, T., Pace, N. and Altman, S. (1983) The RNA moiety of ribonuclease P is the catalytic subunit of the enzyme. *Cell*, **35**, 849-857.
121. Brown, J.W. (1998) The ribonuclease P database. *Nucleic Acids Res.*, **26**, 351-352.

122. Smith, D., Burgin, A.B., Haas, E.S. and Pace, N.R. (1992) Influence of metal ions on the ribonuclease P reaction. Distinguishing substrate binding from catalysis. *J. Biol. Chem.*, **267**, 2429-2436.
123. Altman, S. (1990) Ribonuclease P. Postscript. *J. Biol. Chem.*, **265**, 20053-20056.
124. Pace, N.R. and Smith, D. (1990) Ribonuclease P: function and variation. *J. Biol. Chem.*, **265**, 3587-3590.
125. Altman, S., Kirsebom, L. and Talbot, S. (1995) In Soll, D. and RajBhandary (eds.), *tRNA: Structure and Function*. American Society for Microbiology Press, Washington, DC, pp. 67-78.
126. Peck-Miller, K.A. and Altman, S. (1991) Kinetics of the processing of the precursor to 4.5S RNA, a naturally occurring substrate for RNase P from *Escherichia coli*. *J. Mol. Biol.*, **221**, 1-5.
127. Li, Y. and Altman, S. (2003) A specific endoribonuclease, RNase P, affects gene expression of polycistronic operon mRNAs. *Proc. Natl. Acad. Sci. USA*, **100**, 13213-13218.
128. Mohanty, B.K. and Kushner, S.R. (2007) Ribonuclease P processes polycistronic tRNA transcripts in *Escherichia coli* independent of ribonuclease E. *Nucleic Acids Res.*, **35**, 7614-7625.
129. Mohanty, B.K. and Kushner, S.R. (2008) Rho-independent transcription terminators inhibit RNase P processing of the *secG leuU* and *metT* tRNA polycistronic transcripts in *Escherichia coli*. *Nucleic Acids Res.*, **36**, 364-375.
130. Otsuka, Y., Ueno, H. and Yonesaki, T. (2003) *Escherichia coli* endoribonucleases involved in cleavage of bacteriophage T4 mRNAs. *J. Bacteriol.*, **185**, 983-990.
131. Otsuka, Y. and Yonesaki, T. (2005) A novel endoribonuclease, RNase LS, in *Escherichia coli*. *Genetics*, **169**, 13-20.

132. Kai, T. and Yonesaki, T. (2002) Multiple mechanisms for degradation of bacteriophage T4 *soc* mRNA. *Genetics*, **160**, 5-12.
133. Kanesaki, T., Hamada, T. and Yonesaki, T. (2005) Opposite roles of the *dmd* gene in the control of RNase E and RNase LS activities. *Genes Genet. Syst.*, **80**, 241-249.
134. Yamanishi, H. and Yonesaki, T. (2005) RNA cleavage linked with ribosomal action. *Genetics*, **171**, 419-425.
135. Schiffer, S., Rosch, S. and Marchfelder, A. (2002) Assigning a function to a conserved group of proteins: the tRNA 3'processing enzymes. *EMBO J.*, **21**, 2769-2677.
136. Pellegrini, O., Nezzar, J., Marchfelder, A., Putzer, H. and Condon, C. (2003) Endonucleolytic processing of CCA-less tRNA precursors by RNase E in *Bacillus subtilis*. *EMBO J.*, **22**, 4534-4543.
137. Minagawa, A., Takaku, H., Takagi, M. and Nashimoto, M. (2004) A novel endonucleolytic mechanism to generate the CCA 3'-terminai of tRNA molecules in *Thermotoga maritima*. *J. Biol. Chem.*, **279**, 15688-15697.
138. de la Sierra-Gallay, I.L., Pellegrini, O. and Condon, C. (2005) Structural basis for substrate binding, cleavage and allostery in the tRNA maturase RNase Z. *Nature*, **433**, 657-661.
139. Rudd, K.E. (2000) EcoGene: a genome sequence database for *Escherichia coli* K-12. *Nucleic Acids Res.*, **28**, 60-64.
140. Perwez, T. and Kushner, S.R. (2006) RNase Z in *Escherichia coli* plays a significant role in mRNA decay. *Mol. Microbiol.*, **60**, 723-737.
141. Ezraty, B., Dahlgren, B. and Deutscher, M.P. (2005) The RNase Z homologue encoded by *Escherichia coli* *elaC* gene is RNase BN. *J. Biol. Chem.*, **280**, 16542-16545.
142. Schmidt, F.J. and McClain, W.H. (1978) An *Escherichia coli* ribonuclease which removes an extra nucleotide from a biosynthetic intermediate of bacteriophage T4 proline transfer

- RNA. *Nucleic Acids Res.*, **5**, 4129-4139.
143. Cohen, S.N. and McDowall, K.J. (1997) RNase E: still a wonderfully mysterious enzyme. *Mol. Microbiol.*, **23**, 1099-1106.
 144. Coburn, G.A. and Mackie, G.A. (1999) Degradation of mRNA in *Escherichia coli*: An old problem with some new twists. *Prog. Nucleic Acid Res.*, **62**, 55-108.
 145. Regnier, P. and Arraiano, C.M. (2000) Degradation of mRNA in bacteria: emergence of ubiquitous features. *Bioessays*, **22**, 235-244.
 146. McDowall, K.J., Hernandez, R.G., Lin-Chao, S. and Cohen, S.N. (1993) The *ams-1* and *rne-3071* temperature-sensitive mutations in the *ams* gene are in close proximity to each other and cause substitutions within a domain that resembles a product of the *Escherichia coli rne* locus. *J. Bacteriol.*, **175**, 4245-4249.
 147. Kaberdin, V.R., Miczak, A., Jakobsen, J.S., Lin-Chao, S., McDowall, K.J. and von Gabain, A. (1998) The endoribonucleolytic N-terminal half of *Escherichia coli* RNase E is evolutionarily conserved in *Synechocystis* sp. and other bacteria but not the C-terminal half, which is sufficient for degradosome assembly. *Proc. Natl. Acad. Sci. USA*, **95**, 11637-11642.
 148. Condon, C. and Putzer, H. (2002) The phylogenetic distribution of bacterial ribonucleases. *Nucleic Acids Res.*, **30**, 5339-5346.
 149. Lee, k. and Cohen, S.N. (2003) A *Streptomyces coelicolor* functional orthologue of *Escherichia coli* RNase E shows shuffling of catalytic and PNPase-binding domains. *Mol. Microbiol.*, **48**, 349-360.
 150. Bollenbach, T.J., Schuster, G. and Stern, D.B. (2004) Cooperation of endo- and exoribonucleases in chloroplast mRNA turnover. *Prog. Nucleic Acid Res.*, **78**, 305-337.
 151. Schein, A., Sheffy-Levin, S., Glaser, F. and Schuster, G. (2008) The RNase E/G-type endoribonuclease of higher plants is located in the chloroplast and cleaves RNA similarly

- to the *E. coli* enzyme. *RNA*, **14**, 1057-1068.
152. Ghora, B.K. and Apirion, D. (1978) Structural analysis and *in vitro* processing to p5 rRNA of a 9S RNA molecule isolated from an *rne* mutant of *E. coli*. *Cell*, **15**, 1055-1066.
 153. Misra, T.K. and Apirion, D. (1979) RNase E, an RNA processing enzyme from *Escherichia coli*. *J. Biol. Chem.*, **254**, 11154-11159.
 154. Kuwano, M., Ono, M., Endo, H., Hori, K., Nakamura, K., Hirota, Y. and Ohnishi, Y. (1977) Gene affecting longevity of messenger RNA: a mutant of *Escherichia coli* with altered mRNA stability. *Mol. Gen. Genet.*, **154**, 279-285.
 155. Ono, M. and Kuwano, M. (1979) A conditional lethal mutation in an *Escherichia coli* strain with a longer chemical lifetime of mRNA. *J. Mol. Biol.*, **129**, 343-357.
 156. Mudd, E.A., Krisch, H.M. and Higgins, C.F. (1990) RNase E, an endoribonuclease, has a general role in the chemical decay of *Escherichia coli* mRNA: evidence that *rne* and *ams* are the same genetic locus. *Mol. Microbiol.*, **4**, 2127-2135.
 157. Babitzke, P. and Kushner, S.R. (1991) The Ams (altered mRNA stability) protein and ribonuclease E are encoded by the same structural gene of *Escherichia coli*. *Proc. Natl. Acad. Sci. USA*, **88**, 1-5.
 158. Melefors, Ö. and von Gabain, A. (1991) Genetic studies of cleavage-initiated mRNA decay and processing of ribosomal 9S RNA show that the *Escherichia coli* *ams* and *rne* loci are the same. *Mol. Microbiol.*, **5**, 857-864.
 159. Taraseviciene, L., Miczak, A. and Apirion, D. (1991) The gene specifying RNase E (*rne*) and a gene affecting mRNA stability (*ams*) are the same gene. *Mol. Microbiol.*, **5**, 851-855.
 160. Casarégola, S., Jacq, A., Laoudj, D., McGurk, G., Margaron, S., Tempête, M., Norris, V. and Holland, I.B. (1992) Cloning and analysis of the entire *Escherichia coli* *ams* gene. *ams* is identical to *hmp-1* and encodes a 114 kDa protein that migrates as a 180 kDa

- protein. *J. Mol. Biol.*, **228**, 30-40.
161. Cormack, R.S., Genereaux, J.L. and Mackie, G.A. (1993) RNase E activity is conferred by a single polypeptide: Overexpression, purification, and properties of the *ams/rne/hmp1* gene product. *Proc. Natl. Acad. Sci. USA*, **90**, 9006-9010.
 162. Ray, B.K. and Apirion, D. (1981) Transfer RNA precursors are accumulated in *Escherichia coli* in the absence of RNase E. *Eur. J. Biochem.*, **114**, 517-524.
 163. Li, Z. and Deutscher, M.P. (2002) RNase E plays an essential role in the maturation of *Escherichia coli* tRNA precursors. *RNA*, **8**, 97-109.
 164. Ow, M.C. and Kushner, S.R. (2002) Initiation of tRNA maturation by RNase E is essential for cell viability in *Escherichia coli*. *Genes Dev.*, **16**, 1102-1115.
 165. Li, Z., Pandit, S. and Deutscher, M.P. (1999) RNase G (CafA protein) and RNase E are both required for the 5' maturation of 16S ribosomal RNA. *EMBO J.*, **18**, 2878-2885.
 166. Wachi, M., Umitsuki, G., Shimizu, M., Takada, A. and Nagai, K. (1999) *Escherichia coli* *cafA* gene encodes a novel RNase, designated as RNase G, involved in processing of the 5' end of 16S rRNA. *Biochem. Biophys. Res. Comm.*, **259**, 483-488.
 167. Lundberg, U. and Altman, S. (1995) Processing of the precursor to the catalytic RNA subunit of RNase P from *Escherichia coli*. *RNA*, **1**, 327-334.
 168. Lin-Chao, S. and Cohen, S. (1991) The rate of processing and degradation of antisense RNA I regulates the replication of ColE1-type plasmids *in vivo*. *Cell*, **65**, 1233-1242.
 169. Lin-Chao, S., Wei, C.-L. and Lin, Y.-T. (1999) RNase E is required for the maturation of *ssrA* and normal *ssrA* RNA peptide-tagging activity. *Proc. Natl. Acad. Sci. USA*, **96**, 13406-12411.
 170. Masse, R., Escorcia, F.E. and Gottesman, S. (2003) Coupled degradation of a small regulatory RNA and its mRNA targets in *Escherichia coli*. *Genes Dev.*, **17**, 2374-2383.
 171. Zhang, A., Wassarman, K.M., Rosenow, C., Tjaden, B.C., Storz, G. and Gottesman, S.

- (2003) Global analysis of small RNA and mRNA targets of Hfq. *Mol. Microbiol.*, **50**, 1111-1124.
172. Arraiano, C.M., Yancey, S.D. and Kushner, S.R. (1988) Stabilization of discrete mRNA breakdown products in *ams pnp rnb* multiple mutants of *Escherichia coli* K-12. *J. Bacteriol.*, **170**, 4625-4633.
173. Hajnsdorf, E., Braun, F., Haugel-Nielsen, J., Le Derout, J. and Régnier, P. (1996) Multiple degradation pathways of the *rpsO* mRNA of *Escherichia coli*. RNase E interacts with the 5' and 3' extremities of the primary transcript. *Biochimie*, **78**, 416-424.
174. Ow, M.C., Liu, Q. and Kushner, S.R. (2000) Analysis of mRNA decay and rRNA processing in *Escherichia coli* in the absence of RNase E-based degradosome assembly. *Mol. Microbiol.*, **38**, 854-866.
175. Bernstein, J.A., Lin, P.-H., Cohen, S.N. and Lin-Chao, S. (2004) Global analysis of *Escherichia coli* RNA degradosome function using DNA microarrays. *Proc. Natl. Acad. Sci. USA*, **101**, 2748-2763.
176. Takada, A., Nagai, K. and Wachi, M. (2005) A decreased level of FtsZ is responsible for inviability of RNase E-deficient cells. *Genes Cells*, **10**, 733-741.
177. Tamura, M., Lee, K., Miller, C.A., Moore, C.J., Shirako, Y., Kobayashi, M. and Cohen, S.N. (2006) RNase E maintenance of proper FtsZ/FtsA ratio required for nonfilamentous growth of *Escherichia coli* cells but not for colony-forming ability. *J. Bacteriol.*, **188**, 5145-5152.
178. McDowall, K.J. and Cohen, S.N. (1996) The N-terminal domain of the *rne* gene product has RNase E activity and is non-overlapping with the arginine-rich RNA-binding motif. *J. Mol. Biol.*, **255**, 349-355.
179. Caruthers, J.M., Feng, Y., McKay, D.B. and Cohen, S.N. (2006) Retention of core catalytic functions by a conserved minimal ribonuclease E peptide that lacks the domain

- required for tetramer formation. *J. Biol. Chem.*, **281**, 27046-27051.
180. Callaghan, A.J., Marcaida, M.J., Stead, J.A., McDowall, K.J., Scott, W.G. and Luisi, B.F. (2005) Structure of *Escherichia coli* RNase E catalytic domain and implications for RNA turnover. *Nature*, **437**, 1187-1191.
181. Callaghan, A.J., Redko, Y.U., Murphy, L.M., Grossman, J.G., Yates, D., Garman, E., Ilag, L.L., Robinson, C.V., Symmons, M.F., McDowall, K.J. *et al.* (2005) "Zn-Link": a metal sharing interface that organizes the quaternary Structure and catalytic site of endoribonuclease, RNase E. *Biochemistry*, **44**, 4667-4775.
182. Taraseviciene, L., Bjork, G.R. and Uhlin, B.E. (1995) Evidence for a RNA binding region in the *Escherichia coli* processing endoribonuclease RNase E. *J. Biol. Chem.*, **270**, 26391-26398.
183. Coburn, G.A., Miao, X., Briant, D.J. and Mackie, G.A. (1999) Reconstitution of a minimal RNA degradosome demonstrates functional coordination between a 3' exonuclease and a DEAD-box RNA helicase. *Genes Dev.*, **13**, 2594-2603.
184. Tompa, P. (2002) Intrinsically unstructured proteins. *Trends Biochem. Sci.* , **27**, 527-533.
185. Callaghan, A.J., Aurikko, J.P., Ilag, L.L., Grossman, J.G., Chandran, V., Kuhnel, K., Poljak, L., Carpousis, A.J., Robinson, C.V., Symmons, M.F. *et al.* (2004) Studies on the RNA degradosome-organizing domain of the *Escherichia coli* ribonuclease RNase E. *J. Mol. Biol.*, **340**, 965-979.
186. Py, B., Causton, H., Mudd, E.A. and Higgins, C.F. (1994) A protein complex mediating mRNA degradation in *Escherichia coli*. *Mol. Microbiol.*, **14**, 717-729.
187. Miczak, A., Kaberdin, V.R., Wei, C.-L. and Lin-Chao, S. (1996) Proteins associated with RNase E in a multicomponent ribonucleolytic complex. *Proc. Natl. Acad. Sci. USA*, **93**, 3865-3869.
188. Carpousis, A.J. (2002) The *Escherichia coli* degradosome: Structure, function and

- relationship to other ribonucleolytic multienzyme complexes. *Biochem. Soc. Trans.*, **30(Part 2)**, 150-156.
189. Blum, E., Py, B., Carpousis, A.J. and Higgins, C.F. (1997) Polyphosphate kinase is a component of the *Escherichia coli* RNA degradosome. *Mol. Microbiol.*, **26**, 387-398.
190. Regonesi, M.E., Del Favero, M., Basilico, F., Briani, F., Benazzi, L., Tortora, P., Mauri, P. and Deho, G. (2006) Analysis of the *Escherichia coli* RNA degradosome composition by a proteomic approach. *Biochimie*, **88**, 151-161.
191. Morita, T., Maki, K. and Aiba, H. (2005) RNase E-based ribonucleoprotein complexes: mechanical basis of mRNA destabilization mediated by bacterial noncoding RNAs. *Genes Dev.*, **19**, 2276-2186.
192. Morita, T., Kawamoto, H., Mizota, T., Inada, T. and Aiba, H. (2004) Enolase in the RNA degradosome plays a crucial role in the rapid decay of glucose transporter mRNA in the response to phosphosugar stress in *Escherichia coli*. *Mol. Microbiol.*, **54**, 1063-1075.
193. Kido, M., Yamanaka, K., Mitani, T., Niki, H., Ogura, T. and Hiraga, S. (1996) RNase E polypeptides lacking a carboxyl-terminal half suppress a *mukB* mutation in *Escherichia coli*. *J. Bacteriol.*, **178**, 3917-3925.
194. Lopez, P.J., Marchand, I., Joyce, S.A. and Dreyfus, M. (1999) The C-terminal half of RNase E, which organizes the *Escherichia coli* degradosome, participates in mRNA degradation but not rRNA processing *in vivo*. *Mol. Microbiol.*, **33**, 188-199.
195. Mohanty, B.K. and Kushner, S.R. (2002) Polyadenylation of *Escherichia coli* transcripts plays an integral role in regulating intracellular levels of polynucleotide phosphorylase and RNase E. *Mol. Microbiol.*, **45**, 1315-1324.
196. Leroy, A., Vanzo, N.F., Sousa, S., Dreyfus, M. and Carpousis, A.J. (2002) Function in *Escherichia coli* of the non-catalytic part of RNase E: role in the degradation of ribosome-free mRNA. *Mol. Microbiol.*, **45**, 1231-1243.

197. Khemici, V. and Carpousis, A.J. (2004) The RNA degradosome and poly(A) polymerase of *Escherichia coli* are required *in vivo* for the degradation of small mRNA decay intermediates containing REP-stabilizers. *Mol. Microbiol.*, **51**, 777-790.
198. Taghbalout, A. and Rothfield, L. (2007) RNase E and the other constituents of the RNA degradosome are components of the bacterial cytoskeleton. *Proc. Natl. Acad. Sci. USA*, **104**, 1667-1672.
199. Taghbalout, A. and Rothfield, L. (2008) RNaseE and RNA Helicase B Play Central Roles in the Cytoskeletal Organization of the RNA Degradosome. *J. Biol. Chem.*, **283**, 13850-13855.
200. Jaeger, S., Fuhrmann, O., Heck, C., Hebermehl, M., Schiltz, E., Rauhut, R. and Klug, G. (2001) An mRNA degrading complex in *Rhodobacter capsulatus*. *Nucleic Acids Res.*, **29**, 4581-4588.
201. Carpousis, A.J., Vanzo, N.F. and Raynal, L.C. (1999) mRNA degradation. A tale of poly(A) and multiprotein machines. *Trends Genet.*, **15**, 24-28.
202. Ehretsmann, C.P., Carpousis, A.J. and Krisch, H.M. (1992) Specificity of *Escherichia coli* endoribonuclease RNase E: *In vivo* and *in vitro* analysis of mutants in a bacteriophage T4 mRNA processing site. *Genes Dev.*, **6**, 149-159.
203. Lin-Chao, S., Wong, T.-T., McDowall, K.J. and Cohen, S.N. (1994) Effects of nucleotide sequence on the specificity of *rne*-dependent and RNase E-mediated cleavages of RNA I encoded by the pBR322 plasmid. *J. Biol. Chem.*, **269**, 10797-10803.
204. McDowall, K.J., Lin-Chao, S. and Cohen, S.N. (1994) A + U content rather than a particular nucleotide order determines the specificity of RNase E cleavage. *J. Biol. Chem.*, **269**, 10790-10796.
205. Mackie, G.A. (1998) Ribonuclease E is a 5'-end-dependent endonuclease. *Nature*, **395**, 720-723.

206. Mackie, G.A. (2000) Stabilization of circular *rpsT* mRNA demonstrates the 5'-end dependence of RNase E action *in vivo*. *J. Biol. Chem.*, **275**, 25069-25072.
207. Baker, K.E. and Mackie, G.A. (2003) Ectopic RNase E sites promote bypass of 5'-end-dependent mRNA decay in *Escherichia coli*. *Mol. Microbiol.*, **47**, 75-88.
208. Redko, Y., Tock, M.R., Adams, C.J., Kaberdin, V.R., Grasby, J.A. and McDowall, K.J. (2003) Determination of the catalytic parameters of the N-terminal half of *Escherichia coli* ribonuclease E and the identification of critical functional groups in RNA substrates. *J. Biol. Chem.*, **278**, 44001-44008.
209. Jiang, X. and Belasco, J.G. (2004) Catalytic activation of multimeric RNase E and RNase G by 5'-monophosphorylated RNA. *Proc. Natl. Acad. Sci. USA*, **101**, 9211-9216.
210. Feng, Y., Vickers, T.A. and Cohen, S.N. (2002) The catalytic domain of RNase E shows inherent 3' to 5' directionality in cleavage site selection. *Proc. Natl. Acad. Sci. USA*, **99**, 14746-14751.
211. Jourdan, S.S. and McDowall, K.J. (2008) Sensing of 5' monophosphate by *Escherichia coli* RNase G can significantly enhance association with RNA and simulate the decay of functional mRNA transcripts *in vivo*. *Mol. Microbiol.*, **67**, 102-115.
212. Mudd, E.A. and Higgins, C.F. (1993) *Escherichia coli* endoribonuclease RNase E: autoregulation of expression and site-specific cleavage of mRNA. *Mol. Microbiol.*, **3**, 557-568.
213. Jain, C. and Belasco, J.G. (1995) RNase E autoregulates its synthesis by controlling the degradation rate of its own mRNA in *Escherichia coli*: unusual sensitivity of the *rne* transcript to RNase E activity. *Genes Dev.*, **9**, 84-96.
214. Diwa, A., Bricker, A.L., Jain, C. and Belasco, J.G. (2000) An evolutionarily conserved RNA stem-loop functions as a sensor that directs feedback regulation of RNase E gene expression. *Genes Dev.*, **14**, 1249-1260.

215. Jiang, X., Diwa, A. and Belasco, J.G. (2000) Regions of RNase E important for 5'-end-dependent RNA cleavage and autoregulated synthesis. *J. Bacteriol.*, **182**, 2468-2475.
216. Lee, K., Zhan, X., Gao, J., Feng, Y., Meganathan, R., Cohen, S.N. and Georgiou, G. (2003) RraA: a protein inhibitor of RNase E activity that globally modulates RNA abundance in *E. coli*. *Cell*, **114**, 623-634.
217. Gao, J.J., Lee, K., Zhao, M., Qiu, J., Zhan, X.M., Saxena, A., Moore, C.J., Cohen, S.N. and Georgiou, G. (2006) Differential modulation of *E. coli* mRNA abundance by inhibitory proteins that alter the composition of the degradosome. *Mol. Microbiol.*, **61**, 394-406.
218. Okada, Y., Wachi, M., Hirata, A., Suzuki, K., Nagai, K. and Matsushashi, M. (1994) Cytoplasmic axial filaments in *Escherichia coli* cells: possible function in the mechanism of chromosome segregation and cell division. *J. Bacteriol.*, **176**, 917-922.
219. Goldblum, K. and Apirion, D. (1981) Inactivation of the ribonucleic acid-processing enzyme ribonuclease E blocks cell division. *J. Bacteriol.*, **146**, 128-132.
220. Wang, M. and Cohen, S.N. (1994) *ard-1*: a human gene that reverses the effects of temperature-sensitive and deletion mutations in the *Escherichia coli rne* gene and encodes an activity producing RNase E-like cleavages. *Proc. Natl. Acad. Sci. USA*, **91**, 10591-10595.
221. Umitsuki, G., Wachi, M., Takada, A., Hikichi, T. and Nagai, K. (2001) Involvement of RNase G in *in vivo* mRNA metabolism in *Escherichia coli*. *Genes Cells*, **6**, 403-410.
222. Tock, M.R., Walsh, A.P., Carroll, G. and McDowall, K.J. (2000) The CafA protein required for the 5'-maturation of 16 S rRNA is a 5'- end-dependent ribonuclease that has context-dependent broad sequence specificity. *J. Biol. Chem.*, **275**, 8726-8732.
223. Wachi, M., Naoko, K., Umitsuki, G., Clarke, D.P. and Nagai, K. (2001) A novel RNase G mutant that is defective in degradation of *adhE* mRNA but proficient in the processing of 16S rRNA precursor. *Biochem. Biophys. Res. Comm.*, **289**, 1301-1306.

224. Kaga, N., Umitsuki, G., Nagai, K. and Wachi, M. (2002) RNase G-dependent degradation of the *eno* mRNA encoding a glycolysis enzyme enolase in *Escherichia coli*. *Biosci. Biotechnol. Biochem.*, **66**, 2216-2220.
225. Lee, K., Bernstein, J.A. and Cohen, S.N. (2002) RNase G complementation of *rne* null mutation identified functional interrelationships with RNase E in *Escherichia coli*. *Mol. Microbiol.*, **43**, 1445-1456.
226. Wachi, M., Doi, M., Ueda, T., Ueki, M., Tsuritani, K., Nagai, K. and Matsuhashi, M. (1991) Sequence of the downstream flanking region of the shape-determining genes *mreBCD* of *Escherichia coli*. *Gene*, **106**, 135-136.
227. Briant, D.J., Hankins, J.S., Cook, M.A. and Mackie, G.A. (2003) The quaternary Structure of RNase G from *Escherichia coli*. *Mol. Microbiol.*, **50**, 1381-1390.
228. Marcaida, M.J., DePristo, M.A., Chandran, V., Carpousis, A.J. and Luisi, B.F. (2006) The RNA degradosome: life in the fast lane of adaptive molecular evolution. *Trends Biochem. Sci.*, **31**, 359-365.
229. Wachi, M. and Nagai, K. (2001) *Escherichia coli* ribonuclease G. *Methods Enzymol.*, **342**, 55-63.
230. Bycroft, M., Hubbard, T.J.P., Proctor, M., Freund, S.M.V. and Murzin, A.G. (1997) The solution Structure of the S1 RNA binding domain: a member of an ancient nucleic acid-binding fold. *Cell*, **88**, 235-242.
231. Kaberdin, V.R. and Bizebard, T. (2005) Characterization of *Aquifex aeolicus* RNase E/G. *Biochem. Biophys. Res. Comm.*, **327**, 382-392.
232. Zeller, M.E., Csanadi, A., Miczak, A., Rose, T., Bizebard, T. and Kaberdin, V.R. (2007) Quaternary Structure and biochemical properties of mycobacterial RNase E/G. *Biochemical J.*, **403**, 207-215.
233. Callaghan, A.J., Grossman, J.G., Redko, Y.U., Ilag, L.L., Moncrieffe, M.C., Symmons,

- M.F., Robinson, C.V., McDowall, K.J. and Luisi, B.F. (2003) Quaternary Structure and catalytic activity of the *Escherichia coli* ribonuclease E amino-terminal catalytic domain. *Biochemistry*, **42**, 12848-13855.
234. Wachi, M., Umitsuki, G. and Nagai, K. (1997) Functional relationship between *Escherichia coli* RNase E and the CafA protein. *Mol. Gen. Genet.*, **253**, 515-519.
235. Ow, M.C., Perwez, T. and Kushner, S.R. (2003) RNase G of *Escherichia coli* exhibits only limited functional overlap with its essential homologue, RNase E. *Mol. Microbiol.*, **49**, 607-622.
236. Apirion, D. and Lassar, A.B. (1978) Conditional lethal mutant of *Escherichia coli* which affects processing of ribosomal RNA. *J. Biol. Chem.*, **253**, 1738-1742.
237. Masaaki, W., Genryou, U., Miwa, S., Ayako, T. and Kazuo, N. (1999) *Escherichia coli* *cafA* gene encodes a novel RNase, designated as RNase G, involved in processing of the 5' end of 16S rRNA. *Biochem. Biophys. Res. Comm.*, **259**, 483-488.
238. Deana, A. and Belasco, J.G. (2004) The function of RNase G in *Escherichia coli* is constrained by its amino and carboxyl termini. *Mol. Microbiol.*, **51**, 1205-1217.

Table 1.1. 3' to 5' exoribonucleases in *E. coli*.

Enzyme	Gene	Map position (min)	Subunit MW (kDa)	Catalytic mechanisms	Suggested Function(s)
RNase II	<i>rnb</i>	29	72.5	Hydrolytic cleavage, a processive exoribonuclease	mRNA degradation, stable RNA maturation
RNase D	<i>rnd</i>	40.6	42.7	Hydrolytic cleavage, a distributive exoribonuclease	Stable RNA maturation
RNase R	<i>rnr</i>	94.9	92.1	Hydrolytic cleavage, a processive exoribonuclease	Degradation of both mRNAs and defective stable RNAs
RNase T	<i>rnt</i>	37.2	23.5	Hydrolytic cleavage, a distributive exoribonuclease	Stable RNA maturation
Oligoribonuclease	<i>orn</i>	94.6	20.7	Hydrolytic cleavage, a processive exoribonuclease	Completion of mRNA and stable RNA degradation
PNPase	<i>pnp</i>	71.3	77.1	Phosphorolytic cleavage, a processive exoribonuclease	Degradation of both mRNAs and defective stable RNAs

RNase PH	<i>rph</i>	82.2	25.5	Phosphorolytic cleavage, a processive exoribonuclease	Stable RNA maturation
RNase BN*	<i>rbn</i> (<i>rnz</i>)	87.8	32.8	Hydrolytic cleavage, a distributive exoribonuclease	Stable RNA maturation

*RNase BN same as RNase Z (see the Table 1.2).

Table 1.2. Endoribonucleases in *E. coli* that are involved in either mRNA degradation or stable RNA maturation.

Enzyme	Gene	Map position (min)	Subunit MW (kDa)	Catalytic mechanisms	Suggested Function(s)
RNase E	<i>rne</i>	24.6	118.2	Activated by 5' monophosphate ssRNA specific endoribonuclease	mRNA degradation, stable RNA maturation
RNase G	<i>rng</i>	73.2	55.2	Activated by 5' monophosphate ssRNA specific endoribonuclease	mRNA degradation, stable RNA maturation
RNase I	<i>rna</i>	13.9	27.2	Active in the absence of divalent cation a nonspecific endoribonuclease	Degradation of both mRNAs and defective stable RNAs
RNase III	<i>rnc</i>	58.2	25.6	Recognizes specific stem-loop structures dsRNA specific endoribonuclease	mRNA degradation, stable RNA maturation
RNase LS	<i>rnlA/yfjN</i>	59.6	39.9	Hydrolytic endoribonuclease Preferentially cleaves RNA 3' to pyrimidines	Degradation of both mRNAs and defective stable RNAs
RNase P	<i>rnpA</i> ^a <i>rnpB</i> ^b	83.7 70.4	13.8 130	Hydrolytic endoribonuclease Mg ²⁺ ion dependent	mRNA degradation, stable RNA maturation

RNase Z ^c	<i>rnz/elaC</i>	51.3	32.8	Hydrolytic endoribonuclease Zn ²⁺ ion dependent	mRNA degradation, stable RNA maturation
----------------------	-----------------	------	------	---	--

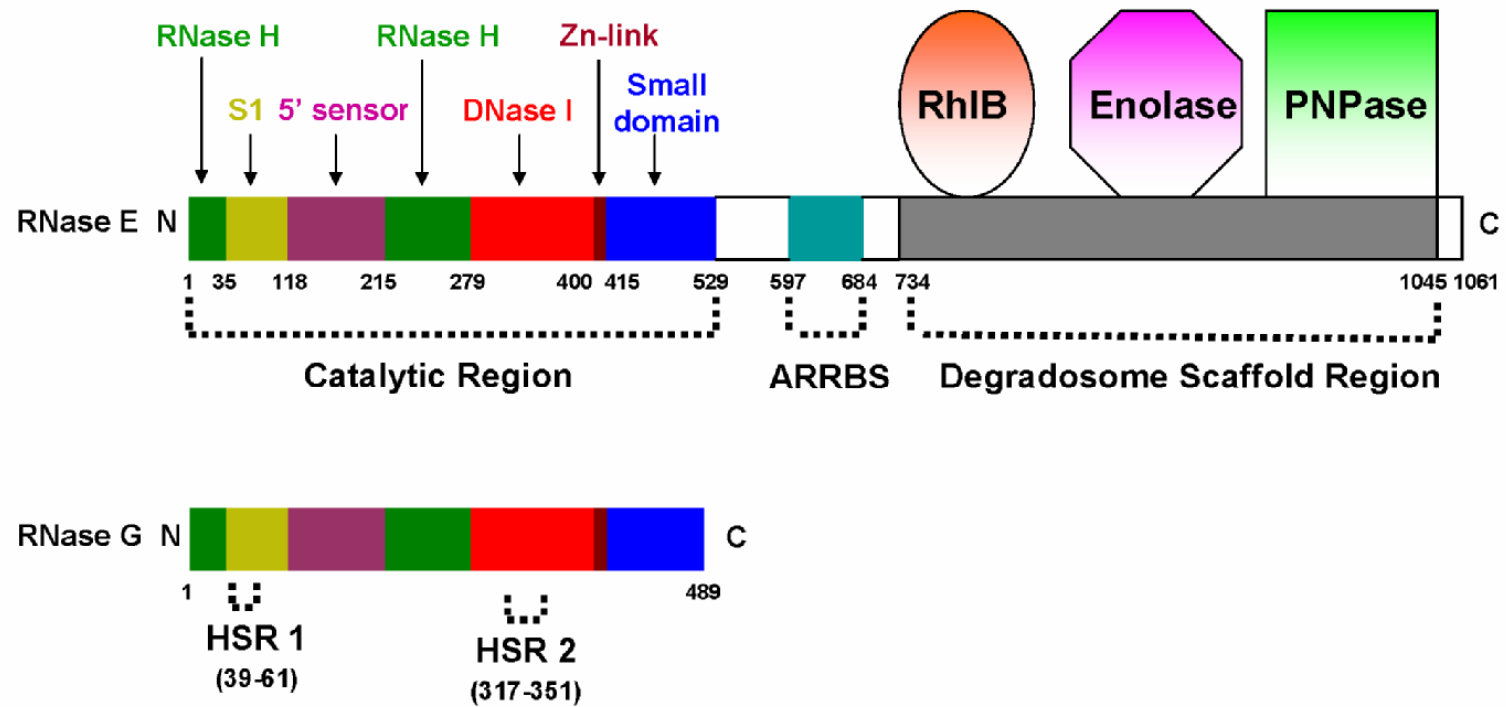
^a *rnpA* encodes for C5 protein subunit of RNase P.

^b *rnpB* encodes for M1 RNA subunit of RNase P. RNase P is unique in *E. coli* in that the RNA subunit contains the catalytic site.

^c RNase Z same as RNase BN (see the Table 1.1).

Figure 1.1. Comparison of the *E. coli* RNase E and RNase G proteins.

A schematic representation of 1061 amino acid long RNase E is presented showing the N-terminal catalytic region (amino acid 1 - 529), ARRBS (arginine-rich RNA binding site, amino acid 597 - 684), and the degradosome scaffolding region (amino acid 734 - 1045) including the 3' to 5' exoribonuclease PNPase (polynucleotide phosphorylase), the RNA helicase RhlB, and enolase binding regions. The six subdomains in the N-terminal catalytic region as identified by the crystallographic analysis (Callaghan *et. al.*, 2005) are color coded: S1 RNA binding domain, a 5' sensor region, an RNase H domain, a DNase 1 domain, a Zn²⁺ link, and a small domain. There is 34.1% of sequence identity between RNase G and RNase E over the first 488 aa of both proteins. The HSR 1 (amino acid 39 - 61) and HSR 2 (amino acid 317 - 351), regions are 59% and 73% identical, respectively, between the two proteins. Drawing is not to scale.



CHAPTER 2

Single amino acid changes in the predicted RNase H domain of *E. coli*

RNase G lead to complementation of RNase E deletion mutants¹

¹ Dae-hwan Chung, Zhao Min, Bi-Cheng Wang, and Sidney R. Kushner. Submitted to *Nucleic Acids*

ABSTRACT

The endoribonuclease RNase E of *Escherichia coli* is an essential enzyme that plays a major role in all aspects of RNA metabolism. In contrast, its homologue, RNase G, seems to have more limited functions. It is involved in the processing of the 5' terminus of 16S rRNA and the initiation of decay of a limited number of mRNAs, but is not required for cell viability, does not appear to participate in tRNA maturation, and cannot substitute for RNase E under normal physiological conditions. Using a combination of molecular genetics and computer modeling, we show that two different spontaneously occurring single amino acid substitutions (*rng-219* and *rng-248*) within the predicted RNase H domain of RNase G result in complementation of the growth defect associated with various RNase E mutants, suggesting that this region of the two proteins may help distinguish their *in vivo* biological activities. In addition, analysis of *rneΔ1018/rng-219* and *rneΔ1018/rng-248* double mutants has provided interesting insights into the distinct roles of RNase E and RNase G in mRNA decay and tRNA maturation.

INTRODUCTION

Endoribonuclease E (RNase E) of *Escherichia coli*, encoded by the *rne* gene, is essential for cell viability and plays a major role in mRNA decay (1,2), rRNA processing (3-5), tRNA maturation (6-8), and a variety of other aspects of RNA metabolism (9-11). In contrast, RNase G, a protein that is 34% identical to the amino terminal catalytic region of RNase E (amino acids 1-489) (12,13), is not required for cell viability, is present in low abundance, and under normal physiological conditions, cannot complement RNase E mutations (13-15).

While both enzymes employ a 5'-end-dependent mechanism for degrading RNA molecules (16,17), *in vivo* they appear to have significantly different substrate specificities. For example, RNase E is required for the processing of many tRNA precursors (7,8), but these

molecules are not effective substrates for RNase G (14,18). In addition, although both proteins are involved in generating the mature 5' terminus of the 16S rRNA *in vivo*, they cleave the precursor at distinct sites (4,5).

Based on these data, it was not surprising that increased expression (>4-fold, see below) of the native RNase G protein, achieved by changing the copy number of the *rng* locus, did not lead to complementation of RNase E mutants (13,14,18). However, higher level expression (174-1440-fold, see below) of an extended form of RNase G [containing either six additional chromosomally encoded amino acids at its amino terminus or six histidine at its carboxy terminus] either from its own mutationally altered promoter (18), a *lacZ* promoter (15,18) or a pBAD arabinose promoter (19) resulted in some growth in various *rne* mutants.

However, none of these experiments addressed what features distinguished the observed differences in the biological activities among the native RNase G, the extended form of RNase G, and RNase E. The solution of the X-ray crystallographic structure of the first 529 amino acids of RNase E (20) has provided a potential means to answer this question. In particular, Callaghan *et al.* (20) determined the presence of five distinct subregions (S1, 5' sensor, RNase H, DNase I, Zn-link) within the first 415 amino acids that presumably all play a role in the activity of RNase E (Fig. A1.1). In fact, it has been shown that only 415 N-terminal amino acids are sufficient for the essential biological function of RNase E, since the *rne* Δ 645 allele supports cell viability at both 30°C and 44°C (8). In addition, it has been demonstrated that the Zn-link motif helps promote the multimerization of the protein *in vitro* (21,22). Furthermore, the isolation of temperature-sensitive mutants with substitutions at amino acids 66 and 68 (*rne-1* and *rne-3071*) has implicated the importance of the S1 RNA binding domain for biological activity (3,23,24). It has also been argued that the DNase I subdomain appears to contain the catalytic site of the protein (20).

The computer generated model for RNase G presented here predicts that the protein has a three-dimensional structure that is remarkably similar to that of RNase E (Fig. A1.1). Even so, a >30-fold increase in the cellular levels of either the native or the extended form of RNase G or chimeric proteins (containing various combinations of the S1, 5' sensor, RNase H and DNase I subdomains from RNase E and RNase G) did not complement either the *rne-1* or *rneΔ1018* alleles. However, we describe spontaneously arising single amino acid substitutions (*rng-219* and *rng-248*) within the predicted RNase H domain of RNase G that lead to complementation of the growth defect associated with *rne* deletion and point mutations at physiologically relevant protein levels. Interestingly, an *rne* deletion mutant growing in the presence of either altered RNase G protein still exhibited dramatic defects in the decay of some mRNAs and the processing of tRNA precursors, while 9S rRNA maturation took place at almost wild-type levels. We also present a comparison in the same genetic background of the RNase G-expressing plasmids described in this study with those used by Lee *et al.* (15) and Deanna and Belasco (18).

RESULTS

Overexpression of either the wild-type (489 aa) or the extended form (495 aa) of RNase G does not complement *rne* mutants

We have previously shown that expression of the wild-type RNase G protein from its own promoter in a high-copy number plasmid (30-50 copies/cell) did not complement an *E. coli rne-1* mutant (14). Accordingly, for the experiments described here we replaced the *rng* regulatory region with the three promoters and ribosome binding site derived from RNase E (25) such that the *rng* locus would be transcribed at a level comparable to the *rne* gene. To ensure that only the native form of RNase G (489 aa) would be synthesized, the upstream GUG codon

was changed to CUG and a canonical ribosome binding site was inserted seven nt upstream of the AUG start codon (pDHK23, Fig. 2.1A). Additionally, in a second construct we changed the upstream GUG start codon to AUG to improve translation of the extended form of RNase G (495 aa; pDHK11, Fig. 2.1A), in order to try and reproduce the results of Lee *et al.* (15) and Deana and Belasco (18). Both plasmids led to at least an ~30-fold increase in the level of the RNase G protein (Fig. 2.1B, lanes 3 and 4 and Table 2.1). The protein produced by pDHK11 had a higher molecular weight, as expected (Fig. 2.1B, lane 3).

Subsequently, we transformed either pDHK11 or pDHK23 into an *rne-1 recA56* strain (SK6610). While both the transformants [SK3475 (*rne-1/pDHK11*) and SK3500 (*rne-1/pDHK23*)] grew at 30°C when streaked on a Luria agar plate (Fig. 2.2A), no growth was detected after 48 hr at 44°C (Fig. 2.2B). If a culture of the untransformed parent (SK6610) was plated at 44°C, we obtained approximately one temperature-resistant revertant for every 10⁸ cells (Table 2.2). These colonies grew when restreaked at 44°C and have subsequently been shown to contain intragenic second-site suppressor mutations (Perwez, *et al.*, submitted). In contrast, there was a ~200-fold increase in the frequency of temperature-resistant survivors in both the pDHK11 or pDHK23 transformants (Table 2.2). However, these isolates did not grow when restreaked at 44°C (Fig. 2.2). In addition, when plasmid DNA was obtained from eight independent colonies picked from the 44°C plates and retransformed into the *rne-1 recA56* strain (SK6610), the frequency of survivors at 44°C was identical to that shown in Table 2.2 (data not shown).

To confirm that neither pDHK11 (Km^r) nor pDHK23 (Km^r) could stably complement the loss of RNase E activity, we attempted to displace a plasmid carrying the wild-type *rne* gene [pSBK1 (*rne*⁺ Cm^r)] from an *rneΔ1018::bla* deletion strain [SK9714, (26)] with both of these plasmids. However, after growing Km^r transformants obtained with either pDHK11 or pDHK23 for over 200 generations in the absence of Cm selection, no Km^r Cm^s transformants were detected amongst the many thousands of colonies tested (data not shown).

Two independent single amino acid changes in RNase G lead to stable complementation of RNase E mutants

Since increased expression of either the native or extended form of RNase G failed to substitute for RNase E in the experiments described above, we designed a protocol to determine if we could isolate spontaneously arising RNase G mutants that could complement a complete *rne* deletion (*rneΔ1018*) (26). We took advantage of the fact that an *rneΔ610* truncation allele supports cell viability in the *rneΔ1018* genetic background at 37°C but not at 44°C (26). Thus, in an *rneΔ1018* strain carrying both the *rneΔ610* (Cm^r) and *rng*⁺ (Km^r) on separate plasmids with identical origins of DNA replication, Km^r Cm^s survivors at 44°C presumably would only contain a mutated *rng* gene.

Accordingly, we transformed a *rneΔ1018::bla/rneΔ610* Cm^r strain (SK9957) with pDHK23 (*rng*⁺ Km^r) (Fig. 2.1A) at 37°C. Km^r Cm^r transformants were subsequently grown for several hundred generations at 44°C in the presence of only Km. When 1000 individual colonies were tested, ~150 were Km^r and Cm^s (See Materials and Methods). However, unlike what we observed in the experiments described in Table 2.2, these temperature-resistant survivors grew when restreaked at 44°C (Fig. 2.2, pDHK28 and pDHK26). In addition, plasmid DNA isolated from six independent isolates displaced pSBK1 (*rne*⁺) from an *rneΔ1018* deletion strain (SK9714) and complemented the temperature-sensitive growth associated with the *rne-1* allele in SK6610 (*rne-1*), in contrast to what was observed with either pDHK11 or pDHK23 (Fig. 2.2A,B, and data not shown). Furthermore, western blot analysis showed no detectable RNase E protein in *rneΔ1018* strains carrying either pDHK26 (*rng*-248) or pDHK28 (*rng*-219) (data not shown).

We sequenced the entire *rng* insert, including the *rne* promoter region, from six independent plasmid isolates in order to determine what, if any, mutational changes had

occurred in pDHK23. In two of the plasmids (one of which was named pDHK28), a G → T transversion mutation in the *rng* coding sequence was observed in the first base-pair of the codon for aa 219, resulting in a Val to Phe substitution (*rng-219*). In the other four plasmids (one of which was named pDHK26), there was a G → A transition in the first base pair of the codon for amino acid 248, causing a Glu to Lys substitution (*rng-248*). In the RNase E protein, the amino acids at these two corresponding positions are Ala and Leu, respectively.

To confirm that the observed complementation resulted from these specific amino acid substitutions, we created pDHK32 (*rng-219*) and pDHK33 (*rng-248*) using site-directed mutagenesis. Both of these plasmids behaved identically to the original plasmids (pDHK26) and (pDHK28) (data not shown). Furthermore, pDHK32 (*rng-219*) and pDHK33 (*rng-248*) restored normal 16S rRNA processing in an *rng::cat* genetic background (data not shown).

Complementation of the growth defect associated with RNase E deficient strains is dependent on the intracellular level of the Rng-219 and Rng-248 proteins

Although we did not obtain complementation of *rne* mutants by overexpressing either the wild-type or extended form of RNase G (Table 2.2, Fig. 2.2), we wanted to find out if the growth observed in an *rneΔ1018* strain carrying either the *rng-219* or the *rng-248* alleles resulted simply from a further increase in the expression of the mutant proteins compared to what was obtained with the wild-type Rng protein from pDHK23 (*rng*⁺). Western blot analysis demonstrated that cells carrying pDHK23 (*rng*⁺), pDHK26 (*rng-248*) or pDHK28 (*rng-219*) produced comparable levels of RNase G protein (Fig. 2.1B, lanes 4 and 5 and Table 2.1).

We next compared the growth properties of strains carrying the *rng-219* or *rng-248* alleles on either 6-8 copy (pDHK26 and pDHK28) or single copy (pDHK29 and pDHK30) number plasmids (Table 2.3). As a control for these experiments, a strain with the *rneΔ645* allele was included because this truncated RNase E protein supports cell viability at 30°C, 37°C,

and 44°C (8). Although strains containing 6-8 copies of either the *rng-248* (SK3541) or *rng-219* (SK3543) mutations grew significantly slower at 37°C than strains carrying either the *rne*⁺, *rne-1* or the *rneΔ645* alleles, we were surprised that the generation times of the *rne*⁺, *rneΔ645*, *rng-219* and *rng-248* strains were similar at 44°C (Table 2.3).

When the *rng-219* and *rng-248* alleles were present on single-copy plasmids, Western blot analysis showed a 3.2-fold reduction in the amount of RNase G protein compared to 6-8 copies/cell (Table 2.1). Under these conditions the *rng-219* and *rng-248* alleles still supported cell viability in the *rneΔ1018* genetic background at 30°C and 37°C, but the mutants had significantly longer generation times compared to strains carrying the *rne*⁺, *rne-1*, and *rneΔ645* alleles (Table 2.3). In addition, the *rng-219* and *rng-248* mutants ceased growing after shift to 44°C (Table 2.3). In fact, the *rng-219* strain displayed a more rapid cessation of growth than the *rne-1* strain (Table 2.3). Analysis of cell viability showed reproducible differences between the *rneΔ1018/rne-1* and *rneΔ1018/rng-219* strains (Fig. 2.3). Cell viability of the *rneΔ1018/rne-1* strain remained largely unchanged after shift to 44°C followed by a gradual decrease after 60 min. In contrast, there was actually a 10-fold increase in cell viability in the *rneΔ1018/rng-219* strain for the first 120 min after the temperature shift (Fig. 2.3).

These data indicated that the complementation of the *rne* deletion was dependent on the cellular level of the mutant RNase G protein. To provide further support for this conclusion we used site-directed mutagenesis to introduce the *rng-219* and *rng-248* alleles into an *rng* gene carried on the 6-8 copy number plasmid pUGK24 (14) that contained its native promoter and ribosome binding site present in to generate pDHK34 and pDHK35, respectively. Based on Western blot analysis, we determined that there was an ~23-fold reduction in RNase G protein levels with these constructions compared to what was obtained with pDHK26 and pDHK28 (Table 2.1). Under these conditions, neither of these plasmids displaced pSBK1 (*rne*⁺) from SK9714 at either 30°C or 37°C or complemented an *rne-1* mutant at 44°C (data not shown).

pRNG3 and pRNG1200 yield more RNase G protein than either pDHK28 (*rng-219*) or pDHK26 (*rng-248*) but support poorer growth in the *rne-1* genetic background

The results described above differ from those of Lee *et al.* (15) and Deana and Belasco (18), who observed growth of RNase E mutants overexpressing of an extended form of RNase G that contained six extra amino acids at the amino terminus. Since their experiments were carried out in different genetic backgrounds, we obtained pRNG3, which expresses an amino terminal extended form of RNase G that also has six additional histidines at the carboxy terminus from a *lacZ* promoter in a plasmid with a pSC101 origin of DNA replication (15) and pRNG1200, which expresses an amino terminal extended form of RNase G from a modified RNase G promoter in a pUC plasmid, and transformed them into SK6610 (*rne-1 recA56*).

Individual purified transformants were patched onto a Luria agar master plate along with *rne-1* derivatives carrying pDHK11 (*rng* extended form), pDHK23 (*rng* wild-type), pDHK28 (*rng-219*), pDHK26 (*rng-248*), an untransformed *rne-1* strain and an isogenic wild type control (Fig. 2.4). Following overnight growth of the master plate at 30°C, replicas were made and grown at 44°C. As shown in Fig. 2.4B, after 24 hr there was no growth in the *rne-1* control or *rne-1* transformants carrying pDHK11 and pDHK23. Very spotty growth was observed with pRNG1200 and with pRNG3 in the presence of IPTG. In contrast, in strains carrying either *rng-219* (pDHK28) or *rng-248* (pDHK26) alleles uniform growth was obtained (Fig. 2.4). After 48 hours of growth at 44°C more growth was observed with pRNG3, but it was still spotty and much less than observed with either pDHK28 (*rng-219*) or pDHK26 (*rng-248*) (Fig. 2.4B). No further improvement in growth was observed with pRNG1200 after 48 hr (Fig. 2.4B).

In a separate experiment, liquid cultures of wild type, *rne-1*, *rne-1*/pRNG3, *rne-1*/pRNG1200 and *rne-1*/pDHK28 (*rng-219*) were grown to $\sim 10^8$ cells/ml at 30°C and then shifted to 44°C. After 24 hrs of shaking, viable cells/ml were determined by plating aliquots on Luria agar plates at 30°C. The number of viable cells in an *rne-1* strain carrying either pRNG3 or pRNG1200 was

19- and 21-fold lower, respectively, than the wild type control. In contrast, in the *rne-1*/pDHK28 strain there was only a 4-fold reduction. By comparison there was a 29-fold decrease in the *rne-1* strain that did not carry any plasmid (data not shown).

Western blot analysis of RNase G protein levels of various strains showed that the *rne-1*/pDHK11, *rne-1*/pDHK23, and *rne-1*/pDHK28 strains had comparable levels of RNase G protein (Fig. 2.1B). In contrast, the total protein samples from *rne-1*/pRNG3 (in the presence of 100 μ M IPTG) and the *rne-1*/pRNG1200 strains had to be reduced 2- and 20-fold, respectively, in order to avoid the overloading the gel (Fig. 2.1B). Taken together, the data in Fig. 2.1B and Table 2.1 indicate that there was a 174- and 1440-fold increase in the amount of RNase G protein in the pRNG3 and pRNG1200 strains, respectively.

Both amino acid changes are located within the predicted RNase H domain of RNase G

The solution of the crystal structure of the catalytic region of RNase E (20) identified five distinguishable subdomains within the catalytic portion of the protein (5' sensor, S1 RNA binding region, RNase H and DNase I domains and a Zn-link). Based on the overall 34.1% sequence identity between RNase G and RNase E proteins within the catalytic region, we used the program Geno 3D (<http://geno3d-pbil-ibcp.fr>), an online homology modeling program (27) to obtain a predicted 3-D structure for RNase G (Fig. A1.1B). This analysis showed that RNase G can be folded, with a high degree of certainty, into the same five distinctive subdomains as RNase E (Fig. A1.1A). Of the five subdomains, the predicted catalytic site contained within the DNase I domain was the most structurally conserved region (45.5% sequence identity), while the RNase H region showed the most divergence (26.6% sequence identity) (Fig. A1.1A and A1.1B). Interestingly, both the *rng-219* and *rng-248* mutations occurred in the predicted RNase H domain. Detailed analysis of the mutationally altered RNase H domains showed very subtle

changes in the side groups extending from two distinct α -helices associated with the RNase H domain in the two RNase G mutants (Fig. A2.2A, A2.2B).

Domain swaps between RNase E and RNase G generate proteins that are not biologically active

Based on the high degree of predicted structural similarity between RNase E and RNase G (Fig. A1.1), we hypothesized that a domain swapping approach, as successfully used with poly(A) polymerase and tRNA nucleotidyltransferase (28), might help distinguish important features of these two homologues. To test this idea directly, we made three chimeric constructs: amino acids 213-281 of the RNase H domain in RNase G were replaced with the same region derived from RNase E; amino acids 1-280 of RNase G were replaced by the S1 binding region, 5' sensor region and the complete RNase H domain from RNase E; and, amino acids 280-489 of RNase G were replaced with the DNase I domain and Zn link from RNase E (amino acids 280-418).

While all three chimeric proteins were expressed at levels comparable to those observed with pDHK26 and pDHK28 (data not shown), none of them could complement either the *rne-1* or *rne Δ 1018* alleles, neither did these proteins improve the maturation of 5S rRNA, or convert the 16.3 S rRNA precursor into its mature 16S form (data not shown). In fact, 5S rRNA processing actually decreased in strains carrying the chimeric plasmids compared to *rne-1* and *rne-1* carrying the native RNase G protein controls (data not shown).

The Rng-219 and Rng-248 proteins effectively restore 9S rRNA processing at 44°C

RNase E was initially discovered based on its role in the processing of the 9S rRNA precursor into the mature 5S rRNA (3). Subsequent analysis of this reaction showed that while

rne-1 mutants are quite defective in 9S rRNA processing (26), truncated RNase E proteins cleaved this substrate quite efficiently (26,29). Furthermore, it has been observed that increased levels of wild-type RNase G partially restored 9S rRNA processing in an *rne-1* mutant at 44°C (14). However, the ability of the Rng-219 and Rng-248 proteins to support cell viability in an *rneΔ1018* strain provided an opportunity to examine 9S rRNA processing in the complete absence of RNase E.

Initially, we measured 9S rRNA processing in strains carrying the various *rne* and *rng* alleles in 6-8 copies/cell. We observed that 9S rRNA processing was less efficient in the *rng* mutants at 30°C compared to wild-type, *rne-1* and *rneΔ645* strains, but reproducibly improved at 44°C (Fig. A1.3A). In particular, at 30°C the processed fractions (PF, defined as the fraction of mature 5S rRNA relative all of 5S rRNA containing species) of 5S rRNA were nearly identical in the wild-type, *rne-1* and *rneΔ645* strains (Fig. A1.3A, lanes 1-3) in agreement with previous results (8). However, the PF was reduced to ~0.70 in the *rng* mutants (Fig. A1.3A, lanes 4, 5). Upon shift to 44°C, the PF in the *rne-1* strain decreased to 0.48 (Fig. A1.3A, lane 7), while the PF for the *rng-248* and *rng-219* alleles actually increased to 0.82 and 0.84 (Fig. A1.3A, lanes 9, 10), respectively.

When the same experiment was performed with strains carrying either the *rng-219* or *rng-248* alleles in single copy, 9S rRNA processing in the two *rng* mutants was comparable at both 30°C and 44°C (Fig. A1.3B, lanes, 14, 15, 19, 20), even though the cells ceased growing at the elevated temperature. Interestingly, the PFs of the two *rng* mutants were more than 2-fold higher than what was observed with the *rne-1* strain at 44°C (Fig. A1.3B, lanes 17, 19, 20). In all cases, the pattern of processing intermediates obtained in the *rne-1*, *rng-219* and *rng-248* strains was nearly identical (Fig. A1.3A, A1.3B) and generally agreed with the results of Lee *et al.* (15).

The absence of RNase E differentially affects the initiation of decay of specific mRNAs

Although experiments using various *rne* alleles (*i.e.*, *rne-1*, *rne131*, *rneΔ610* and *rneΔ645*) from different laboratories have shown that the endonucleolytic decay of specific mRNAs is initiated by RNase E (26,30-32), recent work has suggested that both RNase G and RNase Z can also participate in the decay of certain transcripts (14,15,33-36). The *rneΔ1018/rng-219* and *rneΔ1018/rng-248* strains provided a means to test if the initiation of endonucleolytic decay of specific mRNAs was completely dependent on the presence of RNase E. For our analysis, we determined the half-lives of four mRNAs previously demonstrated to decay in an RNase E-dependent fashion (*rpsO*, *rpsT*, *cspA* and *cspE*) (30,36,37). In agreement with previously published results (14,26), the half-lives of all four transcripts increased significantly in the *rneΔ1018/rne-1* strain when the allele was present in 6-8 copies/cell (Table 2.4). In addition, with the exception of *cspE*, the half-lives increased further when the *rne-1* allele was in single copy (Table 2.4).

Strikingly different results were obtained for the four mRNAs in strains carrying the *rng-219* and *rng-248* alleles in 6-8 copies/cell. The half-lives of both *rpsO* transcripts were dramatically longer compared to the *rne-1* strain (11.6- and 3.0-fold increases in the half-lives of the P1-RIII and P1-t1 species, respectively, in the *rng* mutants versus the *rne-1* strain, Table 2.4). Furthermore, when the mutant alleles were present in single copy, the half-lives of both species increased even further (Table 2.4, Fig. 2.5A), indicating that RNase E was primarily responsible for initiating the endonucleolytic decay of this transcript. Similarly, the half-life of the *cspA* mRNA increased significantly in the *rng-219* and *rng-248* mutants compared to *rne-1* (Table 2.4) suggesting that its decay was also highly dependent on RNase E, in agreement with the recent report of Hankins *et al.* (38). Interestingly, in the *rneΔ1018/rng-219* and *rneΔ1018/rng-248* mutants numerous decay intermediates of *cspA* were present that were not observed in the

rneΔ610/rne-1 strain (Fig. 2.5C). It should be noted that the half-life of the *cspA* mRNA obtained here in wild-type *E. coli* (1-2 min, Table 2.4) was significantly longer than has been reported previously (38,39).

In contrast with what was observed with *rpsO* and *cspA*, the *rpsT* and *cspE* mRNAs had comparable half-lives in the *rne-1*, *rng-219* and *rng-248* strains when the alleles were present in either single copy/cell or 6-8 copies/cell (Table 2.4). In fact, the half-life of *rpsT* in the *rneΔ1018/rng-219* and *rneΔ1018/rng-248* strains was 2.6 and 2.7 min, respectively, when the alleles were present in either 6-8 copies/cell. Since an 8.9 min half-life was observed in an *rne-1 rng::cat* double mutant (14), it would appear that either mutant RNase G protein was able to substitute for RNase E in the initiation of the decay of this mRNA. This idea was supported by the presence of major new *rpsT* decay intermediates in the *rng-219* and *rng-248* strains that were not present in either wild-type or *rne-1* strains (Fig. 2.5B). Interestingly, even when the *rng-219* and *rng-248* alleles were present in single copy, the *rpsT* half-life (between 6-7 min, Table 2.4) was still shorter than that observed in the *rne-1 rng::cat* double mutant.

The maturation of tRNA^{Cys}, tRNA^{His}, and tRNA^{Pro} is completely dependent on RNase E

RNase E is critical for the maturation of many tRNA precursors in *E. coli* (6-8). In fact, it was proposed that the essential function of RNase E involves its role in the initiation of tRNA maturation (7,8), although Deana and Belasco (18) have challenged this hypothesis. However, all the published experiments examining the role of RNase E in tRNA maturation up to now have been carried out using strains that either contained some RNase E activity (*rneΔ610*, *rneΔ645* or *rne* under the control of a *lac* promoter) or have residual activity even at the nonpermissive temperature (*rne-1* and *rne-3071*) (40). Thus, the *rneΔ1018/rng-219* and *rneΔ1018/rng-248* mutants permitted the examination of tRNA maturation in the complete absence of RNase E activity.

We compared the processing of four tRNA species (tRNA^{His}, tRNA^{Pro}, tRNA^{Cys} and tRNA^{Asn}) that have been studied extensively (7,8,14,18) in wild-type, *rne-1*, and *rng* strains. As an additional control we included the *rneΔ645* allele, since the truncated RNase E protein it encodes has been shown to support cell viability at both 30°C and 44°C (8). tRNA^{His}, tRNA^{Cys} and tRNA^{Pro} were chosen because their maturation is highly dependent on RNase E (7,8). In contrast, tRNA^{Asn} was included because each of its four precursors appeared to be processed relatively efficiently in *rne-1* mutants (8).

tRNA maturation was first tested with *rne*⁺, *rne-1*, *rneΔ645*, *rng-219* and *rng-248* alleles present on a single-copy plasmid in a *rneΔ1018* deletion strain (Fig. 2.6A-D). The efficiency of tRNA maturation was quantified by determining the processed fraction (PF) of mature tRNA relative to its total transcript level in each strain. Interestingly, at 30°C, a condition where all the strains were viable, the PF values of all four tRNA species were 2-10-fold lower in the *rng-219* and *rng-248* mutants than in the *rne*⁺, *rneΔ645*, and *rne-1* strains (Fig. 2.6A-D). Furthermore, the processing of tRNA^{His}, tRNA^{Cys} and tRNA^{Pro}, as expected, was more dramatically affected than that of tRNA^{Asn}. For example, the PF of tRNA^{His} (0.05) decreased over 10-fold in the *rng-219* and *rng-248* strains at 30°C (Fig. 2.6A) compared to only an ~2-fold reduction for tRNA^{Asn} (Fig. 2.6C).

In experiments carried out after a two-hour shift to 44°C, the PF values of all four tRNAs decreased significantly in the *rne-1* strain compared to the wild-type and *rneΔ645* controls (Fig. 2.6A-D). In contrast, the PF values for all four tRNA species actually increased 1.3-2.1-fold in the *rng-219* and *rng-248* strains compared to what was observed at 30°C but were still less than or equal to those obtained with the *rne-1* allele (Fig. 2.6A-D).

When the experiments were repeated with each allele present in 6-8 copies/cell, the efficiency of tRNA maturation in the *rne-1*, *rng-219* and *rng-248* strains improved 1.2-2.0 fold for all four tRNA species at 30°C and 44°C compared to what was observed when the alleles were

present in single copy (Figs. 2.6 and Fig. A1.4). However, in all cases except for tRNA^{Pro}, the PF values in the *rng-219* and *rng-248* strains at 44°C were significantly less than in the *rne-1* strain (compare .56 for tRNA^{Cys} in the *rne-1* strain to 0.20 in either *rng* mutant, Appendix 1, Fig. A1.4D), even though under these conditions the *rng-219* and *rng-248* strains were viable, while the *rne-1* mutant was not.

There was a direct correlation between generation time (Table 2.3) and the efficiency of tRNA maturation (Figs. 2.6A-D; A1.4A-D). For example, the growth rate of the *rneΔ645* strain at 44°C did not differ significantly from the wild-type control (37 vs. 29 mins, Table 2.3) and the PFs of the four tRNAs were comparable (Fig. 2.6A-D). In contrast, at 30°C the generation times of the *rng-219* and *rng-248* strains increased from 57 min to 140 min along with a 2-10-fold drop in the processed fractions of the four tRNAs tested (Fig. 2.6A-D).

DISCUSSION

The results reported here demonstrate that even when RNase G levels were increased ~30-fold (Fig. 2.1B, Table 2.1) by employing pDHK23, the native protein did not complement the loss of RNase E activity (Fig. 2.2). Furthermore, in contrast to previous reports (15,18), the presence of six extra amino acids at the amino terminus, a situation that does not occur *in vivo* (41), did not improve the ability of RNase G to substitute for RNase E under our experimental conditions (Figs. 2.2, 2.4).

Furthermore, the data Figs. 2.1B, 2.4 and Table 2.1 provide insights into the differences between the results reported here and the experiments of Lee *et. al.* (15) and Deana and Belasco (18). First, both pRNG3 (15) and pRNG1200 (18) lead to the synthesis of between 5-43-fold more RNase G protein, respectively, than was observed with pDHK28 (Fig. 2.1B, Table 2.1), resulting in intracellular levels of RNase G that are 5-43-fold higher than normal physiological levels of RNase E (Table 2.1). Yet even under these conditions, the extended

form of RNase G only weakly supported cell growth of an *rne-1* strain at 44°C compared to the Rng-219 and Rng-248 proteins (Fig. 2.4). In contrast, when the extended form of RNase G was expressed at levels comparable to either Rng-219 or Rng-248, no growth at 44°C was observed (Fig. 2.4).

Since the sequences of the pRNG3 and pRNG1200 plasmids did not reveal any *rng* mutations (data now shown), it appears that the weak cell growth observed with pRNG3 and pRNG1200 at 44°C (Fig. 2.4) arose primarily from the very high levels of RNase G. In addition, since the survivors obtained with pRNG1200 did not grow when restreaked at 44°C, it seems that the very high a level of RNase G present in these cells may actually be toxic at this temperature, a result also previously observed with artificially increased levels of RNase E (42,43). Furthermore, the ability of the extended form of RNase G to yield survivors compared to the native protein in the experiments of Deana and Belasco (18) could arise from a slight modification of the protein's catalytic activity associated with the extra six amino acids that reduces its toxicity at 37°C but not at 44°C. In contrast, the complementation of the *rneΔ1018* and *rne-1* alleles observed with the *rng-219* and *rng-248* encoded RNase G occurs over a range of mutant protein concentrations that is less than or equal to the normal physiological level of RNase E (Table 2.1), suggesting a possible gain of function for the two altered RNase G proteins.

While it was quite surprising that subtle changes in the predicted RNase H domain of RNase G, a region with the least apparent 3-dimensional similarity to RNase E (Figs. A1.1, A1.2), led to proteins that complemented the absence of RNase E, this result indicates that at least some of the biological differences between the two enzymes are governed by this domain. In fact, these mutants indicate a significant role for the RNase H subdomain in the activity of both proteins. Whether the RNase H domain is critical for initial binding of various RNA molecules or is involved in promoting phosphodiester bond cleavages remains to be determined.

Although the experiments reported here do not provide a definitive explanation for the differences in the catalytic activities of RNase E and RNase G, the ability of the altered Rng proteins to support cell viability at physiological relevant levels in an *rne* deletion strain has provided an opportunity to critically examine the role of RNase E in mRNA decay and tRNA maturation. Since the half-lives of both major *rpsO* transcripts increased dramatically in the complete absence of RNase E (Table 2.4) and no decay intermediates were observed (Fig. 2.5A), it would appear that the *rpsO* mRNAs are not substrates for RNase Z, RNase LS (44), RNase G, and the altered forms of RNase G. Although there might be some concern that the Rng-219 and Rng-248 proteins could have a dominant negative phenotype, as has been observed with certain RNase E mutants (45), the ability of both mutant proteins to support cell viability in an *rneΔ1018 rng::cat* double mutant (data not shown) suggests that this is not the case.

It is also noteworthy that the half-life of the *cspA* mRNA increased significantly in the absence of RNase E (Table 2.4). However, the presence of a number of minor decay intermediates (Fig. 2.6C) suggested that the altered RNase G proteins can very inefficiently cleave this mRNA. The results with both the *rpsO* and *cspA* mRNAs also indicate that the Rne-1 protein retains a significant amount of residual activity at the nonpermissive temperature, a conclusion also supported by Mohanty and Kushner (46).

In contrast, the half-lives of the two major *rpsT* transcripts (*rpsT_{P1}* and *rpsT_{P2}*) did not change significantly among the *rneΔ1018/rne-1*, *rneΔ1018/rng-219* and *rneΔ1018/rng-248* strains under any condition tested (Table 2.4), supporting previous results that other ribonucleases such as RNase G and RNase Z can initiate the decay of these transcripts (14,36). Furthermore, the change in the decay pattern of the *rpsT* transcripts in the *rneΔ1018/rng-219* and *rneΔ1019/rng-248* strains (Fig. 2.5B) demonstrated that the altered RNase G proteins probably cleaved the transcripts at locations different from those recognized by RNase E, and

that the resulting decay intermediates required either RNase E or a functional degradosome for their further degradation. The *cspE* mRNA also appeared to be susceptible to decay by other ribonucleases in the absence of RNase E (Table 2.4). Thus, it appears that some mRNAs (*rpsO* and *cspA*) are much more dependent on RNase E for their decay than others (*rpsT* and *cspE*) (Table 2.4).

The data on tRNA maturation were of equal interest. While RNase E is required for tRNA maturation (7,8), it processes some tRNA precursors more efficiently than others (8). The results presented in Figs. 2.6 and A1.4 confirm that for some tRNAs (notably tRNA^{His}, tRNA^{Pro}, and tRNA^{Cys}) maturation of the polycistronic transcripts containing these species appears to be absolutely dependent on RNase E under normal physiological conditions. For example, when the *mg-219* and *mg-248* alleles were present on single copy plasmids, the PFs of these three tRNAs at 30°C were 0.05-0.12 (Fig. 2.6). When the level of the mutant RNase G proteins was increased ~3.2-fold (Table 2.1), the processed fractions increased to between 0.10-0.18 at the same temperature (Fig. A1.4). These data indicate that the small amount of these three tRNAs arising in the RNase E deletion mutant were a direct result of inefficient processing by the Rng-219 and Rng-248 proteins. Thus, it appears that RNase E is absolutely required to process the polycistronic operons that contain tRNA^{His}, tRNA^{Cys}, and tRNA^{Pro}. Whether the loss of cell viability in the absence of RNase E is the direct result of this defect in tRNA maturation still remains to be determined.

MATERIALS AND METHODS

Bacterial strains

The *E. coli* K-12 strains used in this study were all derived from MG1693 (*rph-1 thyA715*) (2) and are listed in Table 2.5. Strains SK3475, SK3500, SK3538, SK3546, SK3541, SK3543,

SK3563, SK3564, SK5065, and SK5067, were constructed either by standard plasmid transformation protocols or plasmid displacement as previously described (25,26).

Isolation of the *rng-219* and *rng-248* alleles

SK9957 [*rneΔ1018::bla thyA715 rph-1 recA56 srlD300::Tn10 Tc^r/pMOK15 (rneΔ610 Cm^r)*] (26) was transformed with pDHK23 (*rng⁺*, Km^r) and Km^r transformants were selected at 37°C. Individual transformants were grown overnight at 37°C with shaking in Luria broth containing thymine (50 µg/ml) and kanamycin (25 µg/ml). The cultures were then diluted into fresh Luria broth containing thymine and kanamycin and grown at 44°C for several hundred cell divisions. Since both pMOK15 and pDHK23 contained the same pSC101 origin of DNA replication, and the RneΔ610 protein encoded by *rneΔ610* cannot support cell viability at 44°C (26), it was expected that any Cm^s Km^r survivors would contain an altered form of RNase G that could complement the *rneΔ1018* allele. Approximately 150 Km^r Cm^s colonies were identified after replica plating of 1000 individual survivors. Plasmid DNA isolated from six independent survivors displaced pSBK1 (*rne⁺* Cm^r) from SK9714 (*rneΔ1018::bla thyA715 rph-1 recA56 srl-300::Tn10 Tc^r/pSBK1 [rne⁺ Cm^r]*) (26). Accordingly, the 2.2 kb insert in each of the six plasmids was sequenced on both strands using an automated sequencer (Applied Biosystems 3730xl DNA analyzer).

Growth and viability studies

Overnight standing cultures of various strains in Luria broth supplemented with thymine (50 µg/ml) and kanamycin (25 µg/ml), chloramphenicol (20 µg/ml) or spectinomycin (20 µg/ml), where appropriate, were diluted 1:1000 into prewarmed fresh medium and shaken at 30°C or 37°C. Cultures were monitored with a Klett-Summerson Colorimeter (no. 42 green filter). For

the 44°C growth curves, cultures were initially grown with shaking at 37°C until they reached 40 Klett units above background and then were shifted to 44°C. For determination of cell viability, aliquots were removed at the times indicated and plated on Luria agar medium at 30°C. Colonies were counted after 48 hrs of growth.

Oligonucleotide primers

The sequences of the various oligonucleotides used in these experiments are provided in Appendix 1, Table A1.2.

Plasmid constructions

Details of all the plasmid constructions are provided in the Appendix 1.

Site-directed mutagenesis

Experimental details are provided in the Appendix 1.

Western analysis

Western blot analysis of RNase E, RNase G and the RNase E/G chimeric proteins was performed as described by Ow *et al.* (25,26). Protein concentrations were determined by the Bio-Rad protein assay with bovine serum albumin as the standard. Protein samples (10 µg for RNase E and 2-100 µg for RNase G) were electrophoresed in an 8% SDS–polyacrylamide gels and electrotransferred to PVDF membranes (Immobilon™-P; Millipore) using a Bio-Rad Mini-Protean 3 electrophoretic apparatus. The membranes were then probed with either RNase E (1:2000 dilution) or RNase G (1:10000 dilution) antibodies using the ECL Plus™ Western Blotting Detection Kit (GE Healthcare) as specified by the manufacturer. The RNase G antibody

was kindly provided by G. Mackie (41) and was pre-incubated with a one mg of protein extract from RNase G-deficient *E. coli* cells [SK2538 *rng::cat*, (14)] prior to use. The RNase E MAP antibody was raised against the first 20 amino acids of RNase E (26). Protein bands were quantified using a Storm 840™ PhosphorImager (GE Healthcare) equipped with ImageQuant v.5.2 software (Molecular Dynamics).

Northern analysis

Total RNA extraction and mRNA Northern blot analysis were done according to the procedures described by O'Hara *et al.* (47) and Burnett (48). The steady-state RNAs used for the 5S rRNA and tRNA Northern blots were obtained from exponential cultures grown either at 30°C or after shift to 44°C for 120 min. Northern analysis of tRNAs and 5S rRNA (5 µg/lane) were done as described by Ow *et al.* (25,26). Probes for the 5S rRNA (PB5SRNA)(49) and tRNAs (*hisR*, *cysT*, *proM*, *asn*) were oligonucleotides (8) complementary to the mature species and were end-labeled with ³²P using T4 polynucleotide kinase. For quantification, the RNA samples were run on a 1.25% agarose gel and probed for 16S rRNA using the ³²P-5'- end-labeled primer 16S1586 (26). mRNA half-lives were calculated using least squares linear regression analysis.

Computer modeling of RNase G structure

The protein sequence of RNase G was compared against the PDB database by PSI-BLAST (50). Three PDB entries, 2bx2, 2c4r, and 2c0b, were selected as homologous templates for the next step of molecular modeling. All three sequences were derived from the catalytic domain of *E. coli* RNase E. The sequence identity between RNase G and the catalytic domain of RNase E was 34.1%. To generate the model shown in Fig. A1.1, the inter/intra restraints ratio was set to 0.9. The margins in the distance restraints and angle restraints were

0.5 Å and 1.0 Å, respectively. The maximum number of distance restraints was 20,000. Three models were generated using Geno3D (<http://geno3d-pbil.ibcp.fr>), an online homology modeling tool (27). The model with the lowest energy is presented in Fig. A1.1. In this model, 0.9% of the residues occupied disallowed regions of the Ramachandran plot. The root mean square deviation (RMSD) between this model and the RNase E templates range 1.48-1.66 Å. The model of RNase G and the three dimensional structure of RNase E were analyzed and viewed with PyMol. (<http://pymol.sourceforge.net/>).

ACKNOWLEDGEMENTS

The authors wish to thank J. Shivas for excellent technical assistance and B. Mohanty and T. Perwez for reading the manuscript. pRNG3 and pRNG120 were graciously provided by Dr. S. Cohen and Dr. J. G. Belasco, respectively. This work was supported in part by a grant (GM57220) from the National Institute of General Medical Sciences to S.R.K.

REFERENCES

1. Kuwano, M., Ono, M., Endo, H., Hori, K., Nakamura, K., Hirota, Y. and Ohnishi, Y. (1977) Gene affecting longevity of messenger RNA: a mutant of *Escherichia coli* with altered mRNA stability. *Mol. Gen. Genet.*, **154**, 279-285.
2. Arraiano, C.M., Yancey, S.D. and Kushner, S.R. (1988) Stabilization of discrete mRNA breakdown products in *ams pnp rnb* multiple mutants of *Escherichia coli* K-12. *J. Bacteriol.*, **170**, 4625-4633.
3. Apirion, D. and Lasser, A.B. (1978) A conditional lethal mutant of *Escherichia coli* which affects the processing of ribosomal RNA. *J. Biol. Chem.*, **253**, 1738-1742.

4. Li, Z., Pandit, S. and Deutscher, M.P. (1999) RNase G (CafA protein) and RNase E are both required for the 5' maturation of 16S ribosomal RNA. *EMBO J.*, **18**, 2878-2885.
5. Wachi, M., Umitsuki, G., Shimizu, M., Takada, A. and Nagai, K. (1999) *Escherichia coli* *cafA* gene encodes a novel RNase, designated as RNase G, involved in processing of the 5' end of 16S rRNA. *Biochem. Biophys. Res. Comm.*, **259**, 483-488.
6. Ray, B.K. and Apirion, D. (1981) Transfer RNA precursors are accumulated in *Escherichia coli* in the absence of RNase E. *Eur. J. Biochem.*, **114**, 517-524.
7. Li, Z. and Deutscher, M.P. (2002) RNase E plays an essential role in the maturation of *Escherichia coli* tRNA precursors. *RNA*, **8**, 97-109.
8. Ow, M.C. and Kushner, S.R. (2002) Initiation of tRNA maturation by RNase E is essential for cell viability in *Escherichia coli*. *Genes Dev.*, **16**, 1102-1115.
9. Lundberg, U. and Altman, S. (1995) Processing of the precursor to the catalytic RNA subunit of RNase P from *Escherichia coli*. *RNA*, **1**, 327-334.
10. Lin-Chao, S., Wei, C.-L. and Lin, Y.-T. (1999) RNase E is required for the maturation of *ssrA* and normal *ssrA* RNA peptide-tagging activity. *Proc. Natl. Acad. Sci. USA*, **96**, 13406-12411.
11. Masse, R., Escorcia, F.E. and Gottesman, S. (2003) Coupled degradation of a small regulatory RNA and its mRNA targets in *Escherichia coli*. *Genes Dev.*, **17**, 2374-2383.
12. Okada, Y., Wachi, M., Hirata, A., Suzuki, K., Nagai, K. and Matsushashi, M. (1994) Cytoplasmic axial filaments in *Escherichia coli* cells: possible function in the mechanism of chromosome segregation and cell division. *J. Bacteriol.*, **176**, 917-922.
13. Wachi, M., Umitsuki, G. and Nagai, K. (1997) Functional relationship between *Escherichia coli* RNase E and the CafA protein. *Mol. Gen. Genet.*, **253**, 515-519.

14. Ow, M.C., Perwez, T. and Kushner, S.R. (2003) RNase G of *Escherichia coli* exhibits only limited functional overlap with its essential homologue, RNase E. *Mol. Microbiol.*, **49**, 607-622.
15. Lee, K., Bernstein, J.A. and Cohen, S.N. (2002) RNase G complementation of *rne* null mutation identified functional interrelationships with RNase E in *Escherichia coli*. *Mol. Microbiol.*, **43**, 1445-1456.
16. Mackie, G.A. (1998) Ribonuclease E is a 5'-end-dependent endonuclease. *Nature*, **395**, 720-723.
17. Tock, M.R., Walsh, A.P., Carroll, G. and McDowall, K.J. (2000) The CafA protein required for the 5'-maturation of 16 S rRNA is a 5'- end-dependent ribonuclease that has context-dependent broad sequence specificity. *J. Biol. Chem.*, **275**, 8726-8732.
18. Deana, A. and Belasco, J.G. (2004) The function of RNase G in *Escherichia coli* is constrained by its amino and carboxyl termini. *Mol. Microbiol.*, **51**, 1205-1217.
19. Tamura, M., Lee, K., Miller, C.A., Moore, C.J., Shirako, Y., Kobayashi, M. and Cohen, S.N. (2006) RNase E maintenance of proper FtsZ/FtsA ratio required for nonfilamentous growth of *Escherichia coli* cells but not for colony-forming ability. *J. Bacteriol.*, **188**, 5145-5152.
20. Callaghan, A.J., Marcaida, M.J., Stead, J.A., McDowall, K.J., Scott, W.G. and Luisi, B.F. (2005) Structure of *Escherichia coli* RNase E catalytic domain and implications for RNA turnover. *Nature*, **437**, 1187-1191.
21. Callaghan, A.J., Redko, Y.U., Murphy, L.M., Grossman, J.G., Yates, D., Garman, E., Ilag, L.L., Robinson, C.V., Symmons, M.F., McDowall, K.J. *et al.* (2005) "Zn-Link": a metal sharing interface that organizes the quaternary Structure and catalytic site of endoribonuclease, RNase E. *Biochemistry*, **44**, 4667-4775.

22. Jiang, X. and Belasco, J.G. (2004) Catalytic activation of multimeric RNase E and RNase G by 5'-monophosphorylated RNA. *Proc. Natl. Acad. Sci. USA*, **101**, 9211-9216.
23. McDowall, K.J., Hernandez, R.G., Lin-Chao, S. and Cohen, S.N. (1993) The *ams-1* and *rne-3071* temperature-sensitive mutations in the *ams* gene are in close proximity to each other and cause substitutions within a domain that resembles a product of the *Escherichia coli rne* locus. *J. Bacteriol.*, **175**, 4245-4249.
24. Ono, M. and Kuwano, M. (1979) A conditional lethal mutation in an *Escherichia coli* strain with a longer chemical lifetime of mRNA. *J. Mol. Biol.*, **129**, 343-357.
25. Ow, M.C., Liu, Q., Mohanty, B.K., Andrew, M.E., Maples, V.F. and Kushner, S.R. (2002) RNase E levels in *Escherichia coli* are controlled by a complex regulatory system that involves transcription of the *rne* gene from three promoters. *Mol. Microbiol.*, **43**, 159-171.
26. Ow, M.C., Liu, Q. and Kushner, S.R. (2000) Analysis of mRNA decay and rRNA processing in *Escherichia coli* in the absence of RNase E-based degradosome assembly. *Mol. Microbiol.*, **38**, 854-866.
27. Combet, C., Jambon, M., Deleage, G. and Geourjan, C. (2002) Geno3D: Automatic comparative molecular modelling of protein. *Bioinformatics*, **18**, 213-214.
28. Betat, H., Rammelt, C., Martin, G. and Mori, M. (2004) Exchange of regions between bacterial poly(A) polymerase and the CCA-adding enzyme generates altered specificities. *Mol. Cell*, **15**, 389-398.
29. Lopez, P.J., Marchand, I., Joyce, S.A. and Dreyfus, M. (1999) The C-terminal half of RNase E, which organizes the *Escherichia coli* degradosome, participates in mRNA degradation but not rRNA processing *in vivo*. *Mol. Microbiol.*, **33**, 188-199.
30. Mackie, G.A. (1991) Specific endonucleolytic cleavage of the mRNA for ribosomal protein S20 of *Escherichia coli* requires the products of the *ams* gene *in vivo* and *in vitro*. *J. Bacteriol.*, **173**, 2488-2497.

31. Hajnsdorf, E. and Regnier, P. (1999) *E. coli rpsO* mRNA decay: RNase E processing at the beginning of the coding sequence stimulates poly(A)-dependent degradation of the mRNA. *J. Mol. Biol.*, **286**, 1033-1043.
32. Celesnik, H., Deana, A. and Belasco, J.G. (2007) Initiation of RNA decay in *Escherichia coli* by 5' pyrophosphate removal. *Mol. Cell*, **27**, 79-90.
33. Kaga, N., Umitsuki, G., Nagai, K. and Wachi, M. (2002) RNase G-dependent degradation of the *eno* mRNA encoding a glycolysis enzyme enolase in *Escherichia coli*. *Biosci. Biotechnol. Biochem.*, **66**, 2216-2220.
34. Wachi, M., Naoko, K., Umitsuki, G., Clarke, D.P. and Nagai, K. (2001) A novel RNase G mutant that is defective in degradation of *adhE* mRNA but proficient in the processing of 16S rRNA precursor. *Biochem. Biophys. Res. Comm.*, **289**, 1301-1306.
35. Umitsuki, G., Wachi, M., Takada, A., Hikichi, T. and Nagai, K. (2001) Involvement of RNase G in *in vivo* mRNA metabolism in *Escherichia coli*. *Genes Cells*, **6**, 403-410.
36. Perwez, T. and Kushner, S.R. (2006) RNase Z in *Escherichia coli* plays a significant role in mRNA decay. *Mol. Microbiol.*, **60**, 723-737.
37. Hajnsdorf, E., Steier, O., Coscoy, L., Teyssset, L. and Régnier, P. (1994) Roles of RNase E, RNase II and PNPase in the degradation of the *rpsO* transcripts of *Escherichia coli*: stabilizing function of RNase II and evidence for efficient degradation in an *ams pnp rnb* mutant. *EMBO J.*, **13**, 3368-3377.
38. Hankins, J.S., Zappavigna, C., Prud'homme-Genereux, A. and Mackie, G.A. (2007) Role of RNA Structure and susceptibility to RNase E in regulation of a cold shock mRNA, *cspA* mRNA. *J. Bacteriol.*, **189**, 4353-5358.
39. Goldenberg, D., Azar, I. and Oppenheim, A.B. (1996) Differential mRNA stability of the *cspA* gene in the cold-shock response of *Escherichia coli*. *Mol. Microbiol.*, **19**, 241-248.

40. Mohanty, B.K. and Kushner, S.R. (2008) Rho-independent transcription terminators inhibit RNase P processing of the *secG leuU* and *metT* tRNA polycistronic transcripts in *Escherichia coli*. *Nucleic Acids Res.*, **36**, 364-375.
41. Briant, D.J., Hankins, J.S., Cook, M.A. and Mackie, G.A. (2003) The quaternary structure of RNase G from *Escherichia coli*. *Mol. Microbiol.*, **50**, 1381-1390.
42. Claverie-Martin, F., Diaz-Torres, M.R., Yancey, S.D. and Kushner, S.R. (1991) Analysis of the altered mRNA stability (*ams*) gene from *Escherichia coli*: nucleotide sequence, transcription analysis, and homology of its product to MRP3, a mitochondrial ribosomal protein from *Neurospora crassa*. *J. Biol. Chem.*, **266**, 2843-2851.
43. Jain, C. and Belasco, J.G. (1995) RNase E autoregulates its synthesis by controlling the degradation rate of its own mRNA in *Escherichia coli*: unusual sensitivity of the *rne* transcript to RNase E activity. *Genes Dev.*, **9**, 84-96.
44. Otsuka, Y. and Yonesaki, T. (2005) A novel endoribonuclease, RNase LS, in *Escherichia coli*. *Genetics*, **169**, 13-20.
45. Briegel, K.J., Baker, A. and Jain, C. (2006) Identification and analysis of *Escherichia coli* ribonuclease E dominant-negative mutants. *Genetics*, **172**, 7-15.
46. Mohanty, B.K. and Kushner, S.R. (2007) Ribonuclease P processes polycistronic tRNA transcripts in *Escherichia coli* independent of ribonuclease E. *Nucleic Acids Res.*, **35**, 7614-7625.
47. O'Hara, E.B., Chekanova, J.A., Ingle, C.A., Kushner, Z.R., Peters, E. and Kushner, S.R. (1995) Polyadenylation helps regulate mRNA decay in *Escherichia coli*. *Proc. Natl. Acad. Sci. USA*, **92**, 1807-1811.
48. Burnett, W.V. (1997) Northern blotting of RNA denatured in glyoxal without buffer recirculation. *Biotechniques*, **22**, 668-671.

49. Babitzke, P., Granger, L. and Kushner, S.R. (1993) Analysis of mRNA decay and rRNA processing in *Escherichia coli* multiple mutants carrying a deletion in RNase III. *J. Bacteriol.*, **175**, 229-239.
50. Altschul, S.F., Madden, T.L., Schaffer, A.A., Zhang, J., Zhang, Z., Miller, W. and Lipman, D.J. (1997) Gapped BLAST and PSI-BLAST: a new generation of protein database search programs. *Nucleic Acids Res.*, **25**, 3389-3402.
51. Hajsndorf, E., Braun, F., Haugel-Nielsen, J., Le Derout, J. and Régnier, P. (1996) Multiple degradation pathways of the *rpsO* mRNA of *Escherichia coli*. RNase E interacts with the 5' and 3' extremities of the primary transcript. *Biochimie*, **78**, 416-424.
52. Claverie-Martin, F., Diaz-Torres, M.R., Yancey, S.D. and Kushner, S.R. (1989) Cloning of the altered mRNA stability (*ams*) gene of *Escherichia coli* K-12. *J. Bacteriol.*, **171**, 5479-5486.
53. Wang, R.F. and Kushner, S.R. (1991) Construction of versatile low-copy-number vectors for cloning, sequencing and expression in *Escherichia coli*. *Gene*, **100**, 195-199.
54. Deana, A., Ehrlich, R. and Reiss, C. (1996) Synonymous codon selection controls in vivo turnover and amount of mRNA in *Escherichia coli* *bla* and *ompA* genes. *J. Bacteriol.*, **178**, 2718-2720.

Table 2.1. Relative intracellular levels of RNase G.

Genotype	Composition of RNase G	Copies of <i>rng</i> /cell	Relative Amount ¹	Ratio of RNase G/RNase E ²
<i>rng</i> ⁺	Wild type	1	1	0.03 ²
<i>rne</i> ⁺ /pUGK24 (<i>rng</i> ⁺) ³	Wild type	6-8	1.6	0.05
<i>rne</i> ⁺ /pUGK31 (<i>rng</i> ⁺) ³	Wild type	30-50	4.2	0.13
<i>rne</i> ⁺ /pDHK11 (<i>rng</i> ⁺) ⁴	5' extended form	6-8	31.8	0.95
<i>rne</i> ⁺ /pDHK23 (<i>rng</i> ⁺) ⁵	Wild type	6-8	33.5	1.0
<i>rne</i> ⁺ /pDHK26 (<i>rng</i> -248) ⁵	Rng-248	6-8	36.9	1.1
<i>rne</i> ⁺ /pDHK28 (<i>rng</i> -219) ⁵	Rng-219	6-8	36.5	1.1
<i>rne</i> ⁺ /pDHK29 (<i>rng</i> -248) ⁶	Rng-248	1-2	12	0.36
<i>rne</i> ⁺ /pDHK30 (<i>rng</i> -219) ⁶	Rng-219	1-2	11.9	0.36
<i>rne</i> -1/pRNG3 (<i>rng</i> - <i>his</i> ₆) ⁷	5' extended form with six histidines at carboxy terminus	6-8	174	5.2
<i>rne</i> -1/pRNG1200 (<i>rng</i> ⁺) ⁸	5' extended form	>100	1440	43

¹The amount of RNase G detected in MG1693 by Western blotting (Materials and Methods) was set at 1. In order to visualize the protein in wild type cells it was necessary to load 100 μ g of protein. As a control 100 μ g of an extract of SK2538 (*rng::cat*) was run on the same gel.

²The ratio of RNase G protein to RNase E protein *in vivo* is based on the data of Lee *et al.* (15). They estimated that RNase G was less than 4% of the amount of RNase E. However, for the calculations presented here we used a more conservative estimate of 3%.

³pUGK24 is a pSC101 derivative encoding wild type *rng* with its own promoter and ribosome binding site. pUGK31 is a ColE1 derivative carrying wild type *rng* with its own promoter and ribosome binding site. Both plasmids have been described elsewhere (14).

⁴pDHK11 is a pSC101 derivative encoding the 5' extended form of *rng* that is transcribed from the three promoters of *rne* (See Materials and Methods).

⁵pDHK23, pDHK26 and pDHK28 carry *rng* loci that do not encode the extra six amino acids at the amino terminus. Their isolation and construction are described in Materials and Methods.

⁶pDHK29 and pDHK30 encode the *rng* inserts derived from pDHK26 and pDHK28 cloned into the single copy vector pMOK40 (8).

⁷pRNG3 encodes the 5' extended form of RNase G as well as six histidine residues at the carboxy terminus (15) and is transcribed from an inducible *lacZ* promoter (100 μ M IPTG).

⁸pRNG1200 encodes both the 5' extended form and native form of RNase G (see Fig. 2.1B, lane 7) transcribed from a mutated *rng* promoter cloned into a pUC high copy number plasmid (18) In fact, both the extended form and native form of RNase G are synthesized from this construct (Fig. 2.1B, lane 7).

Table 2.2. Frequency of apparent temperature-resistant revertants in the *rne-1* genetic background.

Strain	Genotype	Temperature-resistant revertants/ 10^8 cells ^a
SK6610	<i>rne-1 recA56</i>	0.8 ± 1.2^b
SK3475	<i>rne-1 recA56/pDHK11 (rng[*])</i>	212 ± 39^c
SK3500	<i>rne-1 recA56/ pDHK23 (rng⁺)</i>	247 ± 24^c

rng^{}*, RNase G with six extra amino acids at the amino terminus; *rng⁺*, native form of RNase G.

^aAverage of at least four independent determinations.

^bRevertants obtained from SK6610 represent intragenic second-site suppressor mutations within the *rne* coding sequence (Perwez, *et al.*, submitted).

^cRevertants obtained from SK3475 and SK3500 did not grow when restreaked at 44°C.

Table 2.3. Generation times of strains carrying the *rng-219* and *rng-248* alleles.

Strain	Genotype	Generation Time (min) ^a		
		30°C	37°C	44°C
Alleles present in 6-8 copies				
SK9714	<i>rneΔ1018/rne⁺</i>	ND ^b	35.2 ± 0.3	29.0 ± 3.0
SK9937	<i>rneΔ1018/rne-1</i>	ND ^b	36.0 ± 0.7	ts ^c
SK9987	<i>rneΔ1018/rneΔ645</i>	ND ^b	48.0 ± 2.1	33.7 ± 2.0
SK3543	<i>rneΔ1018/rng-219</i>	ND ^b	66.0 ± 5.0	35.8 ± 0.3
SK3541	<i>rneΔ1018 rng-248</i>	ND ^b	68.7 ± 0.4	34.6 ± 0.3
Alleles present in single copy				
SK10143	<i>rneΔ1018/rne⁺</i>	57.2 ± 0.8	34.5 ± 0.3	29.4 ± 1.0
SK10144	<i>rneΔ1018/rne-1</i>	57.0 ± 1.6	36.4 ± 0.6	ts ^c
SK2685	<i>rneΔ1018/rneΔ645</i>	70.0 ± 2.7	43.5 ± 0.8	37.3 ± 0.2
SK3564	<i>rneΔ1018 rng-219</i>	140 ± 2.0	100 ± 2.0	ts ^d
SK3563	<i>rneΔ1018/rng-248</i>	140 ± 10.0	92 ± 2.0	ts ^c

^aRepresents an average of three independent growth curves.

^bND, not determined.

^cts, temperature sensitive. Growth stopped by 150 min after shift to 44°C.

^dts, temperature sensitive. Growth stopped by 120 min after shift to 44°C.

Table 2.4. Half-lives of mRNAs in various strains^a.

Transcript	Half-life (min) ^b			
	<i>rne</i> ⁺	<i>rne-1</i>	<i>rng-248</i>	<i>rng-219</i>
Alleles present in 6-8 copies/cell				
<i>rpsO</i> _{P1-RIII}	0.9 ± 0.1	1.2 ± 0.1	13.9 ± 0.5	13.7 ± 3.0
<i>rpsO</i> _{P1-t1}	1.4 ± 0.2	5.5 ± 0.5	16.8 ± 2.0	16.8 ± 2.0
<i>rpsT</i> _{P1}	1.5 ± 0.2	4.6 ± 0.6	2.6 ± 0.3	2.7 ± 0.1
<i>rpsT</i> _{P2}	1.8 ± 0.1	2.5 ± 0.6	2.4 ± 0.2	2.4 ± 0.1
<i>cspA</i>	1.1 ± 0.1	2.0 ± 0.2	3.8 ± 0.6	4.3 ± 0.3
<i>cspE</i>	1.1 ± 0.1	13.1 ± 0.1	10.3 ± 2.4	9.8 ± 0.6
Alleles present in single copy/cell				
<i>rpsO</i> _{P1-RIII}	1.2 ± 0.2	2.0 ± 0.3	17.2 ± 2.0	21.2 ± 3.8
<i>rpsO</i> _{P1-t1}	2.6 ± 0.2	10.0 ± 2.0	>30	>30
<i>rpsT</i> _{P1}	1.6 ± 0.2	7.6 ± 0.9	7.0 ± 1.0	6.6 ± 0.9
<i>rpsT</i> _{P2}	1.9 ± 0.4	5.6 ± 0.4	5.6 ± 0.4	6.2 ± 0.9
<i>cspA</i>	2.2 ± 0.2	4.6 ± 0.5	9.6 ± 1.5	11.4 ± 0.6
<i>cspE</i>	2.4 ± 0.2	10.4 ± 1.2	14.5 ± 2.5	13.2 ± 1.2

All mRNA half-lives were measured immediately after shift to 44°C as described in Materials and Methods. Each strain carries an *rneΔ1018* allele on the chromosome. The *rpsO*_{P1-RIII} and *rpsO*_{P1-t1} transcripts are those described by Hajnsdorf *et al.*(51). The *rpsT*_{P1} and *rpsT*_{P2} represent transcripts from the gene's two promoters (30).

^aIn all of these strains, the chromosomal copy of the *rne* gene has been deleted (*rne* Δ 1018) and the alleles indicated are present on either a 6-8 copy number plasmid or a single copy plasmid.

^bRepresents the average of at least four independent determinations.

Table 2.5. Bacterial strains and plasmids DNA used in this study.

Strain	Genotype	Source of reference
MG1693	<i>rph-1 thyA715</i>	<i>E. coli</i> Genetic Stock Center
SK2538	<i>rng::cat rph-1 thyA715 Cm^r</i>	(14)
SK2685	<i>rneΔ1018::bla thyA715 rph-1 recA56¹ pDHK6 (rneΔ645 Sm^r/Sp^r)/pWSK129 (Km^r)</i>	(8)
SK3475	<i>rne-1 rph-1 thyA715 recA56¹/pDHK11²(rng⁺ Km^r)</i>	This study
SK3500	<i>rne-1 rph-1 thyA715 recA56¹/pDHK23(rng⁺ Km^r)</i>	This study
SK3538	<i>rne-1 rph-1 thyA715 recA56¹/pDHK26(rng-248/Km^r)</i>	This study
SK3540	<i>rne-1 rph-1 thyA715 recA56¹/pDHK28(rng-219/Km^r)</i>	This study
SK3541	<i>rneΔ1018::bla thyA715 rph-1 recA56¹/pDHK26 (rng-248 Km^r)</i>	This study
SK3543	<i>rneΔ1018::bla thyA715 rph-1 recA56¹/pDHK28 (rng-219 Km^r)</i>	This study
SK3548	<i>rneΔ1018::bla thyA715 rph-1 recA56¹/pUGK24 (rng⁺/Km^r)</i>	(14)
SK3549	<i>rneΔ1018::bla thyA715 rph-1 recA56¹/pUGK31 (rng⁺/Km^r)</i>	(14)
SK3563	<i>rneΔ1018::bla thyA715 rph-1 recA56¹/pDHK29 (rng-248 Sm^r/Sp^r)/pWSK129 (Km^r)</i>	This study

SK3564	<i>rneΔ1018::bla thyA715 rph-1 recA56¹/pDHK30 (rng-219 Sm^r/Sp^r)/pWSK129 (Km^r)</i>	This study
SK5065	<i>rne-1 rph-1 thyA715 recA56¹/pRNG3 (placZrng⁺ Ap^r)³</i>	This study
SK5067	<i>rne-1 rph-1 thyA715 recA56¹/pRNG1200 (rng⁺ Km^r)⁴</i>	This study
SK6610	<i>rne-1 rph-1 thyA715 recA56¹</i>	(52)
SK9714	<i>rneΔ1018::bla thyA715 rph-1 recA56¹/pSBK1(rne⁺ Cm^r)</i>	(26)
SK9937	<i>rneΔ1018::bla thyA715 rph-1 recA56¹/pMOK13 (rne-1 Cm^r)</i>	(26)
SK9957	<i>rneΔ1018::bla thyA715 rph-1 recA56¹/pMOK15 (rneΔ610 Cm^r)</i>	(26)
SK9987	<i>rneΔ1018::bla thyA715 rph-1 recA56¹/pMOK29 (rneΔ645 Sm^r/Sp^r)</i>	(8)
SK10143	<i>rneΔ1018::bla thyA715 rph-1 recA56¹/pMOK44 (rne⁺ Sm^r/Sp^r)/pWSK129 (Km^r)</i>	(8)
SK10144	<i>rneΔ1018::bla thyA715 rph-1 recA56¹/pMOK45 (rne-1 Sm^r/Sp^R)/pWSK129 (Km^r)</i>	(8)

Plasmids

pDHK6	Single-copy plasmid with <i>rneΔ645</i> Sm ^r /Sp ^r	(8)
pDHK11	6 – 8 copy plasmid with <i>rng⁺</i> [along with 6 additional amino acids (MRKGIN) at 5' –end and the regulatory region and ribosome binding site of <i>rng</i> have been	This study

replaced with those derived from *rne*] Km^r (Fig. 2.1)

pDHK23	6 – 8 copy plasmid with <i>rng</i> ⁺ (<i>rng</i> -native form with the regulatory region and ribosome binding site of <i>rng</i> has been replaced with those from <i>rne</i> and a canonical ribosome binding site) Km ^r (Fig. 2.1)	This study
pDHK26	6 – 8 copy plasmid with <i>rng-248</i> Km ^r	This study
pDHK28	6 – 8 copy plasmid with <i>rng-219</i> Km ^r	This study
pDHK29	Single-copy plasmid with <i>rng-248</i> Sm ^r /Sp ^r	This study
pDHK30	Single-copy plasmid with <i>rng-219</i> Sm ^r /Sp ^r	This study
pDHK32	6 – 8 copy plasmid with <i>rng-219</i> Km ^r (derived by PCR site-directed mutagenesis)	This study
pDHK33	6 – 8 copy plasmid with <i>rng-248</i> Km ^r (derived by PCR site-directed mutagenesis)	This study
pDHK34	6 – 8 copy plasmid with <i>rng-219</i> Km ^r (contains <i>rng</i> regulatory sequences)	This study
pDHK35	6 – 8 copy plasmid with <i>rng-248</i> Km ^r (contains <i>rng</i> regulatory sequences)	This study
pDHK38	6 – 8 copy plasmid with <i>rne-rng</i> Chimera 1 (amino acids 213-281 of RNase G were replaced with those from RNase E) Km ^r	This study
pDHK39	6 – 8 copy plasmid with <i>rne-rng</i> Chimera 2 (amino acids from 1-280 of RNase G	This study

were replaced with those from RNase E) Km^r

pDHK40	6 – 8 copy plasmid with <i>rne-rng</i> Chimera 3 (amino acids 280-489 of RNase G were replaced with amino acids 280-418 from RNase E) Km ^r	This study
pMOK13	6 – 8 copy plasmid with <i>rne-1</i> Cm ^r	(26)
pMOK15	6 – 8 copy plasmid with <i>rneΔ610</i> Cm ^r	(26)
pMOK21	6 – 8 copy plasmid with <i>rneΔ645</i> Sm ^r /Sp ^r	(8)
pMOK40	Single copy plasmid with Sm ^r /Sp ^r	(8)
pMOK44	Single copy plasmid with <i>rne</i> ⁺ Sm ^r /Sp ^r	(8)
pMOK45	Single copy plasmid with <i>rne-1</i> Sm ^r /Sp ^r	(8)
pRNG3	6-8 copy plasmid with extended form of <i>rng</i> ⁺ and six histidines at the carboxy terminus under the control of the <i>lacZ</i> promoter Ap ^r	(15)
pRNG1200	High copy number pUC plasmid with extended form of <i>rng</i> ⁺ with a modified <i>rng</i> promoter Km ^r	(18)2
pSBK1	6 – 8 copy plasmid with <i>rne</i> ⁺ Cm ^r	(26)
pUGK24	6 – 8 copy plasmid with <i>rng</i> ⁺ Km ^r	(14)

pUGK31	30-50 copy plasmid with <i>rng</i> ⁺ Km ^r	(14)
pWSK129	6 – 8 copy plasmid with Km ^r	(53)

¹All strains containing the *recA56* allele also carry the *srID300::Tn10* Tc^r insertion mutation.

²pDHK11 encodes an RNase G protein with six additional amino acids at its amino terminus.

³Plasmid pRNG3 carries *rng*⁺ [along with 6 additional amino acids (MRKGIN) at 5' –end and 6 histidines at the 3' end] under the control of the *lacZ* promoter (15).

⁴Plasmid pRNG1200 carries *rng*⁺ [along with 6 additional amino acids (MRKGIN) at 5' –end] under the control of a modified *rng* promoter (54).

Figure 2.1. (A) Diagrammatic representation of the *rng* constructs in pDHK11 and pDHK23. The chromosomal *rng* sequence is shown at the top. The native translation start, identified by sequencing of the protein purified from *E. coli* (41) is shown as +1. The translation start site employed by Lee *et al.* (15) and Deana and Belasco (18) is indicated as -18. The upstream regulatory region of RNase E (shown to the left in blue), including its three promoters, as identified by Ow *et al.* (25), was used to express *rng* in both pDHK11 and pDHK23. In pDHK11, the GTG translation start codon was changed to ATG and the RNase E ribosome binding site was inserted to increase translation efficiency. In pDHK23, the upstream GTG codon was changed to CTG to block potential translation initiation and a canonical ribosome binding site (underlined) was inserted seven nt upstream of the RNase G native translation start codon (ATG). Altered nucleotides are shown in bold. Rightward black arrows indicate translation start codons for the two constructs. Rightward blue arrows indicate the transcription start sites associated with the three RNase E promoters. (B) Western blot analysis of RNase G in various strains using either 40 (lanes 1-5), 20 (lane 6) or 2 μ g of total cell protein. Lane 1, MG1693; Lane 2, SK6610; Lane 3, SK3475; Lane 4, SK3500; Lane 5, SK3540; Lane 6, SK5065; and Lane 7, SK5067. The Relative Quantities (RQ) of RNase G are reported in Table 2.1. pDHK11 and pRNG1200 encode an RNase G protein the contains an extra six amino acids at the amino terminus (Fig. 2.1A). Based on the construction of pRNG1200 (18) both the native and extended form of the protein will be synthesized (lane 7). pRNG3 encodes the extended form of RNase G along with six histidine residues at the carboxy terminus (15).

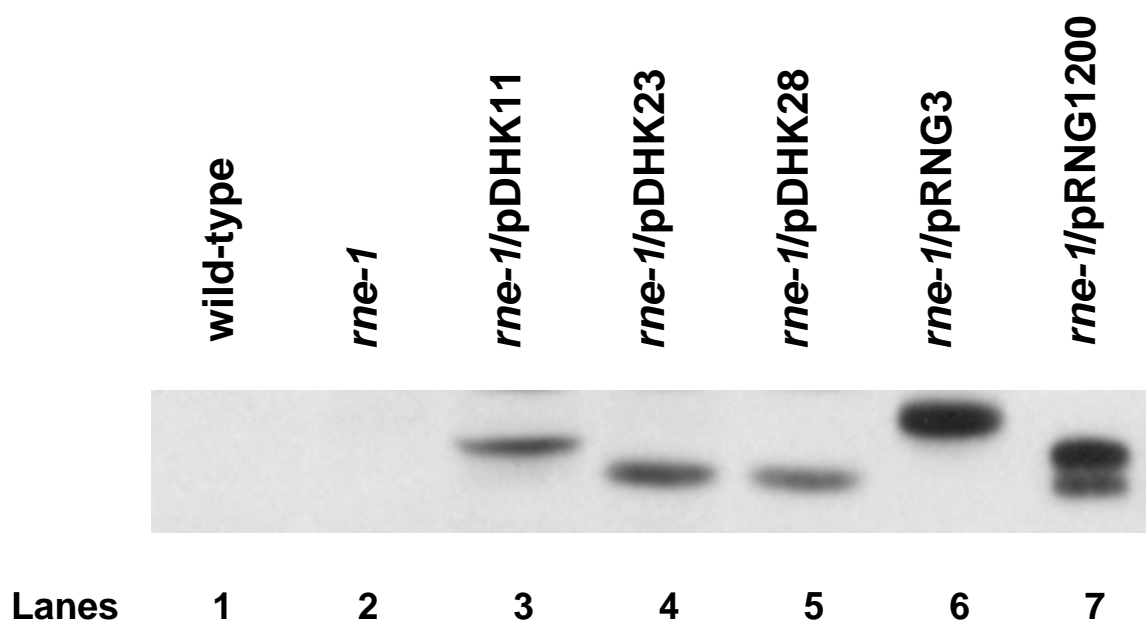
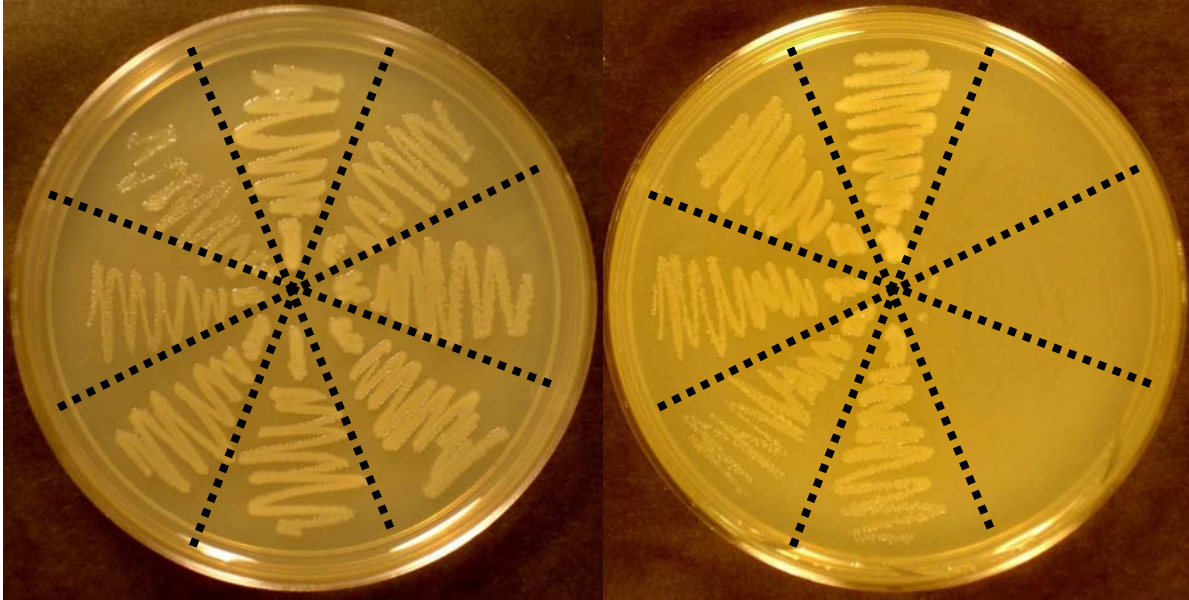
(B)

Figure 2.2. Growth properties of strains carrying wild-type and mutant forms of RNase G. All the strains were freshly streaked on L agar plates containing 50 µg/ml thymine and incubated for 72 hrs at 30°C (A) or for 48 hrs at 44°C (B). The genotypes of the strains are depicted in (C). The strain designations are as follows: *rne*⁺ (MG1693); *rne-1* (SK6610); *rne-1/pDHK23 rng*⁺ (SK3500); *rne-1/pDHK11 rng*⁺ (SK3475, contains six extra amino acids at the N-terminus of RNase G); *rne-1/rne-219* (SK3540); *rne-1/rng-248* (SK3538); *rneΔ1018/rng-219* (SK3543); and *rneΔ1018/rng-248* (SK3541).

(A) 30°C

(B) 44°C



(C)

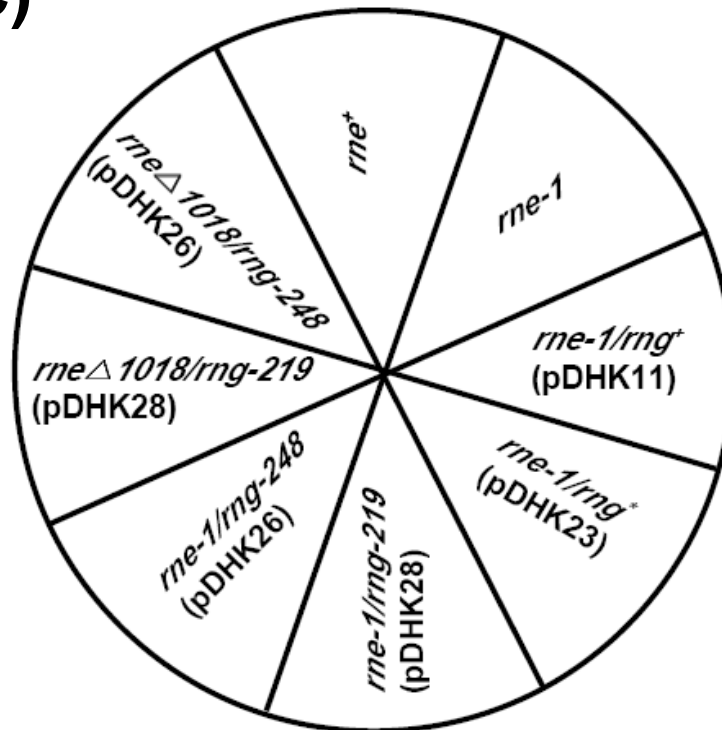


Figure 2.3. Measurement of cell viability in strains carrying single copies of the *rne*⁺ (□, SK10143), *rne-1* (◇, SK10144), and *rng-219* (○, SK3564) alleles in an *rneΔ1018* deletion background. Cell viability was determined as described in Materials and Methods.

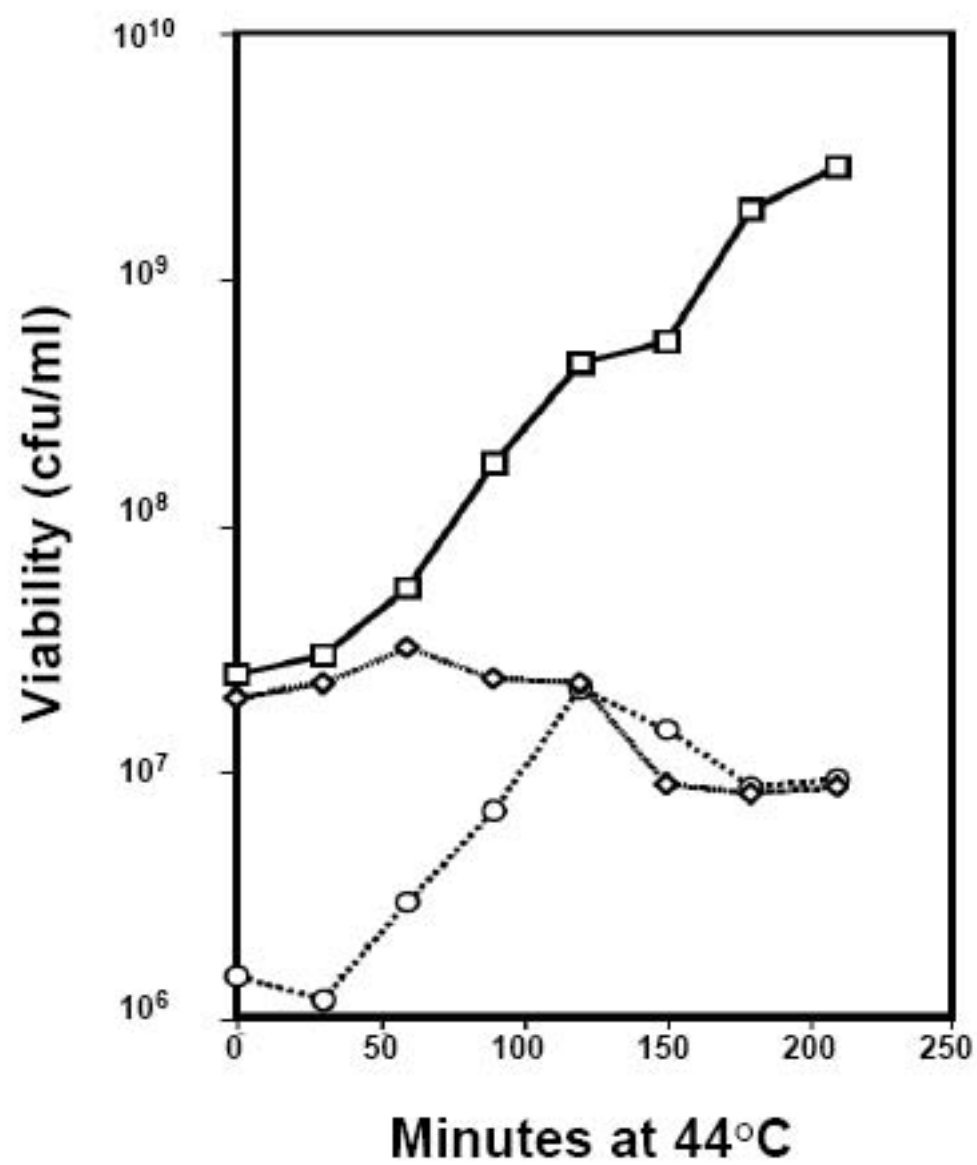


Figure 2.4. Comparison of the growth properties by replica plating on Luria agar medium of an *rne-1* mutant carrying various *rng* plasmids. Individual colonies of the various strains as indicated in (A) were patched onto a Luria agar master plate and grown overnight at 30°C. Replicas were then incubated for either 24 or 48 hours at 44°C.

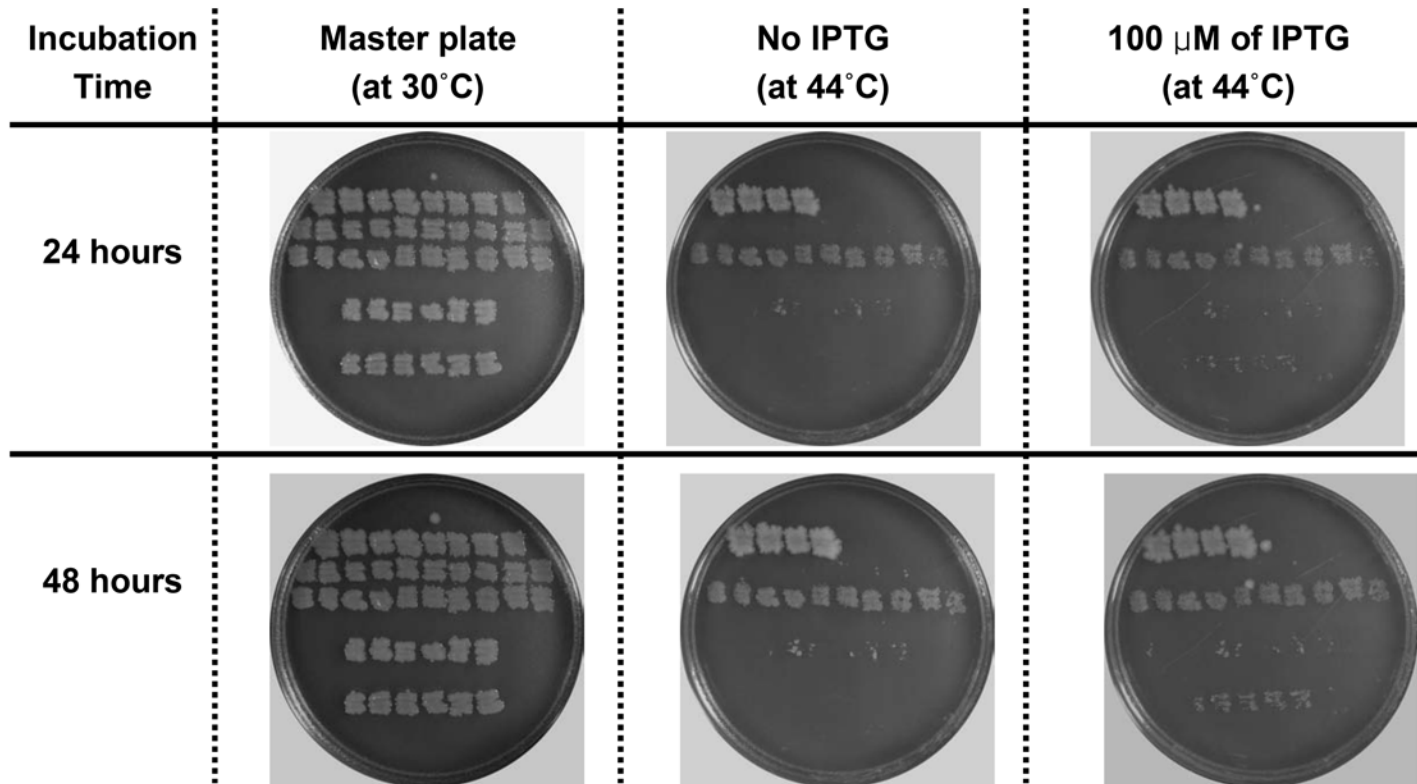
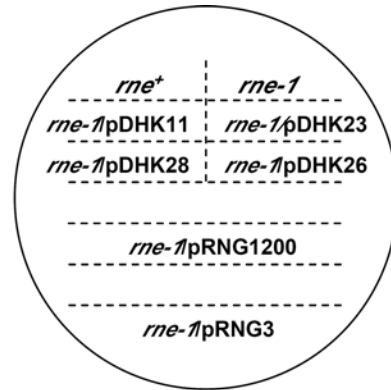
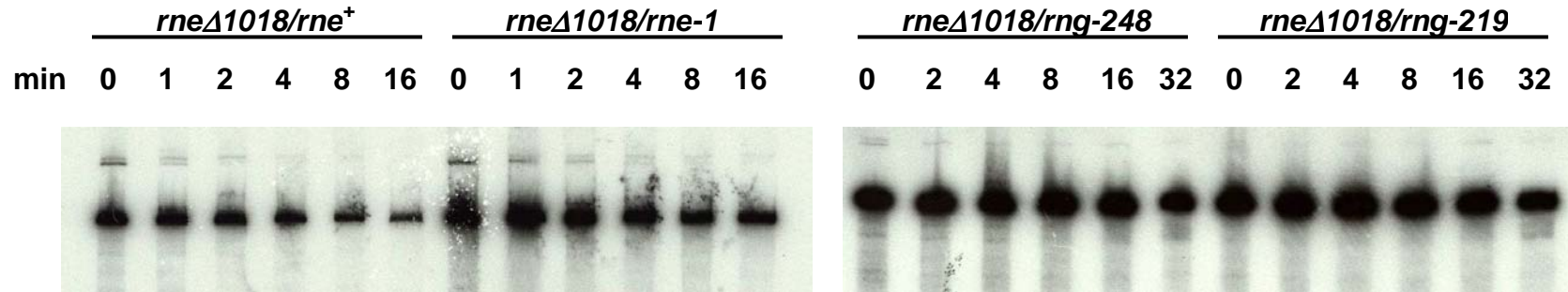
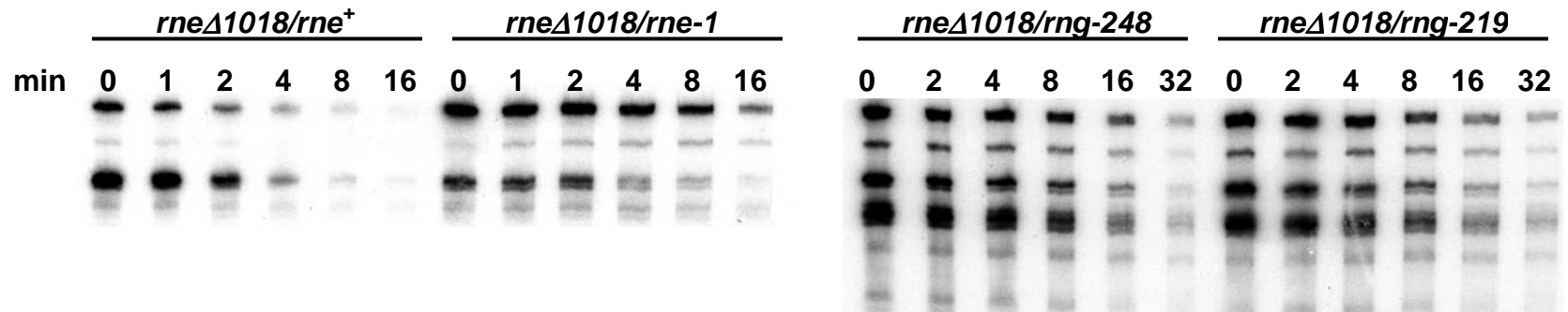


Figure 2.5. mRNA decay profiles of the *rpsO* (A), *rpsT* (B), and *cspA* (C) mRNAs. Total RNA (5 $\mu\text{g}/\text{lane}$) was isolated from cultures of SK10143 (wild-type), SK10144 (*rne-1*), SK3563 (*rng-248*), and SK3564 (*rng-219*) at various times (min) as described in Materials and Methods.

(A) *rpsO***(B) *rpsT***

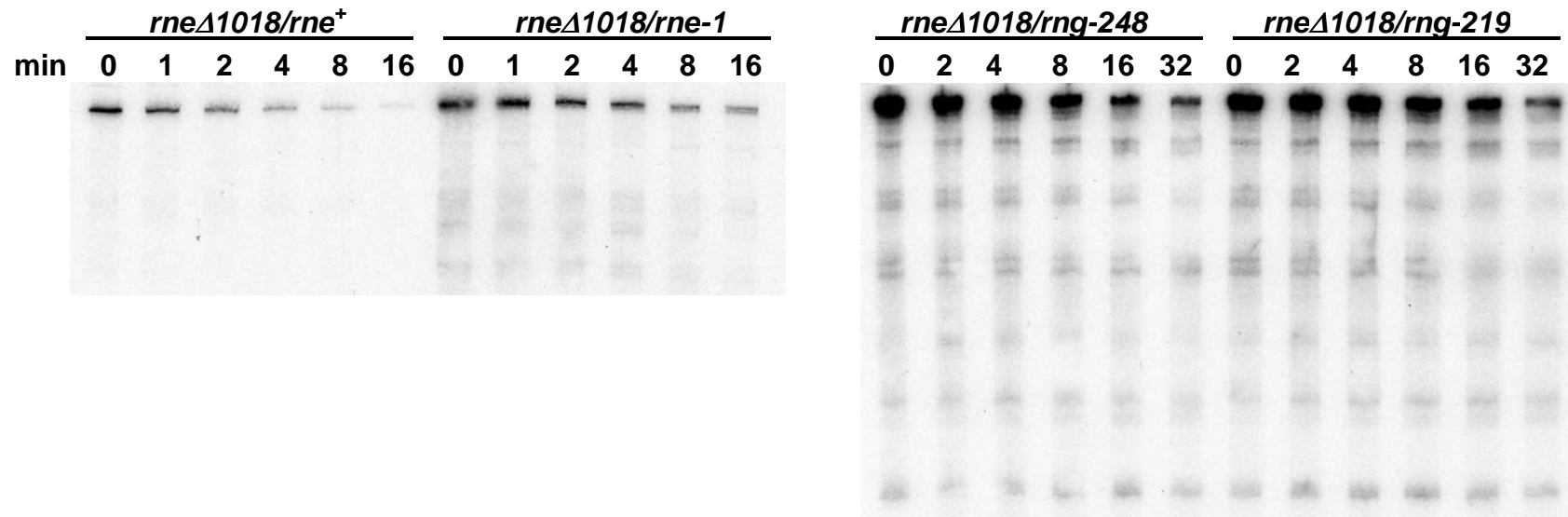
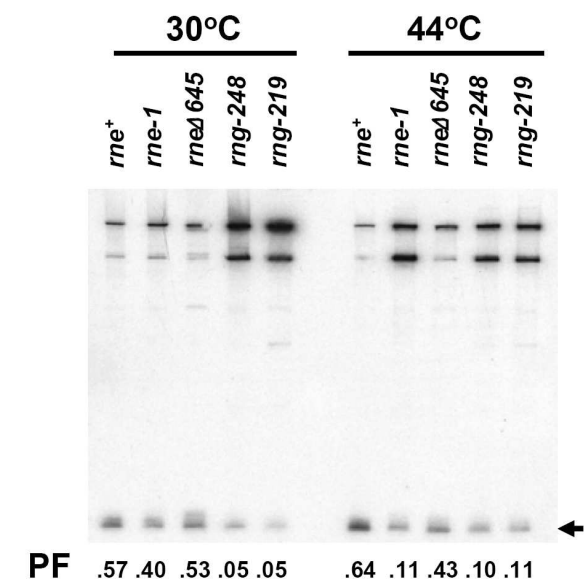
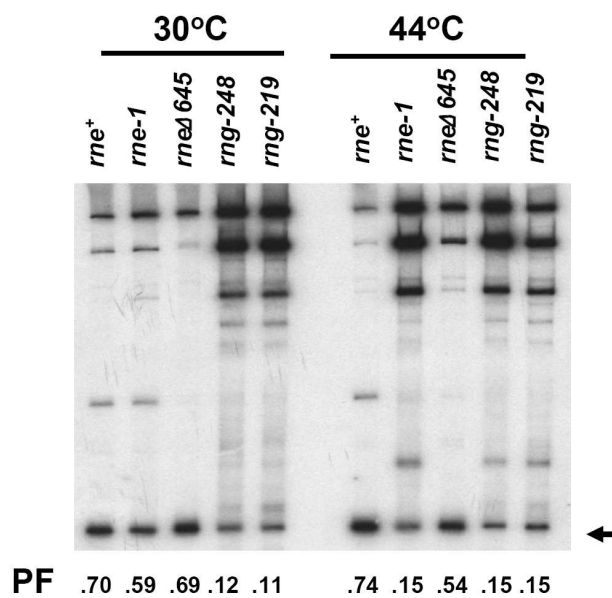
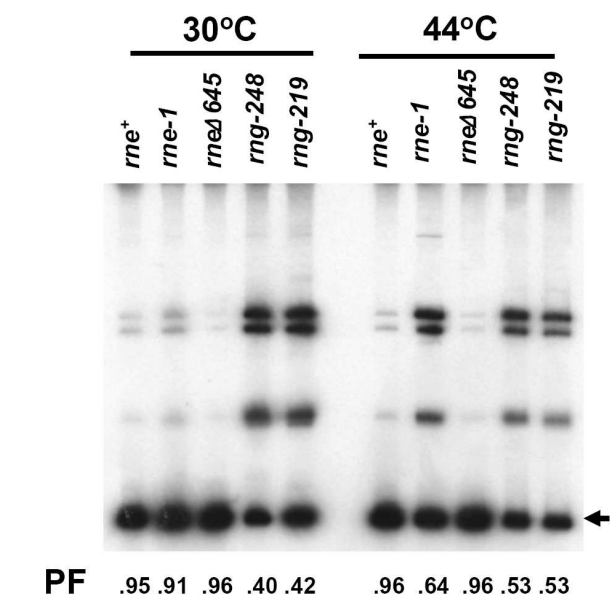
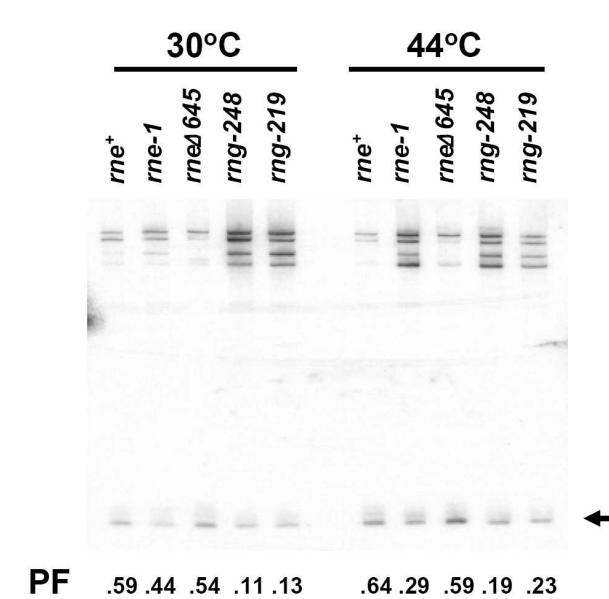
(C) *cspA*

Figure 2.6. Analysis of tRNA maturation in *rneΔ1018/rng-219* and *rneΔ1018/rng-248* mutants when the *rng* alleles were present in single copy. Steady-state RNA (5 μg/lane) isolated from cultures grown either at 30°C or after shift to 44°C was analyzed as described in Materials and Methods. Oligonucleotides specific for tRNA^{His} (A), tRNA^{Pro} (B), tRNA^{Asn} (C), and tRNA^{Cys} (D) were used as probes. PF denotes the processed fraction, which is defined as the amount of a given mature tRNA divided by the total amount of tRNA transcribed (processed and unprocessed). The numbers represent the average of 3-4 independent determinations. The standard deviations from the mean are presented in Appendix 1, Table A1.1. Arrows in the right margins indicate the position of each mature tRNA. RNA levels were normalized as described in Materials and Methods.

(A) tRNA^{His}**(B) tRNA^{Pro}****(C) tRNA^{Asn}****(D) tRNA^{Cys}**

CHAPTER 3

Biochemical Analysis of *E. coli* RNase G reveals significant overlaps in substrate specificity and cleavage site selection with its essential homologue, RNase E¹

¹ Dae-hwan Chung and Sidney R. Kushner. To be Submitted to Journal of Molecular Biology

ABSTRACT

In *Escherichia coli* the endoribonucleases RNase E and RNase G are homologues that are involved in various aspects of RNA metabolism. RNase E is essential for cell viability and plays important roles in mRNA decay, tRNA maturation, rRNA processing and the degradation of small regulatory RNAs and their target mRNAs. In contrast, RNase G is less abundant, is not required for cell viability, and acts on a much more limited set of RNA molecules. While both enzymes employ a 5'-end-dependent reaction mechanism *in vivo*, they cleave the 5' leader region of the immature 16S rRNA at different locations. Furthermore, under normal physiological conditions RNase G is not able to complement the loss of RNase E activity. Recently, we isolated single amino acid mutations in RNase G (*rng-219* and *rng-248*) that lead to complementation of various RNase E mutants. However, while the *rng-219* and *rng-248* alleles complemented the growth defect associated the loss of RNase E activity, mRNA decay and tRNA maturation remained highly defective. Here we show, surprisingly, that *in vitro* the purified RNase G and Rng-219 proteins have, overall, very similar cleavage site specificity to RNase E, particularly on tRNA substrates. The major difference between the RNase G and Rng-219 proteins appears to be increased cleavage specificity such that the Rng-219 protein more closely resembles RNase E. In addition, RNase G is ~50-fold more active in the presence of Mn^{2+} than Mg^{2+} .

INTRODUCTION

Escherichia coli contains two members of the RNase E/G endoribonuclease family, which is widely distributed in eubacteria¹. On the one hand, RNase E, is essential for cell viability and is involved in many aspects of RNA metabolism, including mRNA decay, rRNA

processing and tRNA maturation^{2; 3; 4; 5; 6; 7; 8; 9; 10; 11}. In contrast, inactivation of RNase G does not lead to any obvious growth phenotype and the enzyme is only involved in the decay of a limited number of mRNAs and the generation of the mature 5' end of the 16S rRNA^{10; 11; 12; 13; 14; 15}.

Although the N-terminal catalytic domain of RNase E is 34.1% identical to the sequence of RNase G¹⁶, under normal physiological conditions RNase G cannot substitute for RNase E^{14; 17; 18}. This result is somewhat surprising since both proteins employ a similar 5'-end-dependent mechanism for the cleavage of RNA substrates within A/U rich single-stranded regions^{19; 20; 21; 22; 23}. In fact, the two enzymes cleave the 17S precursor of 16S rRNA at different sites *in vivo*^{10; 11}. In contrast, *in vitro* experiments have suggested that both enzymes can process the 9S precursor of 5S rRNA at similar sites²⁰. Additional biochemical and structural studies have indicated that both RNase G and RNase E are more active in multimeric form^{21; 24; 25; 26; 27; 28} and that multimerization is promoted by the presence of a 5' phosphomonoester terminus on the substrate^{21; 24; 25}.

Studies by Lee *et al.*¹⁵ and Deana and Belasco¹⁸ indicated that over-expression of an extended form of RNase G containing an extra six amino acids at its 5' terminus could lead to the growth of RNase E mutants. Although the extra amino acids are encoded in the *rng* mRNA, analysis of the purified protein demonstrated that the extended form of the protein is not normally synthesized *in vivo*²⁸. These studies raised the interesting question of how RNase G substituted for RNase E under these conditions. In trying to answer this question, Chung *et al.*²⁹ isolated two spontaneously arising mutations in the structural gene for RNase G (*rng-219* and *rng-248*) that led to the complementation of RNase E deletion mutants at physiologically relevant levels of the mutant RNase G proteins. In these strains, it was observed that 9S rRNA processing was restored to almost wild-type levels, while mRNA decay and tRNA maturation remained very defective²⁹. Furthermore, the processing of the 5' terminus of 16S rRNA was also normal²⁹. It was also determined that the growth observed in the presence of the

extended form of RNase G^{15; 18} resulted only after the extended protein was overproduced at 174-1000-fold higher levels than found in wild type *E. coli*²⁹.

Based on these observations, we attempted to determine if there were significant biochemical differences between wild type RNase G and the protein encoded by the *rng-219* allele. Derivatives of both proteins, tagged with six histidine residues at their carboxy termini, were constructed and shown to encode biologically active proteins. The RNase G and Rng-219 proteins were purified to greater than 98% homogeneity from a strain deficient in polynucleotide phosphorylase, a major 3' → 5' exonuclease. Both purified RNase G proteins were subsequently tested, along with purified RNase E on a variety of rRNA, tRNA and mRNA substrates. We show here that RNase G is ~50-fold more active in the presence of Mn²⁺ than Mg²⁺. In addition, all three enzymes cleave a variety of tRNA precursors at identical locations, even though they are not substrates for RNase G *in vivo*^{14; 18}. The data indicate that an important difference between wild type RNase G and the Rng-219 protein is a significant decrease in the nonspecific cleavages associated with the mutant enzyme. Accordingly, the cleavage specificity of Rng-219 is more similar to RNase E than RNase G, even though overall the enzyme is less active than RNase G on the majority of the substrates tested.

RESULTS

Purification of the Rng⁺ and Rng-219 Proteins.

The *rng⁺* and *rng-219* encoded RNase G proteins were purified as C-terminally His-tagged proteins. Prior to purification of either RNase G (His)₆ or Rng-219 (His)₆ each IPTG-inducible plasmid was transformed into SK2538 (*rng::cat*)¹⁴ and the ability of both modified RNase G proteins to complete the 5' end maturation of the 16S rRNA was experimentally

verified (data not shown). Initially, RNase G (His)₆ was purified from MG1693⁴, a wild type strain of *E. coli*, as described in the *Materials and Methods*. Although the purified RNase G looked to be greater than 98% pure based silver staining of a polyacrylamide gel (data not shown), Western blot analysis showed the presence of small amounts of both polynucleotide phosphorylase (PNPase) and RNase E (data not shown).

Since we suspected that the small amount of both contaminating ribonucleases arose from their association in the multiprotein degradosome^{30; 31}, both plasmids were subsequently transformed into SK10019 (*pnpΔ1684::str/spc rph-1 thyA715*)³². The subsequent purification procedure as described in *Materials and Methods* involved ammonium sulfate precipitation, Ni²⁺-NTA agarose chromatography and Mono Q anion exchange chromatography. Interestingly, the Rng-219 protein eluted at a lower salt concentration from the Mono Q column than wild-type RNase G (data not shown). The two proteins were judged greater than 98% pure based on a combination of coomassie blue and silver staining and western blot analysis with anti-RNase G antibodies (Fig. 3.1 and data not shown). Each preparation contained a very small amount of RNase G proteolysis products (Fig. 3.1C). More importantly, neither protein preparation contained any detectable RNase E, PNPase or RNase II as determined by western blot analysis (data not shown).

Optimization of RNase G activity.

In order to optimize the activity of RNase G, we generated an uniformly P³²-labeled 254 nt RNA fragment from the 5' end of the 16S rRNA (Fig. 3.2). Based on *in vivo* experiments^{10; 11}, the 5' terminus of this substrate is two nt downstream of an RNase E cleavage site and contains a single RNase G cleavage that was predicted to yield two fragments, 67 and 187 nt in length (Fig. 3.2A). Previously, RNase G had been assayed in the presence of 5 mM MgCl₂ and 60 mM

KCl^{24; 28}. However, when we assayed our purified RNase G under these conditions, we saw only very weak activity (Fig. 3.2B, lanes 17, 18). While activity improved if the 60 mM KCl was omitted from the reaction mixtures (Fig. 3.2B, lanes 9-12), there were numerous discrete species of which none had the expected sizes. Substitution of MnCl₂ for MgCl₂ led to the production of a single major species of ~155 nt and a second larger band at ~207 nt (Fig. 3.2B, lanes 3-8). Addition of 60 mM KCl inhibited RNase G activity in the presence of MnCl₂ (Fig 3.2B, 13-16). Based on the quantification of the 155 nt species, there was a ~50-fold increase in activity in the presence of 5 mM Mn²⁺ versus 5 mM Mg²⁺. The increase in activity was a ~40-fold in the presence of 1 mM Mn²⁺. Optimal activity in the presence of Mn²⁺ was observed at pH 7.6 and Zn²⁺ had no affect on activity (data not shown). It should be noted that the cleavage pattern with this substrate was similar in the presence of either cation (Fig. 3.2B, data not shown).

Since neither of the two major rRNA cleavage products appeared to arise from the known *in vivo* site at +1 (Fig. 3.2A), we used primer extension analysis to map the 5' termini of the 155 and 207 nt species. We determined that the major 5' terminus was located at +32 to generate the 155 nt species, while the larger 207 nt fragment arose from an RNase G cleavage at - 20 (Fig. 3.2A). The 99 nt fragment observed in Fig. 3.2B (lanes 3-8) represents the upstream product derived from cleavage at the G1 site based on Northern blot analysis (data not shown).

Analysis of 16S rRNA processing by RNase G, Rng-219, and RNase E.

Briant *et al.*²⁸ used a 671 nt 16S rRNA fragment was used to analyze RNase G activity and showed that RNase G cut the fragment at the same location *in vitro* and *in vivo*. Accordingly, for the comparative analysis of RNase G, Rng-219 and RNase E, we made a

different run-off transcript that started at the upstream RNase III cleavage site of the *rrnB* 16S rRNA precursor (-154), yielding a fragment of 344 nt (Fig. 3.3A). Again based on *in vivo* data^{24;}²⁸, we expected fragments of 157 and 187 from cleavage with RNase G compared to fragments of 91 and 253 nt with RNase E (Fig. 3.3A). To our surprise, all three enzymes cleaved the 344 nt substrate to generate a 155 nt fragment at the same site (verified by primer extension analysis, data not shown) that was obtained with the shorter substrate used in Fig. 3.2B (Fig. 3.3B). The secondary cleavages by the three proteins, however, were significantly different. Thus there were two additional RNase E cleavages at -39 and -34 (Fig. 3.3B, lanes 8-10), as well as an Rng-219 cleavage at -20 that was not evident with the RNase G protein (Fig. 3.3B, lanes 2-7). When taking into account that the RNase G reactions contained 10-fold more protein than the RNase E digestion, we estimated an overall five-fold difference in the activity of RNase G versus RNase E on this substrate. The composition of the smaller cleavage products denoted by the ★ in Fig. 3.3B was not determined.

RNase G, Rng-219 and RNase E process the 9S rRNA precursor at identical sites.

RNase E was first identified based on its ability to process a 9S rRNA precursor to generate a pre-5S form that has three extra nt at both its 5' and 3' termini^{2;33}. Interestingly, Tock *et al.*²⁰ found that their RNase G preparation did not cleave at the upstream RNase E cleavage site (Fig. 3.4A). However, *in vivo* data has suggested that RNase G can substitute for RNase E in the maturation of 5S rRNA^{14;29}. Accordingly, we generated a 288 nt 9S rRNA precursor molecule from the *rrnD* rRNA operon (Fig. 3.4A). As shown in Fig. 3.4B, all three proteins cleaved the 288 nt 9S rRNA precursor to yield a 126 nt product, that had an extra three nt at the 5' terminus (based on primer extension analysis, data not shown) indicating that the enzymes were cleaving at the sites observed *in vivo*. Based on the amount of each protein

added, the activity of RNase G was less reduced by ~two-fold compared to RNase E. It also appeared that RNase G had more nonspecific activity on this RNA molecule than the Rng-219 protein in that the 126 nt species began to disappear at longer time points (Fig. 3.4B and data not shown). In addition, all three enzymes appeared to have multiple cleavage sites within the upstream and downstream sequences, since neither the 96 nt upstream cleavage product nor the 63 nt downstream fragment were detected in any significant amounts (data not shown).

RNase G and Rng-219 cleave the *rpsT* mRNA at unique sites compared to RNase E.

A variety of studies have shown that RNase E is involved in the decay of a large number in specific mRNAs^{4; 15; 34}, while RNase G appears to have a much more limited role in mRNA decay^{12; 15; 35}. In fact, it has been suggested that RNase G plays a backup role in the decay of a variety of *E. coli* mRNAs¹⁴. To compare the activities of RNase G, Rng-219 and RNase E on specific mRNA substrates, we chose the *rpsT* and *cspA* mRNAs. Both have been shown *in vivo* to be dependent on RNase E for their decay^{6; 36}. However, It has also been demonstrated that RNase G can also degrade the *rpsT* mRNA in the absence of RNase E¹⁴. A 450 nt *rpsT* mRNA was generated that included the entire 5' UTR starting from the P1 promoter transcription start site and included the Rho-independent transcription terminator (Fig. 3.5A). As expected from previous work⁶, there was a major RNase E cleavage site that resulted in removal of the Rho-independent transcription terminator when the substrate had a 5' phosphomonoester terminus, as well as a nearby second site that produced a slightly shorter species at longer time points (Fig. 3.5B, lanes 10-13). There were also a number of smaller fragments and it appeared that that the initial cleavage product was degraded further as a function time. In the case of both RNase G and the Rng-219 protein, the cleavage pattern was almost completely different with RNase E (Fig 3.5B, lanes 2-9). There appeared to be a primary

cleavage site slightly upstream of the major RNase E cleavage site as well as a large number of additional sites that led to a large number of smaller degradation products (Fig. 3.5B, lanes 2-9). Furthermore, the fragment pattern obtained with the Rng-219 protein was slightly different than that derived with wild type RNase G (Fig. 3.5B & 3.5C, lanes 2-9). Overall, it appeared as if the Rng-219 protein was less active on the *rpsT* mRNA than RNase G.

Since both enzymes have been shown to be 5'-end-dependent and to be inhibited by the presence of a 5' triphosphate, we repeated the experiment without pretreatment of the run-off transcript with TAP (See *Materials and Methods*). The presence of the 5' triphosphate reduced the activity of RNase G approximately two-fold but interestingly, did not significantly change the overall degradation profile (compare Fig. 3.5B, lanes 2-5 and Fig. 3.5C, lanes 2-5). In the case of the Rng-219 enzyme, its activity was also decreased by a factor of ~two-fold (Fig. 3.5B, lanes 6-9 and Fig. 3.5C, lanes 6-9). With RNase E, there was four-five-fold inhibition of catalytic activity, in general agreement with the results of Mackie²³ along with a significant change in the profile of degradation products (Fig. 3.5B, lanes 10-13 and Fig. 3.5C, lanes 10-13).

RNase G, Rng-219 and RNase E generate recognize the same major cleavage site in the *cspA* mRNA.

Hankins *et al.*³⁶ have demonstrated a single major RNase E cleavage site within the *cspA* mRNA located 34 nt upstream of the Rho-independent transcription termination site. In the experiments described in Fig. 3.6, we used a PCR DNA fragment that generated two distinct run-off transcripts. A 461 nt transcript that contained the entire 5' UTR as well as an extra 32 nt downstream of the Rho-independent transcription terminator and a 429 nt species corresponding to the *in vivo* derived mRNA (Fig. 3.6A). In agreement with the previously reported results³⁶, RNase E cleaved both species once to generate a 395 nt product that accumulated over the

course of the reaction (Fig. 3.6B, lanes 8-10). Surprisingly, the reaction was equally efficient in the presence or absence of the 5' terminal triphosphate (Fig. 3.6B, lanes 8-10; 18-20). The cleavage profile generated with the Rng-219 protein looked very similar to that obtained with RNase E although the reaction was less efficient (Fig. 3.6B, lanes 5-7; 15-17). In the case of RNase G, both transcripts were rapidly degraded, in the presence or absence of the 5' terminal triphosphate, without the appearance of a significant amount of the 395 nt decay intermediate (Fig. 3.6B, lanes 2-4; 12-14). When the Northern blots were reprobed with an oligonucleotide specific for the terminator region of the *cspA* transcript (Fig. 3.6A, oligo b), both a 66 nt (derived from the 461 nt transcript) and a 34 nt (derived from the 429 nt transcript) species accumulated in the RNase E digestion (Fig. 3.6C, lanes 8-10, 18-20). In contrast, the 66 nt species was only weakly observed in the Rng-219 digestion and was barely detected with RNase G (Fig. 3.6C, lanes 2-7, 12-17).

RNase G, Rng-219 and RNase E process the monocistronic *pheU* precursor tRNA at the same site.

It has been previously shown *in vivo* that the *pheU* tRNA transcript is a substrate for RNase E but not for RNase G^{9; 14; 18}. Accordingly, we expected to see a significant difference between the ability of the two RNase G proteins and RNase E to process a primary *pheU* tRNA transcript. For these experiments, we used a *pheU* DNA template that contained an extra G at the 5' mature terminus, the 76 nt mature *pheU* tRNA and 63 downstream nt that included the Rho-independent transcription terminator (Fig. 3.7A). This template gave three distinct transcription products with T7 RNA polymerase (Fig. 3.7B and 3.7C, lane 1). The unlabeled *pheU* run-off transcript was digested with either RNase G, Rng-219 or RNase E over a time course of 35 min and was subsequently analyzed on Northern blots using either probe a

(mature tRNA) or probe b (downstream sequences) (Fig. 3.7A). To our surprise, all three enzymes generated a primary processing intermediate of 78-79 nt, which arose from cleavage either 1-2 downstream of the encoded CCA determinate (Fig. 3.7B). Furthermore, neither of the RNase G proteins were inhibited more than 2.7-fold by the presence of the 5' triphosphate (Fig. 3.7B, lanes 2-9 and Fig. 3.7C, lanes 2-9 and Table 3.1). In contrast, the activity of RNase E was inhibited by 15-fold (Fig. 3.7B, lanes 10-13 and Fig. 3.7C, lanes 10-13 and Table 3.1). In addition, the Rng-219 protein had five-fold less activity on this substrate than the RNase G protein (Fig. 3.7B, 3.7C).

Analysis of the processing of polycistronic tRNA transcripts.

Since the analysis of the monocistronic *pheU* tRNA transcript demonstrated that it was cleaved efficiently by RNase G, we decided to test two additional polycistronic transcripts (*argX hisR leuT proM* and *glyW cysT leuZ*) that have been shown to be processed efficiently *in vivo* by RNase E^{8;9} but are not substrates for RNase G^{14;18}. Unlabeled *argX* operon (*argX hisR leuT proM*) transcripts were generated from a PCR fragment that produced two species. A 481 nt transcript derived from termination at the encoded Rho-independent terminator and a 505 nt species that arose from run-off transcription of the entire template fragment (Fig. 3.8A). Digestion products generated by treatment with RNase G, Rng-219 and RNase E were analyzed using Northern blot analysis with the oligonucleotide probes shown in Fig. 3.8A. In the first experiment, we used probe a to determine the nature of the pre-tRNA^{Arg} that was cleaved from the polycistronic transcript. As shown in Fig. 3.8B, all three enzymes generated a species of 140-141 nt that represented the 5' leader, *argX* and 3' trailer sequences up to positions of +140 or 141. In the case of RNase E, there was a second major species of 228-229 nt that represented an *argX hisR* fragment (Fig. 3.8B, lanes 12-16). Both RNase G proteins produced

some additional processing intermediates that were not observed with RNase E (Fig. 3.8B, lanes 2-11). The RNase G protein was ~four-fold more active than the Rng-219 protein. Compared to RNase E, the ability of RNase G to release the pre-*argX* tRNA from the *argX* polycistronic transcript was only reduced by a factor of two. The precise location of the E1/G1 cleavage sites shown in Fig. 3.8A were determined using primer extension analysis (Fig. 3.9B, lanes 6-11). All three enzymes produced two distinct primer extension products located at +140 and +141 (Fig. 3.9B, lanes 6-11).

When the Northern analysis was repeated with a probe specific for *hisR* (probe c, Fig. 3.8A) the major species observed was ~86 nt in length (Fig. 3.8D). As observed with *argX*, RNase G was considerable more active than the Rng-219 protein (Fig. 3.8D, lanes 2-11). Both RNase G proteins generated a series of minor processing intermediates that were not observed with RNase E. In addition, RNase G also produced a product that was smaller than 86 nt (Fig. 3.8D, lanes 3-6). Primer extension analysis (Fig. 3.9B) revealed all three enzymes cleaved the *argX* precursor at either position +228 or 229 with almost equal affinity (Fig. 3.9C, lanes 6-11). In the case of RNase G, additional cleavages were also observed at positions +234, 235, and 242 (Fig. 3.9C, lanes 6-7), but were either greatly diminished in the presence of Rng-219 (Fig. 3.9C, lanes 8-9), or absent with the RNase E protein (Fig. 3.9C, lanes 10-11).

Reprobing the membrane with an oligonucleotide specific for *leuT* (Fig. 3.8A, oligo e) resulted in a distinct pattern of processing intermediates with a major species of ~107 nt arising from cleavages at E2/G2 and E3/G3 (Fig. 3.8A and 3.8F, lanes 2-16). As seen with the *argX* and *hisR* probes, the RNase G protein produced more processing intermediates than were observed with RNase E (Fig. 3.8F, lanes 2-6). In addition, RNase G appeared to further degrade the 107 nt species at later points in the digestion, as was also observed with the *argX* species (Fig. 3.8B). Primer extension analysis also showed a cleavage site at +370, three nt upstream for the mature 5' terminus (E4/G4 for all three enzymes and well as a weaker

cleavage site at position +380 for wild type RNase G (G11, Fig. 3.8A and data not shown). Cleavage at the +380 position, which falls within the mature *proM* was greatly diminished with the Rng-219 protein (data not shown). As seen with both *argX* and *hisR*, there was significantly less activity with the Rng-219 protein compared to RNase G along with some modification of the cleavage profile (see the 206 nt species in Fig. 3.8F, lanes 2-11).

In the final experiment with the 5' monophosphorylated *argX* precursor, the membrane was reprobed with oligo g, which was specific for the mature *proM* tRNA (Fig. 3.8A). In this case, the primary species was ~84 nt length and represented the *proM* tRNA that had been cleaved at both the 5' and 3' ends by either RNase G, Rng-219 or RNase E (Fig. 3.8A E4/G4 and E5/G5; Fig. 3.8E). Some additional cleavage products, such as a 110 nt species that retained the Rho independent transcription terminator were specific for the two RNase G proteins were also observed (Fig. 3.8H, lanes 2-11). As observed with the other three tRNAs in the operon, RNase G was ~four-fold more active than the Rng-219 protein. Additional probings with oligonucleotides specific for intercistronic and terminator regions (probes b, d, f, h and i, Fig. 3.8A) were used to help establish the identity of the various fragments shown in Fig. 3.8 (data not shown).

Based on our observation that the processing of the *pheU* tRNA precursor was significantly affected by the presence of a 5' triphosphate (Fig. 3.7, Table 3.1), we repeated the experiments described in Fig. 3.8B, D, F, and H, using a 5' triphosphate terminated *argX* polycistronic transcript. As seen with *pheU*, RNase E activity on this polycistronic transcript was reduced between 10- 25-fold depending on the individual pre-tRNA species in the presence of a 5' triphosphate (Table 3.1). In contrast, the decrease in the activity of RNase G varied between 1.5-5.6- fold for the wild type protein and 3.7-12-fold for Rng-219 (Table 3.1). Furthermore, while the presence of a triphosphate led to reduced catalytic activity for all three enzymes, it did not change the profile of processing intermediates for any of the four tRNAs tested (compare

Fig. 3.8B, C; 3.8D, E; 8F, G; and 3.8H, I). The presence of the triphosphate did appear to reduce the nonspecific cleavages associated with RNase G (Fig. 3.8C and 3.8G).

As a final experiment we also examined the processing of the *glyW cysT leuZ* polycistronic transcript, which has also been shown to undergo RNase E dependent processing to generate pre-tRNAs^{8;9}. Initially, we used a uniformly labeled transcript and examined the pattern of processing intermediates. While the overall processing profiles looked quite similar (Fig. 3.10), an approximately 142 nt species (Fig. 3.10B, lanes 7, 8) was missing with both the RNase G and Rng-219 proteins. When the experiment was repeated with an unlabeled *glyW cysT leuZ* substrate and probed with a variety of oligonucleotides, it became clear that RNase G cleavage only occurred at a site (E2/G1) that was four nt upstream of *cysT* (Fig. 3.10A) generating a fragment of 142 nt. In contrast, digestion with RNase E produced a 113 nt fragment that arose from cleavage 2-3 nt downstream of the *glyW* CCA determinant (E1) (Fig. 3.10A, data not shown). The *glyW cysT leuZ* transcript also differed in on other important aspect, namely the inhibition of enzyme activity in the presence of a 5' triphosphate. Unlike what was observed with the *pheU* and *argX* transcripts, the highest level of inhibition was less than two-fold for RNase E (Table 3.1).

RNase E and RNase G process polycistronic tRNA transcripts in the 5' → 3' direction.

In order to determine if RNase G, Rng-219 and RNase E processed the polycistronic tRNA transcripts in the 5' → 3' as would be expected based on the 5' end dependence of both ribonucleases^{19; 20; 22}, we examined the fraction of full-length tRNA precursor processed into individual pre-tRNAs as a function of digestion time. In the case of the *argX hisR leuT proM* polycistronic transcript, an indication of 5' → 3' directionality would be the initial appearance of the pre-*argX* precursor, followed by pre-*hisR* and subsequently pre-*leuT* and pre-*proM*.

Separation of the last two tRNAs would be predicted to occur with the same reaction kinetics. As shown in Fig. 3.11, these predictions were reflected in the appearance of the four pre-tRNAs in the order of *argX*, *hisR*, and (*leuT*, *proM*).

DISCUSSION

While RNase E and RNase G are homologues¹⁷ and act on RNA molecules employing a similar 5' end-dependent reaction mechanism^{20;22}, *in vivo* they seem to have very different substrate specificities. It thus of considerable interest that single amino acid substitutions in the predicted RNase H domain of RNase G led to the complementation of the growth defects associated with RNase E mutations²⁹. In the experiments reported here we have compared the catalytic activities of purified RNase G, Rng-219 and RNase E on a variety of rRNA, mRNA and tRNA substrates *in vitro*. The data provide some fascinating insights into the complex world of these two related ribonucleases.

In the first place, RNase G is over 50-fold more active in the presence of Mn^{2+} than Mg^{2+} (Fig. 3.2), suggesting that there could be considerably more RNase G activity *in vivo* than previously thought if the Mn^{2+} cofactor is tightly bound to the protein. This would be a required since the *in vivo* the Mn^{2+} concentration is predicted to be in the micromolar range with most of it being bound to proteins rather than being free in solution (Simon Silver, personal communication). Thus it is possible that besides there being fewer RNase G protein molecules, relative to RNase E¹⁵, if Mn^{2+} is not available, the enzyme is probably only active on a very limited number of substrates, including the 17S rRNA precursor^{10;11} accounting for its inability to substitute for RNase E. Since 16S rRNA is a very abundant in the cell and is matured very efficiently, it would seem that RNase G may in fact be more active than previously envisioned.

This is a very important issue because on the hypotheses regarding the essential function of RNase E *in vivo* involves its role in the processing of tRNA precursors such as *pheU* and the *argX* and *glyW* polycistronic operons^{8,9}. As shown here, it turns out that *in vitro* RNase G and RNase E, overall, process these tRNA precursors at the same major cleavage sites (Figs 3.7-3.10) to generate identical pre-tRNAs for further processing. The only apparent exception is the failure of RNase G to cleave immediately downstream of *glyW* (Fig. 3.10), but a slightly downstream cleavage by RNase G (Fig. 3.10) would still generate a pre-*glyW* tRNA that could be exonucleolytic processed into its mature form. The biggest problem, however, is that while the pre-tRNAs are generated by RNase E are relatively stable to further degradation *in vitro*, that is not the case with RNase G. Thus with the *argX* operon at the later time points the major species begin to disappear in the RNase G digestions but build up in the RNase E reactions (Fig. 3.8). In fact, a number of RNase G cleavage sites were mapped within the mature *hisR* and *proM* tRNAs (Fig. 3.8A). The fact that the Rng-219 protein has less nonspecific activity on the tRNA substrates, suggests that if there were sufficient levels of the Rng-219 protein, sufficient pre-tRNAs could be produced to generate to yield enough functional tRNAs needed for cell survival. In contrast, high levels of the wild type RNase G would tend to produce nonfunctional tRNA processed products.

The observed overall lack of cleavage specificity on the part of RNase G observed here (Figs. 3.2-3.8) suggests that if it is using Mn^{2+} as a cofactor *in vivo* the enzyme breaks down the initial cleavage products into many smaller fragments. While it is possible that the preparation of RNase G used in these experiments is contaminated with another ribonuclease, its purification from a PNPase deficient strains and a failure to show the presence of any RNase II or RNase E protein, tends to suggest that this is an inherent property of RNase G. This lack of specificity provides a possible explanation for the observations of Lee et al.¹⁵ and Deana and Belasco¹⁸, in which they observed some growth of RNase E mutants in the presence of 174-1000-fold

increase in the level of a modified form of RNase G²⁹ that contained an extra six amino acids at the amino terminus. Specifically, such a large increase in RNase G protein levels, whether it was using Mn²⁺ or Mg²⁺ as its cofactor *in vivo*, would lead to a great deal of nonspecific processing of tRNA precursors (Figs. 3.7, 3.8, and 3.10). Thus only a very small fraction of cells might contain enough functional tRNAs, for example, to be able to survive. In fact, as was observed by Chung et al.,²⁹ in the case of pRNG1200¹⁸, the survivors obtained in the temperature sensitive *rne-1* genetic background did not survive when restreaked at 44°C²⁹.

In contrast, the levels of the *rng-219* and *rng-248* encoded RNase G proteins were able to support cell viability at protein concentrations that did not exceed that normal intracellular RNase E levels²⁹. This observation is very significant since the *in vitro* data with the Rng-219 protein shows that its cleavage specificity has been increased somewhat for a number of substrates, particularly tRNAs, even though its overall catalytic activity has been reduced (Figs. 3.7, 3.8, 3.10). Since it is still not clear why RNase E is an essential enzyme, what simply may account for the ability of the *rng-219* and *rng-248* to complement *rne* mutations while the wild enzyme cannot is the slight increase in substrate specificity that results from subtle changes in the predicted RNase H domain of the protein. If the processing, maturation or decay of only a limited number of substrates needs to be improved marginally to support cell viability, a minor modification in the activity of RNase G might be all that is required.

In contrast to the data derived with the tRNA precursors, the picture with the mRNA substrates tested here was significantly different. In one case, *cspA* the two enzymes had the same major cleavage site immediate downstream of the translation stop site (Fig. 3.6A), but again the RNase G protein cleaved the initial product at many additional locations (Fig. 3.6B, lanes 2-4). The 395 nt primary cleavage product was more stable in the Rng-219 digestion and very stable in the presence of RNase E (Fig. 3.6B, lanes 5-10). Furthermore, the downstream cleavage products derived from the RNase E cleavage were also stable (Fig. 3.6C, lanes 8-10),

while they were only barely detectable in the RNase G digestion and weakly visible with Rng-219. These data were very distinct from the observations with the *rpsT* mRNA where the cleavage patterns were essentially completely different (Fig. 3.5). Thus unlike what was seen with tRNAs, the two homologues can have very distinct specificities on the same RNA substrate.

The fact that the activity of RNase G and RNase E can vary widely on mRNA substrates provides another alternative explanation for the failure of RNase G to substitute for RNase E, even when there are increased levels of the protein in the cell. Recent work by Perwez et al. (manuscript in preparation) with intragenic suppressors of temperature sensitive RNase E mutations has suggested that normal mRNA decay is not essential for cell viability, it cannot be ruled out that the decay or processing of a particular mRNA might be essential for the cell to survive. If it happens to be a mRNA which is cleaved in a completely different manner by RNase E versus RNase G, there would be no way for the two enzymes to substitute for each other. What was observed for *rpsT* (Fig. 3.5) would be an example of this type of behavior. A similar type of situation could exist for the processing or decay of a small regulatory RNA.

Finally, it is important to note that none of the three enzymes cleaved a shortened form of a 16S rRNA precursor at the observed *in vivo* sites (Figs. 3.2 and 3.3). It is thus important to realize that the choice of a substrate for *in vitro* analysis must be carefully chosen and the cleavage pattern obtained verified *in vivo* if the data is to have any real significance. Clearly, there is still much to be learned about overlapping and non overlapping functions of these two homologues.

MATERIALS AND METHODS

Construction of His-tagged Rng and Rng-219.

The *rng* gene segment (1.5 kb) was amplified via PCR using oligonucleotides RNG-His(up) (5'-GGAGGGGGATCCATGACGGCTGAATTGTTAG -3') and RNG-His(down) (5'-CCAGCGAATTCTTAGTGATGGTGATGGTGATGCATCATTACGACGTCAAAGT-3'), *Pfu* DNA polymerase (Stratagene) and pUGK31 (*rng*⁺, Ap^r) plasmid DNA¹⁴ as a template. The PCR product was cleaved with *Bam*H1 and *Eco*R1 and cloned into pBMK31 [a regulated expression vector containing a pBR322 origin of DNA replication that was derived from cloning the *lacI*^f gene from pAG702³⁷ into pLAC11³⁸] digested with *Bgl*II and *Eco*RI to generate pJSK1 (*rng*⁺, Ap^r). To construct pJSK3 (*rng-219*, Ap^r), the experiment was identical to that describe above for pJSK1, except that pDHK28 (*rng-219*, Km^r)²⁹, which contains the Val to Phe substitution at 219 amino acid position in *rng* gene, used as a template. DNA sequencing demonstrated that the cloned *rng* and *rng-219* genes were in frame with the six histidine codons followed by a translation stop codon. Western blot analysis using anti-(His)₆ antibody confirmed that induction of pJSK1 and pJSK3 with IPTG led to the synthesis of the expected 56 kDa of C-terminal His-tagged RNase G protein derivatives. We confirmed that the His-tagged Rng and Rng-219 were biologically active *in vivo* by showing that each protein could complement the defect in 16S rRNA processing in SK2538 (*rng::cat*)¹⁴ (data not shown).

Purification of His-tagged Rng, Rng-219 and Rne.

Purification of His-tagged Rng and Rng-219 was similar to the method described by Briant *et al.*²⁸. In outline, two L cultures of SK10019 (*thyA715 rph-1 pnpΔ683::str/spc*^r) cells

harboring either pJSK1 and pJSK3 were grown at 37°C in LB medium containing ampicillin (200 µg/ml) to Klett 50 (No. 42 green filter) and then further incubated 2.5 hours in the presence of 0.2 mM IPTG. Cells were harvested at 3000 x g, and resuspended in Lysis Buffer [10 mM Tris-HCl, pH 7.6, 1 mM EDTA, 0.1 mM DTT, 10 mM imidazole, 0.1 mM phenylmethylsulphonyl fluoride (PMSF), 0.1 % Tween 20, 5 % glycerol, 1 mg/ml lysozyme (Sigma), and protease inhibitor (Complete, EDTA-free from Roche)]. The suspension was sonicated (20 W, three 20 s bursts with intermittent 60 s cooling by using Sonifier cell disruptor, Model W185) followed by centrifugation at 15000 x g for 30 min at 4°C. Each supernatant fraction was precipitated with ammonium sulfate (~40% saturation). The pellets were suspended in 5 ml of sterile water and dialyzed immediately against Dialysis Buffer (10 mM Tris-HCl, pH 7.6, 1 mM EDTA, 0.1 mM DTT, 0.1 % Tween 20, 5 % Glycerol, and 0.1 mM PMSF). The dialyzed protein sample was mixed with 0.5 ml of Ni²⁺-NTA agarose resin (Qiagen) pre-equilibrated with Lysis buffer (without Lysozyme). The lysate/resin mix was incubated for 1 h at 4°C with gentle agitation and the entire suspension was poured into a column. The mixed resin was washed twice with 20 ml each of Wash Buffer (10 mM Tris-HCl, pH 7.6, 1 mM EDTA, 0.1 mM DTT, 0.1 % Tween 20, 0.1 mM PMSF, and 20 mM imidazole). Proteins were eluted in two steps with 12 ml each of Elution Buffer (10 mM Tris-HCl, pH 7.6, 1 mM EDTA, 0.1 mM DTT, 0.1 % Tween 20, and 0.1 mM PMSF) containing either 50 mM or 300 mM imidazole, respectively. Elution fractions from the 300 mM imidazole wash were pooled and further purified by anion-exchange chromatography on a one ml Mono Q column (GE Healthcare), eluted with a salt gradient (50 to 600 mM NaCl gradient in Dialysis buffer). The peak fractions were pooled and dialyzed overnight against Dialysis Buffer and stored at -70°C. Under these conditions the purified proteins were stable for over six months. His-tagged (carboxy terminus) RNase E was purified from SK10154 (*ompT1000::kan*) grown in LB broth as described previously³⁹.

Protein aliquots were diluted with 1X reaction buffer just before their use in cleavage assays. Protein concentrations were determined by the Bio-Rad protein assay using bovine serum albumin as the standard. Protein purity was verified using both Coomassie brilliant blue G-250 as described by Sedmak and Grossberg⁴⁰ and Silver staining as described in Sambrook and Russell⁴¹. Based on the SDS-PAGE analysis, the protein purity was estimated at <98%. Further analysis of the purified RNase G proteins for the presence of trace amounts of RNase E, RNase II or polynucleotide phosphorylase was carried out using Western blot analysis. Three µg of purified Rng and Rng-219 were electrophoresed in an 8% SDS–polyacrylamide gel and electrotransferred to a PVDF membrane (ImmobilonTM-P; Millipore) using a Bio-Rad Mini-Protein 3 electrophoretic apparatus. The membranes were then probed with either polyclonal anti-RNase G, polyclonal anti-RNase II or a MAP-anti-RNase E antibody⁴ using the ECL PlusTM Western Blotting Detection Kit (Amersham Biosciences) as specified by the manufacturer. The RNase G antibody was kindly provided by George A. Mackie and was pre-incubated with a 1 mg of protein extract from RNase G-deficient *E. coli* cells [SK2538 (*rng::cat*)¹⁴] prior to use. The anti-RNase II antibody was kindly provided by Cecelia Arraiano.

Preparation of RNA substrates.

Both internally ³²P-labeled and unlabeled rRNAs, mRNAs, and tRNAs were prepared by *in vitro* transcription of DNA templates using T7 RNA polymerase (Promega). The templates were generated using PCR with *Taq* DNA polymerase (Sigma) along with an upstream primer that in each case contained a T7 RNA polymerase promoter sequence. The DNA template for the 254 nt 16S rRNA *in vitro* run-off transcript encoding three Gs, 64 nt of the 5' leader sequence and part of the 16S rRNA coding sequence (up to + 187 nt) from the *rrnB* operon was made by PCR amplification using primers 16S (G)-up (5'-TAATACGACTCACTATAGGGACCA

AGTCTCAAGAGTGAACA -3'), 16S rRNA-Down (5'-CGACGTTATGCGGTATTAGCT -3'), and MG1693 genomic DNA as a template. The DNA template for the 344 nt 16S rRNA *in vitro* run-off transcript encoding three Gs, 154 nt of 5' leader sequence, and part of the 16S rRNA coding sequence (up to + 187 nt) in the *rrnB* operon was made by PCR amplification using primers 16S rRNA-up (5' -TAATACGACTCACTATAGGGAGAAGCGGCACTGCTCTTTAACA - 3'), 16S rRNA-Down (5'-CGACGTTATGCGGTATTAGCT-3'), and MG1693 genomic DNA as a template. The 344 nt 16S (b) rRNA substrate was the same as the 16S (a) rRNA substrate except that it contained 90 additional nt from the 5' leader region, which contained the known *in vivo* RNase E cleavage site at -66 nt position ¹¹. The DNA template for the 288 nt 9S rRNA *in vitro* run-off transcript encoding three Gs, 99 nt of 5' leader sequence, 120 nt of 9S rRNA whole coding sequence, and 66 nt of 3' trailer region in the *rrnD* operon was made by PCR amplification using primers 5S rRNA-up (5'- TAATACGACTCACTATAGGGATAACCTTACAA CGCCGAAGC-3'), 5S rRNA-Down (5'- ACTGGGGACCTCACCTTAC-3'), and MG1693 genomic DNA as a template. The DNA template for the 450 nt *rpsT* mRNA was amplified using primers PT7-RPST (5'-TAATACGACTCACTATAGGGAGAGCCATCA CTACGTAACGAGTG-3'), RPST-ANTI (5'-CGCATCACAAAAGCAGCAGGC - 3'), and MG1693 genomic DNA as a template, while the DNA template for the 461 nt *cspA* mRNA *in vitro* run off transcript was amplified using primers *cspA* - 5' UP (5'- TAATACGACTCACTATAGAACGGTTTGACGTAC AGACC -3'), *cspA* - 3' Down (5'- CGCGATCGATTATTTATT TCCTG -3'), and MG1693 genomic DNA as a template. The DNA template for the 140 nt *pheU* tRNA *in vitro* run-off transcript encoded three Gs, the entire *pheU* coding sequence and 63 nt of downstream sequence was amplified using primers PT-7 *pheU* (5'-TAATACGACTCACTATAGGCCCGGATAGCTCAGTC GG-3'), *pheU* antisense II (5'- CGCTTA AATCGTGGCGTCCTG-3'), and MG1693 genomic DNA as a template. The DNA template for the 505 nt *argX hisR leuT proM* *in vitro* run-off transcript was amplified using primers ArgX 5-end (5'-TAATA CGACTCACTATAGGCAACGGCGCTAAG CGCCCGTA-3'),

ProM-ter (5'-AGGGTGACGAAATGCACAGA-3'), and MG1693 genomic DNA as a template. The DNA template for the 452 nt *glyW-cysT-leuZ* *in vitro* run off transcript was amplified using primers GlyW 5' (5'-TAATACGACTCACTATAGGAACGGCGGCACTGATT GCC-3'), GlyW 3' (5'- ACGACAAGTTGCAGGCAC AT), and MG1693 genomic DNA as a template. *In vitro* transcription reactions were carried out at 30°C for 2-4 hours in 50 µl reaction volumes using 0.5 µg of DNA template, 500 µM each of GTP, ATP and UTP, 20 µM of CTP, 50 µCi [α -³²P]-CTP, 20 U RNasin (Promega), and 20 U T7 RNA polymerase (Promega) in a buffer containing 40 mM Tris-Cl pH 7.9, 6 mM MgCl₂, 10 mM NaCl, 10 mM DTT, 2 mM spermidine. Unlabeled run-off transcripts were transcribed as described above except that only non-radiolabeled nucleotides were added. All run-off transcripts (5'-triphosphorylated RNA) were extracted from 6% polyacrylamide/ 7M urea gels with phenol–chloroform–isoamyl alcohol (20:19:1), and then precipitated with ethanol. To generate 5'-monophosphorylated RNA, the 5'-triphosphorylated RNA was treated with Tobacco Acid Pyrophosphatase according to the manufacturer's instructions (Epicentre Technologies, Madison, WI, USA) as described previously ⁴².

RNase E and RNase G Cleavage Assays and Northern blot analysis

RNA cleavage assays with purified Rng and Rng-219 were carried out at 37°C in 60 µl reaction buffer (25 mM Tris-HCl pH 7.6, 100 mM NH₄Cl, 5 mM MnCl₂, 0.1 mM DTT, 0.1 mM EDTA, and 5% Glycerol). RNase E cleavage reactions were performed as described previously ³⁹. Approximately 1×10^5 - 2×10^5 Cerenkov counts of a uniformly labeled RNA substrate or 300-400 ng of non-radiolabelled RNA substrates were used per assay. The amount of purified proteins (RNase E, RNase G, and Rng-219) in each cleavage reaction is noted in each figure legend. For endonuclease activity assays, RNA transcripts were heated in the appropriate reaction buffer for 2 min at 50°C, 10 min at 37°C and chilled on ice prior to adding either purified

RNase E or RNase G protein preparations. Eight μ l samples were withdrawn at various time points and mixed with equal volume of 2 X RNA gel-loading buffer (95% Formamide, 18mM EDTA, and 0.025% SDS, Xylene Cyanol, and Bromophenol Blue). Samples were denatured at 95°C for 5 min and chilled on ice prior to loading onto either 6% or 8% polyacrylamide/7 M urea gels depending on the size of the particular substrate. For Northern blot analysis, the cleavage products were separated electrophoretically on a 6 % or 8% polyacrylamide/7 M urea gel and electroblotted to a Biotrans⁺ membrane. All oligonucleotide probes were 5'-end-labeled with [γ -³²P]-ATP using T4 polynucleotide kinase. The membranes were scanned with a PhosphorImager scanner (Storm 840 PC, Amersham Biosciences) and quantified using ImageQuant 5.2 software.

Primer extension analysis.

The unlabeled *argX hisR leuT proM* or *glyW cyst leuZ* run-off transcripts containing a 5'-monophosphate were prepared as described in above. Approximately 400 ng of the RNA substrate was used in cleavage reactions with purified Rng (60 ng), Rng-219 (60 ng), or Rne (12 ng). Reaction conditions were same as described above. Cleavage reactions were done in 60 μ l reaction volumes at 37°C. Aliquots were removed at 4 and 16 min, phenol extracted and precipitated with ethanol prior to primer extension. Primers 'c' (*HisR*), 'e' (*LeuT*), and 'g' (*ProM*) in Fig. 3.8, were end-labelled with [γ -³²P] ATP using T4 polynucleotide kinase (BioLabs). Primer extensions were carried out using ThermoScript[™] Reverse Transcriptase (Invitrogen) at 60°C according to the manufacturer's specification. The substrate RNA was degraded by adding RNase A and each reaction mixture was phenol-extracted before running on 6% polyacrylamide/7 M urea sequencing gels. Sequencing reactions performed with the same set of primers were electrophoresed along with the respective primer extension products to map the

cleavage sites. Similar reactions were carried out with the unlabeled *glyW cysT leuZ* run-off transcript.

Oligonucleotide probes and primers.

The sequences of the primers used in the experiments reported here are available on request.

ACKNOWLEDGEMENTS

We thank Bijoy Mohanty and Tariq Perwez for their help in preparation of this manuscript. This work was supported in part by a grant from the National Institutes of Health to S.R. K. (GM57220).

REFERENCES

1. Condon, C. & Putzer, H. (2002). The phylogenetic distribution of bacterial ribonucleases. *Nucleic Acids Res.* **30**, 5339-46.
2. Apirion, D. & Lassar, A. B. (1978). Conditional lethal mutant of *Escherichia coli* which affects processing of ribosomal RNA. *J. Biol. Chem.* **253**, 1738-1742.
3. Ono, M. & Kuwano, M. (1979). A conditional lethal mutation in an *Escherichia coli* strain with a longer chemical lifetime of mRNA. *J. Mol. Biol.* **129**, 343-357.
4. Ow, M. C., Liu, Q. & Kushner, S. R. (2000). Analysis of mRNA decay and rRNA processing in *Escherichia coli* in the absence of RNase E-based degradosome assembly. *Mol. Microbiol.* **38**, 854-866.

5. Arraiano, C. M., Yancey, S. D. & Kushner, S. R. (1988). Stabilization of discrete mRNA breakdown products in *ams pnp rnb* multiple mutants of *Escherichia coli* K-12. *J. Bacteriol.* **170**, 4625-4633.
6. Mackie, G. A. (1991). Specific endonucleolytic cleavage of the mRNA for ribosomal protein S20 of *Escherichia coli* requires the products of the *ams* gene *in vivo* and *in vitro*. *J. Bacteriol.* **173**, 2488-2497.
7. Regnier, P. & Hajnsdorf, E. (1991). Decay of mRNA encoding ribosomal protein S15 of *Escherichia coli* is initiated by an RNase E-dependent endonucleolytic cleavage that removes the 3' stabilizing stem and loop Structure. *J. Mol. Biol.* **187**, 23-32.
8. Li, Z. & Deutscher, M. P. (2002). RNase E plays an essential role in the maturation of *Escherichia coli* tRNA precursors. *RNA* **8**, 97-109.
9. Ow, M. C. & Kushner, S. R. (2002). Initiation of tRNA maturation by RNase E is essential for cell viability in *Escherichia coli*. *Genes Dev.* **16**, 1102-1115.
10. Wachi, M., Umitsuki, G., Shimizu, M., Takada, A. & Nagai, K. (1999). *Escherichia coli* *cafA* gene encodes a novel RNase, designated as RNase G, involved in processing of the 5' end of 16S rRNA. *Biochem. Biophys. Res. Comm.* **259**, 483-488.
11. Li, Z., Pandit, S. & Deutscher, M. P. (1999). RNase G (CafA protein) and RNase E are both required for the 5' maturation of 16S ribosomal RNA. *EMBO J.* **18**, 2878-85.
12. Umitsuki, G., Wachi, M., Takada, A., Hikichi, T. & Nagai, K. (2001). Involvement of RNase G in *in vivo* mRNA metabolism in *Escherichia coli*. *Genes Cells* **6**, 403-410.
13. Wachi, M., Naoko, K., Umitsuki, G., Clarke, D. P. & Nagai, K. (2001). A novel RNase G mutant that is defective in degradation of *adhE* mRNA but proficient in the processing of 16S rRNA precursor. *Biochem. Biophys. Res. Comm.* **289**, 1301-1306.

14. Ow, M. C., Perwez, T. & Kushner, S. R. (2003). RNase G of *Escherichia coli* exhibits only limited functional overlap with its essential homologue, RNase E. *Mol. Microbiol.* **49**, 607-622.
15. Lee, K., Bernstein, J. A. & Cohen, S. N. (2002). RNase G complementation of *rne* null mutation identified functional interrelationships with RNase E in *Escherichia coli*. *Mol. Microbiol.* **43**, 1445-1456.
16. Okada, Y., Wachi, M., Hirata, A., Suzuki, K., Nagai, K. & Matsushashi, M. (1994). Cytoplasmic axial filaments in *Escherichia coli* cells: possible function in the mechanism of chromosome segregation and cell division. *J. Bacteriol.* **176**, 917-922.
17. Wachi, M., Umitsuki, G. & Nagai, K. (1997). Functional relationship between *Escherichia coli* RNase E and the CafA protein. *Mol. Gen. Genet.* **253**, 515-519.
18. Deana, A. & Belasco, J. G. (2004). The function of RNase G in *Escherichia coli* is constrained by its amino and carboxyl termini. *Mol. Microbiol.* **51**, 1205-1217.
19. Jiang, X., Diwa, A. & Belasco, J. G. (2000). Regions of RNase E important for 5'-end-dependent RNA cleavage and autoregulated synthesis. *J. Bacteriol.* **182**, 2468-75.
20. Tock, M. R., Walsh, A. P., Carroll, G. & McDowall, K. J. (2000). The CafA protein required for the 5'-maturation of 16 S rRNA is a 5'-end-dependent ribonuclease that has context-dependent broad sequence specificity. *J. Biol. Chem.* **275**, 8726-8732.
21. Jourdan, S. S. & McDowall, K. J. (2008). Sensing of 5' monophosphate by *Escherichia coli* RNase G can significantly enhance association with RNA and simulate the decay of functional mRNA transcripts *in vivo*. *Mol. Microbiol.* **67**, 102-115.
22. Mackie, G. A. (1998). Ribonuclease E is a 5'-end-dependent endonuclease. *Nature* **395**, 720-723.
23. Mackie, G. A. (2000). Stabilization of circular *rpsT* mRNA demonstrates the 5'-end dependence of RNase E action *in vivo*. *J. Biol. Chem.* **275**, 25069-25072.

24. Jiang, X. & Belasco, J. G. (2004). Catalytic activation of multimeric RNase E and RNase G by 5'-monophosphorylated RNA. *Proc. Natl. Acad. Sci. USA* **101**, 9211-9216.
25. Callaghan, A. J., Grossman, J. G., Redko, Y. U., Ilag, L. L., Moncrieffe, M. C., Symmons, M. F., Robinson, C. V., McDowall, K. J. & Luisi, B. F. (2003). Quaternary Structure and catalytic activity of the *Escherichia coli* ribonuclease E amino-terminal catalytic domain. *Biochemistry* **42**, 12848-13855.
26. Callaghan, A. J., Redko, Y. U., Murphy, L. M., Grossman, J. G., Yates, D., Garman, E., Ilag, L. L., Robinson, C. V., Symmons, M. F., McDowall, K. J. & Luisi, B. F. (2005). "Zn-Link": a metal sharing interface that organizes the quaternary Structure and catalytic site of endoribonuclease, RNase E. *Biochemistry* **44**, 4667-4775.
27. Callaghan, A. J., Marcaida, M. J., Stead, J. A., McDowall, K. J., Scott, W. G. & Luisi, B. F. (2005). Structure of *Escherichia coli* RNase E catalytic domain and implications for RNA turnover. *Nature* **437**, 1187-1191.
28. Briant, D. J., Hankins, J. S., Cook, M. A. & Mackie, G. A. (2003). The quaternary Structure of RNase G from *Escherichia coli*. *Mol. Microbiol.* **50**, 1381-1390.
29. Chung, D.-H., Min, Z., Wang, B.-C. & Kushner, S. R. (2008). Single amino acid changes in the predicted RNase H domain of *E. coli* RNase G lead to the complementation of RNase E mutants. *Nucleic Acids Res.*, submitted.
30. Carpousis, A. J., Van Houwe, G., Ehretsmann, C. & Krisch, H. M. (1994). Copurification of *E. coli* RNAase E and PNPase: Evidence for a specific association between two enzymes important in RNA processing and degradation. *Cell* **76**, 889-900.
31. Py, B., Higgins, C. F., Krisch, H. M. & Carpousis, A. J. (1996). A DEAD-box RNA helicase in the *Escherichia coli* RNA degradosome. *Nature* **381**, 169-172.

32. Mohanty, B. K. & Kushner, S. R. (2003). Genomic analysis in *Escherichia coli* demonstrates differential roles for polynucleotide phosphorylase and RNase II in mRNA abundance and decay. *Mol. Microbiol.* **50**, 645-658.
33. Ghora, B. K. & Apirion, D. (1978). Structural analysis and *in vitro* processing to p5 rRNA of a 9S RNA molecule isolated from an *rne* mutant of *E. coli*. *Cell* **15**, 1055-1066.
34. Bernstein, J. A., Lin, P.-H., Cohen, S. N. & Lin-Chao, S. (2004). Global analysis of *Escherichia coli* RNA degradosome function using DNA microarrays. *Proc. Natl. Acad. Sci. USA* **101**, 2748-2763.
35. Kaga, N., Umitsuki, G., Nagai, K. & Wachi, M. (2002). RNase G-dependent degradation of the *eno* mRNA encoding a glycolysis enzyme enolase in *Escherichia coli*. *Biosci. Biotechnol. Biochem.* **66**, 2216-2220.
36. Hankins, J. S., Zappavigna, C., Prud'homme-Genereux, A. & Mackie, G. A. (2007). Role of RNA Structure and susceptibility to RNase E in regulation of a cold shock mRNA, *cspA* mRNA. *J. Bacteriol.* **189**, 4353-5358.
37. Mohanty, B. K. & Kushner, S. R. (1999). Analysis of the function of *Escherichia coli* poly(A) polymerase I in RNA metabolism. *Mol. Microbiol.* **34**, 1094-1108.
38. Warren, J. W., Walker, J. R., Roth, J. R. & Altman, E. (2000). Construction and characterization of a highly regulable expression vector, pLAC11, and its multipurpose derivatives, pLAC22 and pLAC33. *Plasmid* **44**, 138-151.
39. Perwez, T. & Kushner, S. R. (2006). RNase Z in *Escherichia coli* plays a significant role in mRNA decay. *Mol. Microbiol.* **60**, 723-737.
40. Sedmak, J. J. & Grossberg, S. E. (1977). A rapid, sensitive, and versatile assay for protein using Coomassie brilliant blue G250. *Anal. Biochem.* **79**, 544-552.
41. Sambrook, J. & Russell, D. W. (2001). *Molecular cloning: A laboratory manual*. 3rd edit, Cold Spring Harbor Laboratory Press.

42. Mohanty, B. K. & Kushner, S. R. (2008). Rho-independent transcription terminators inhibit RNase P processing of the *secG leuU* and *metT* tRNA polycistronic transcripts in *Escherichia coli*. *Nucleic Acids Res.* **36**, 364-375.
43. Roy, M. K., Singh, B., Ray, B. K. & Apirion, D. (1983). Maturation of 5S rRNA: Ribonuclease E cleavages and their dependence on precursor sequences. *Eur. J. Biochem.* **131**, 119-127.

Table 3.1 Relative activity of RNase G, Rng-219 and RNase E on tRNA transcripts terminated with either a 5' phosphomonoester or 5' triphosphate.

Ratio of Activity on 5' P versus 5' PPP terminated substrate ¹			
Enzyme/Transcript	RNase G	Rng-219	RNase E
<i>pheU</i>	2.4	2.7	15.5
<i>argX</i>	1.5	3.7	10.1
<i>hisR</i>	5.6	12	25.7
<i>leuT</i>	5.6	10.0	22.3
<i>proM</i>	4.0	8.1	14.3
<i>glyW</i>	0.9	1.2	1.1
<i>cysT</i>	1.3	1.2	0.9
<i>leuZ</i>	1.8	1.8	1.9
<i>rpsT</i>	2.7	2.4	4.9

¹Ratios were determined from the data presented in Figures 3.7-3.9 and other experiments with the *glyW* operon that are not shown.

Figure 3.1. Purification of His-tagged Rng and Rng-219 proteins.

Three μg of purified His-tagged Rng and Rng-219 derived from the pooled Mono Q column fractions (*Materials and Methods*) were electrophoresed in an 8% SDS–polyacrylamide gel. (A) Coomassie blue stained SDS-PAGE gel. (B) Silver stained SDS-PAGE gel. (C) Western blot analysis of purified His-tagged RNase G protein derivatives probed with polyclonal anti-RNase G antibody as described in *Materials and Methods*. Lane M contains size standards, which are indicated on the left. The ~ 56 kDa of purified His-tagged RNase G protein derivatives are indicated by an arrow on the right.

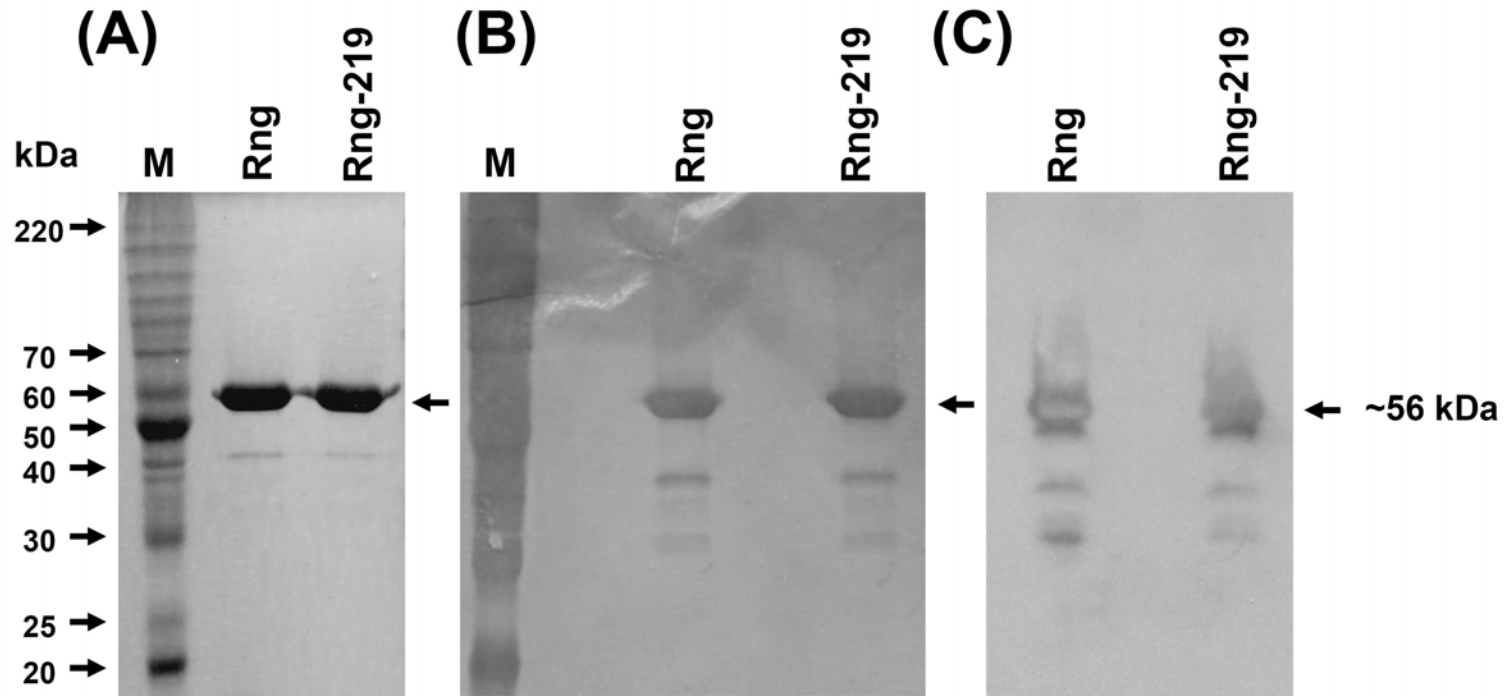
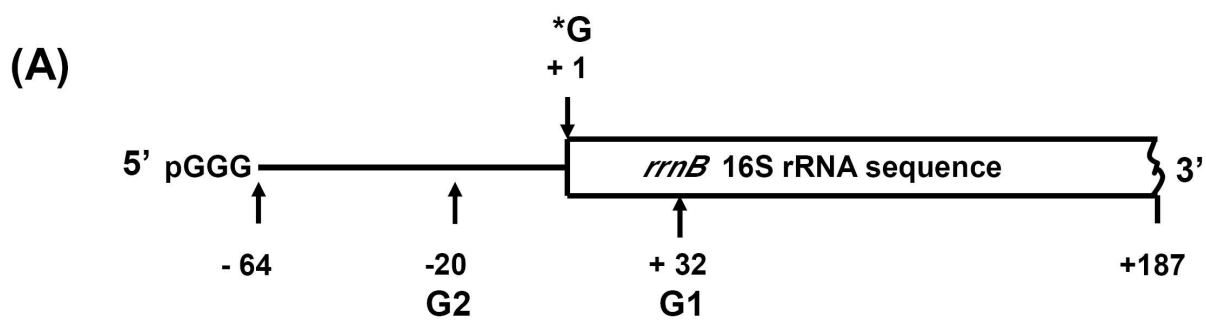


Figure 3.2. Analysis of RNase G activity at various reaction conditions.

(A) Schematic diagram of 16S rRNA *in vitro* run-off transcript containing a 5'-monophosphate, synthesized as described in *Materials and methods*. The 254-nt RNA, which contains three extra 'G's at the 5' end of transcript encompasses residues from – 64 of the 5' leader sequence to residue +187 (the 5' portion of the 16s rRNA coding sequence from the *rrnB* rRNA operon). The rRNA region is shown as an open box, and +1 position is the mature 5'-terminus of 16S rRNA. Based on the *in vitro* analysis described in (B) the major RNase G cleavage sites (G1 and G2) are marked with upward arrows. *G (+1), marked with a downward arrow is the known *in vivo* RNase G cleavage site^{10;11}. (B) Reactions (60 µl total volume) were carried out for 5 and 10 min at 37°C in the presence of 120 ng of purified RNase G (except reaction 'a') and an internally ³²P-labeled 16S (a) rRNA substrate containing a 5'-monophosphate. The products were separated on an 8% polyacrylamide/7 M urea gel. Reaction 'a' (lanes 1 and 2), incubated without enzyme in standard reactions conditions (25 mM Tris-HCl pH 7.6, 100 mM NH₄Cl, 5 mM MnCl₂, 0.1 mM DTT, 0.1 mM EDTA, and 5% Glycerol); reaction 'b' (lanes 3 and 4), same as reaction 'a' except 1 mM MnCl₂ instead of 5 mM MnCl₂; reaction 'c' (lanes 5 and 6), same as reaction 'a' except 3 mM MnCl₂ instead of 5 mM MnCl₂; reaction 'd' (lanes 7 and 8), same as reaction 'a'; reaction 'e' (lanes 9 and 10), same as reaction 'a' except 1 mM MgCl₂ instead of 5 mM MnCl₂; reaction 'f' (lanes 11 and 12), same as reaction 'a' except for 5 mM MgCl₂ instead of 5 mM MnCl₂; reaction 'g' (lanes 13 and 14), same as reaction 'c' except for adding 60 mM KCl; reaction 'h' (lanes 15 and 16), same as reaction 'a' except for adding 60 mM KCl; reaction 'i' (lanes 17 and 18), same as reaction 'f' except for adding 60 mM KCl and pH 7.7, which was the identical reaction condition as described in Briant *et al.*²⁸. The time of digestion is shown above each lane. The positions of the full-length substrate (254 nt) and the two major products (155 and 207 nt) are shown in the left margin with arrows.



(B)

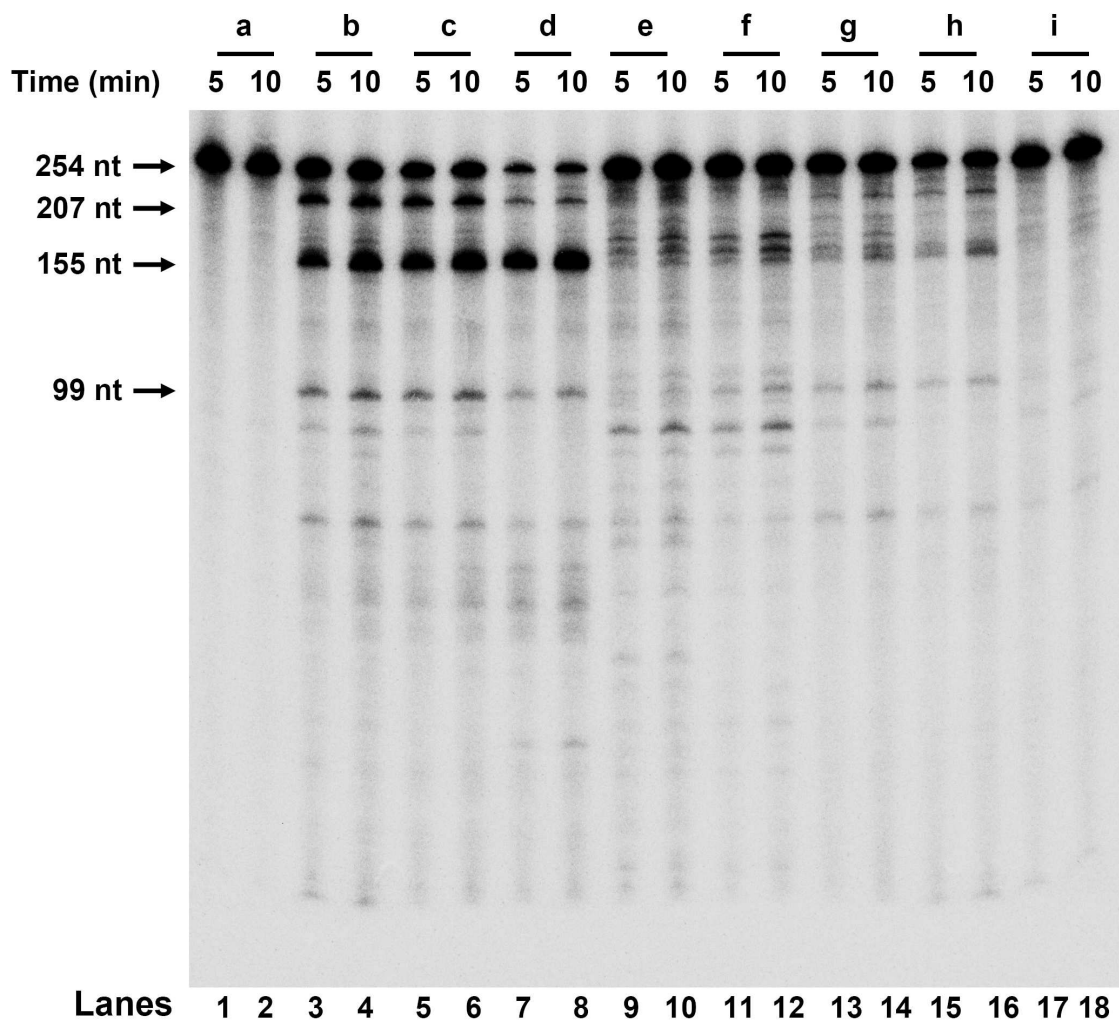
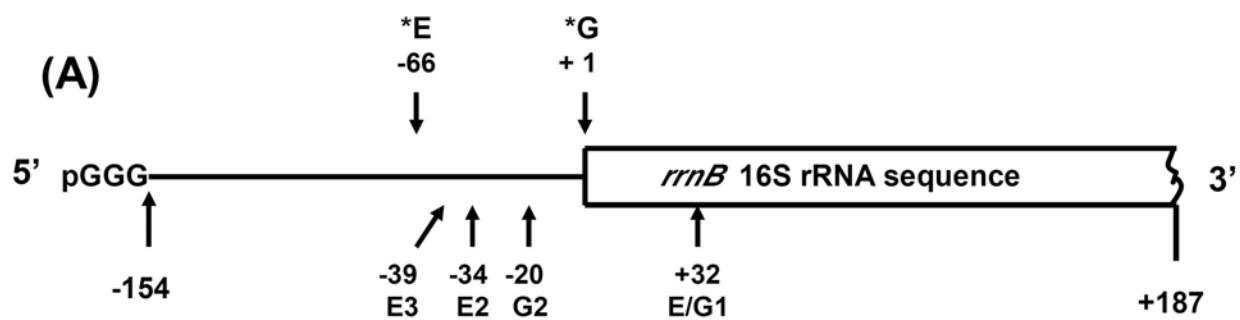


Figure 3.3. Processing of the 16S rRNA by RNase G, Rng-219 and RNase E.

(A) Schematic diagram of 16S rRNA *in vitro* run-off transcript. A 344 nt RNA, which contained three extra 'G's at the 5' end of transcript and encompassed residues from -154 of 5' leader sequence (including *in vivo* cleavage sites of RNase E and RNase G¹¹) to residue +187 (the 5' portion of the 16S rRNA coding sequence). The rRNA region is shown as an open box with the +1 position being the mature 5'-terminus of 16S rRNA. Based on the *in vitro* analysis, the overlapping RNase G and RNase E cleavage site that generates the 155 nt product is designated at E/G1 (upward arrow). Other RNase E and RNase G cleavage sites mapped by primer extension analysis (data not shown) are marked by upward arrows. marked at the top with arrows, The known *in vivo* RNase E and RNase G cleavage sites [*E (-66) and *G (+1)] are marked with downward arrows. (B) Internally ³²P-labeled 344 nt 16S rRNA substrate containing a 5'-monophosphate, was incubated without enzyme (lane 1), with 60 ng of RNase G (lanes 2 to 4), with 60 ng of Rng-219 (lanes 5 to 7), and with 6 ng of RNase E (lanes 8 to 10), the products were separated on a 6 % polyacrylamide/7 M urea gel (see *Materials and Methods*). The time of digestion is shown above each lane. The positions of the full length substrate (344 nt), and the major products derived by RNase E and RNase G cleavage activity are designated by leftward arrows. The composition of the bands are indicated by the star were not determined.



(B)

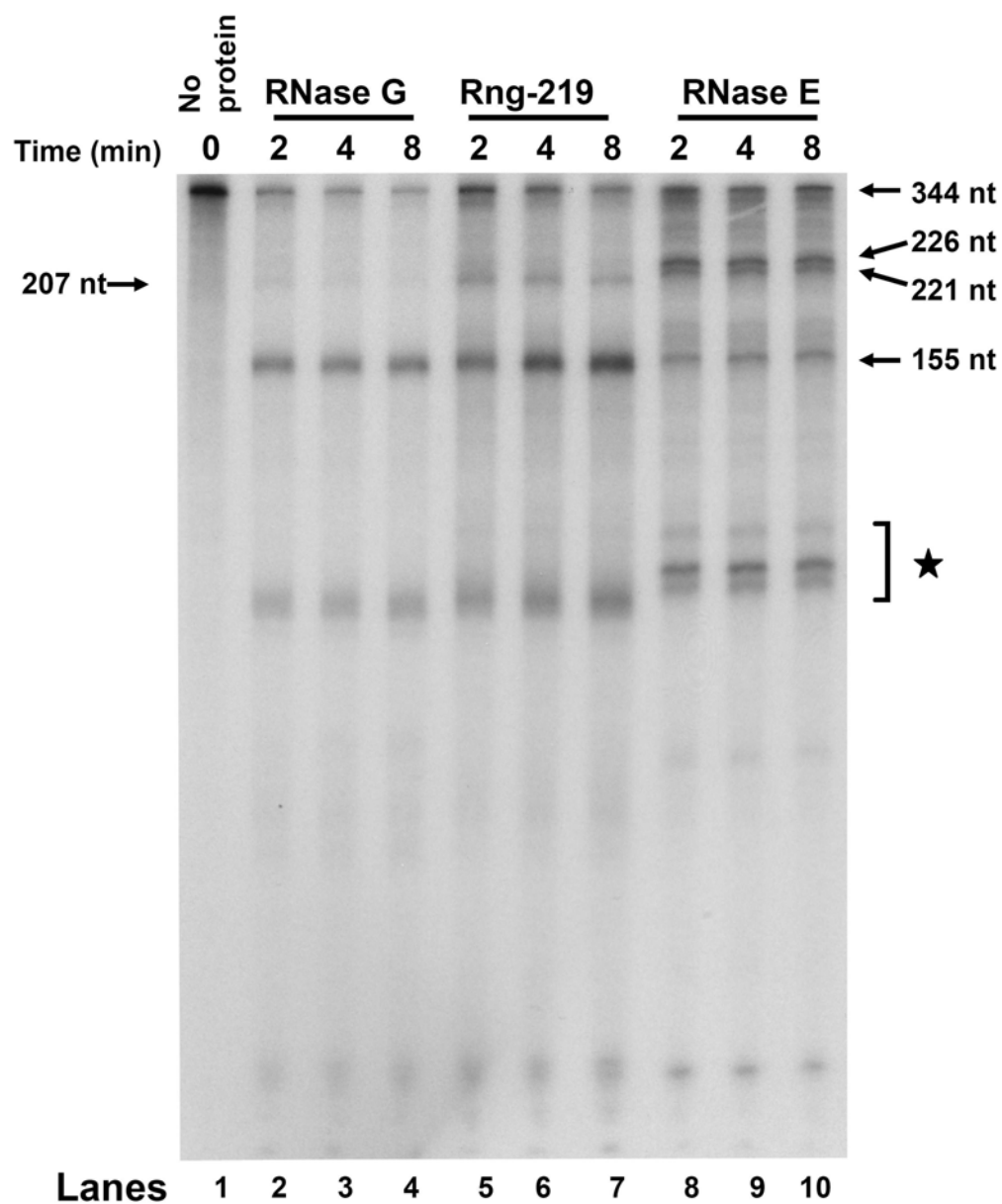


Figure 3.4. *In vitro* analysis of the processing of 9S rRNA.

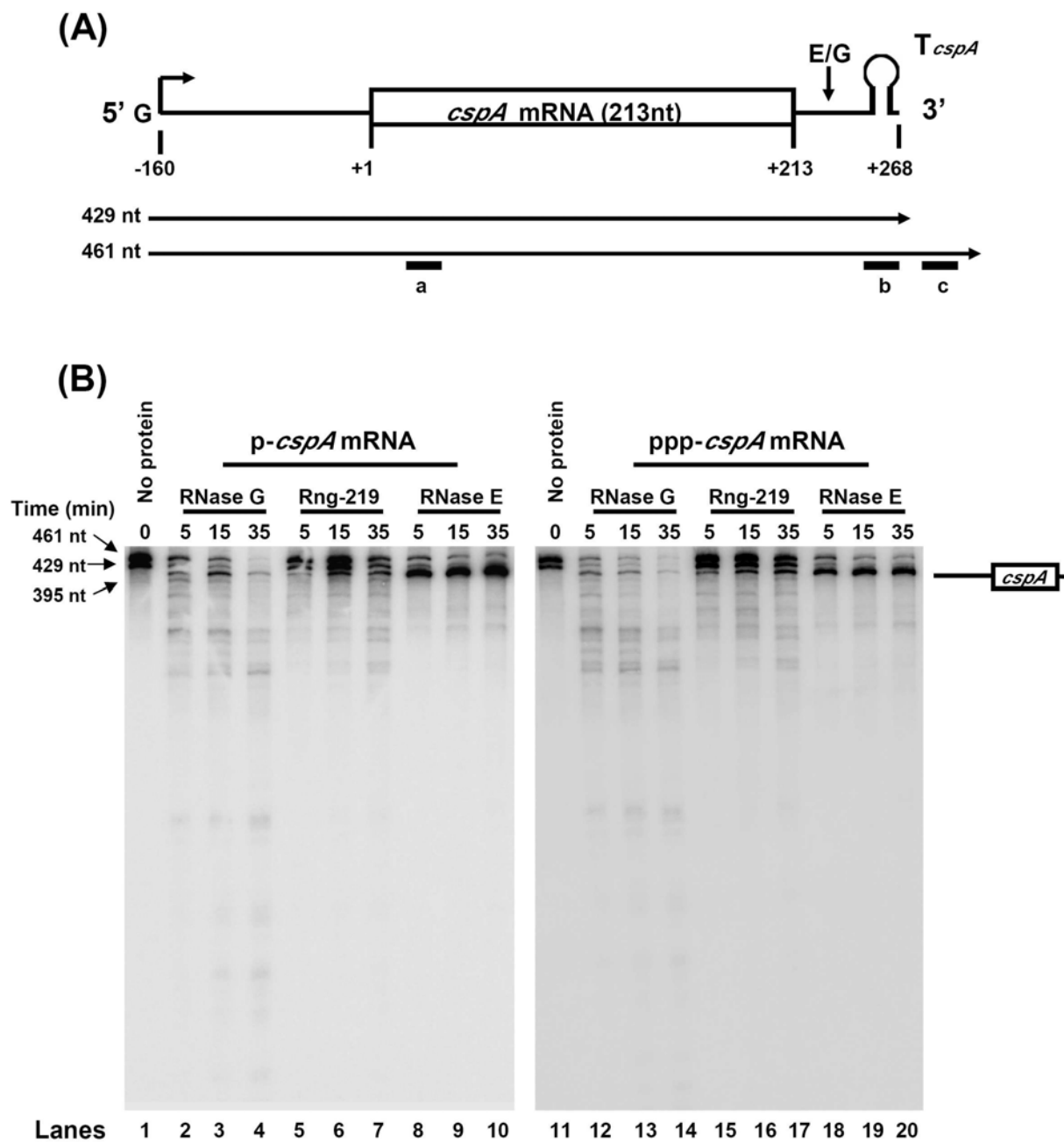
(A) Schematic diagram of 9S rRNA *in vitro* run-off transcript. The 288 nt RNA, which represents the 9S rRNA processing intermediate contains 3 extra 'G's at the 5' end of the transcript. The mature 5S rRNA is shown as an open rectangle and the extra sequences are shown as lines. Based on our *in vitro* analysis, which is in agreement with previous studies⁴³, the RNase E and RNase G cleavage sites [E1/G1 (located at 3 nt upstream from 5' mature end of 5S rRNA) and E2/G2 (located at 3 nt downstream from 3' mature end of 5S rRNA)] are marked with upward arrows. (B) Internally ³²P-labeled 9S rRNA substrate with a 5'-monophosphate terminus derived by treatment with TAP (see *Materials and Methods*) was incubated without enzyme (lane 1), with 60 ng of RNase G (lanes 2 to 5), with 60 ng of Rng-219 (lanes 6 to 9), and with 12 ng of RNase E (lanes 10 to 13). The products were separated on an 8% polyacrylamide/ 7 M urea gel (see *Materials and Methods*). The time of digestion is shown above each lane. The positions of the full-length substrate (288 nt) and the p5S product (126 nt) derived from either RNase E or RNase G cleavage activity are marked in the right margin. The presence of the extra nt at the 5' end of the 126 nt fragment was determined by primer extension analysis (data not shown).

Figure 3.5. *In vitro* analysis of the processing of the *rpsT* mRNA.

(A) Schematic diagram of the *rpsT* mRNA *in vitro* transcript used in this study. The *rpsT* mRNA coding region is indicated as an open rectangle and the extra sequences are shown as lines. The 450 nt *in vitro* generated mRNA substrate contains three extra 'G's at the 5' end of transcript along with the P1 promoter initiation site (-133) and ends at the encoded Rho independent transcription terminator. The internally ³²P-labeled transcript was synthesized as described in *Materials and Methods*. (B and C) The *rpsT* mRNA terminated with either a 5'-monophosphate (B) or a 5'-triphosphate (C) was incubated without enzyme (lane 1), with 120 ng of RNase G (lanes 2 to 5), with 120 ng of Rng-219 (lanes 6 to 9), and with 24 ng of RNase E (lanes 10 to 13), the products were separated on a 6 % polyacrylamide/7 M urea gel (see *Materials and Methods*). The time of digestion is shown above each lane. The primary RNase E digestion products as predicted from earlier work^{6; 39} are marked in the right margin. The full-length transcript is marked in the left margin.

Figure 3.6. *In vitro* analysis of the processing of the *cspA* mRNA.

(A) Schematic diagram of the *cspA* mRNA *in vitro* transcripts. A schematic of the two *cspA* transcripts are shown. They contain one extra 'G' at the 5' terminus, 160 nt from the *in vivo* encoded 5' UTR, the *cspA* ORF (open rectangle) and 268 downstream nt that contains the Rho independent transcription terminator. Based on our *in vitro* analysis and the work of ³⁶, the primary RNase E/G cleavage site (located 20 nt downstream of the translation terminator codon) with a downward arrow. The 429 nt transcripts arose from termination at the encoded Rho independent transcription terminator, while the 461 nt occurred through run-off transcription to the end of the DNA template. The probes used for the Northern analyses are positioned below the transcript. (B and C) Unlabeled *cspA* mRNA substrates containing either 5'-triphosphate or 5'-monophosphate was incubated without enzyme (lanes 1 and 11), with 120 ng of RNase G (lanes 2 to 4, and 12 to 14), with 120 ng of Rng-219 (lanes 5 to 7, and 15 to 17), and with 18 ng of RNase E (lanes 8 to 10, and 18 to 20). The reactions products were separated electrophoretically on an 8% polyacrylamide/7 M urea gel (see *Materials and Methods*). The time (min) of digestion is shown above each lane. The same membrane was used for probing with each oligonucleotide after stripping following the recommendations of the membrane manufacturer. The positions of the two full-length substrates and major cleavage products are shown in the right margin of each gel picture. (B) Probe a. (C) Probe b.



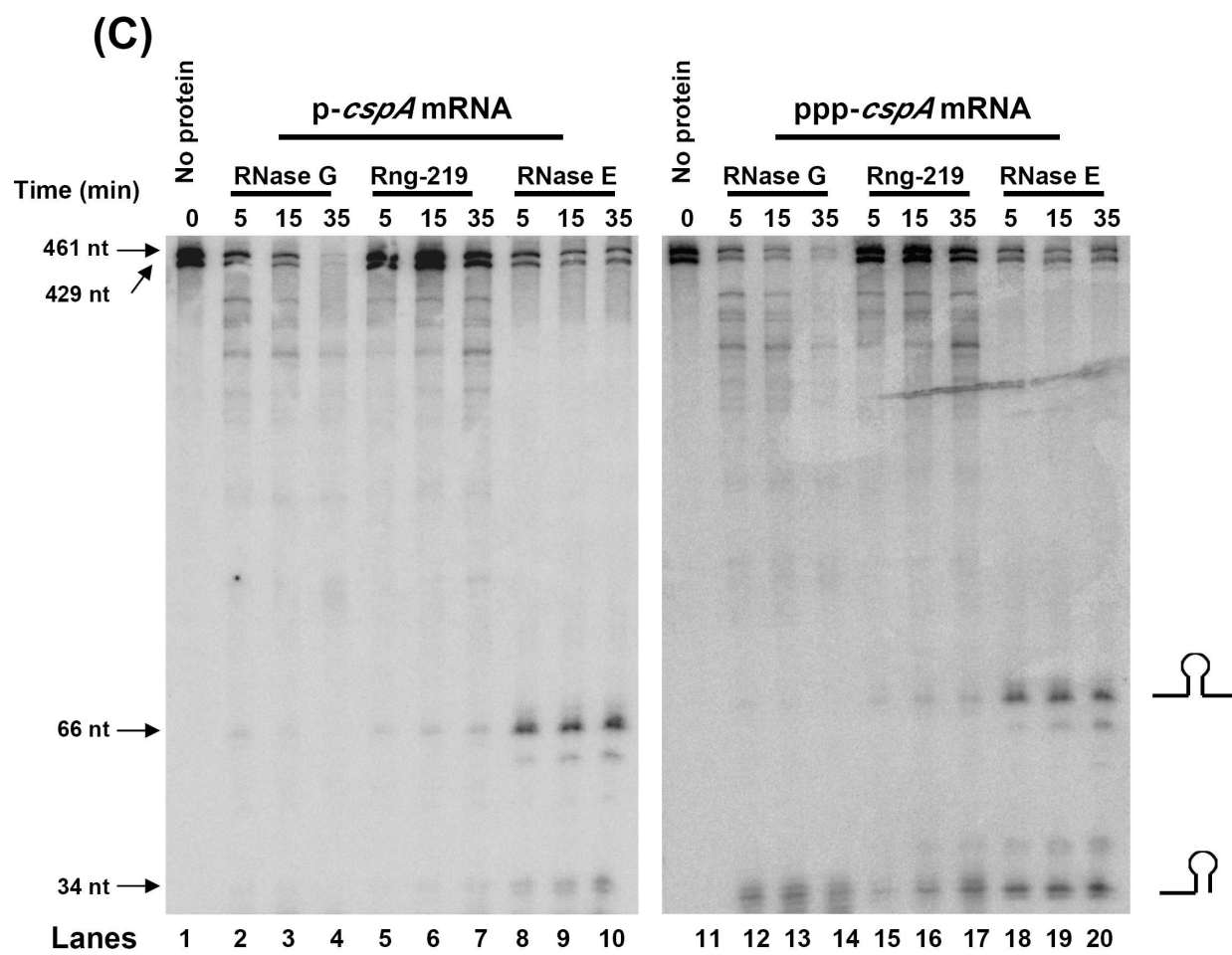
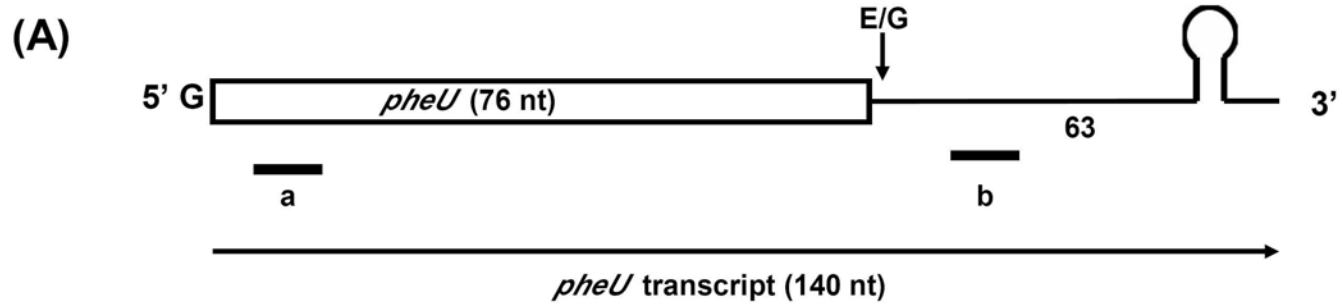
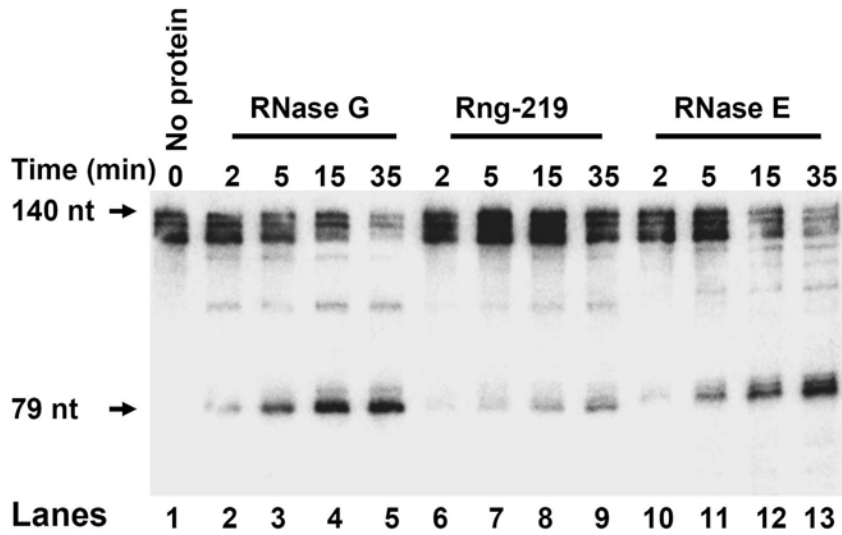


Figure 3.7. *In vitro* analysis of processing of the *pheU* tRNA substrate.

(A) Schematic diagram of the *pheU* tRNA *in vitro* run-off transcript. The DNA template used for the *in vitro* transcription contained one extra 'G' upstream of the mature *pheU* tRNA, the 76 nt mature *pheU* sequence (open rectangle) and 63 downstream nt including the Rho independent transcription terminator. Transcription with T7 RNA polymerase (see *Materials and Methods*) generated a full-length 140 nt species as well as two slight smaller premature termination products. The probes used for the analysis are also positioned below the transcript. The major RNase E/G [E/G (located at 1-2 nt downstream from the encoded CCA element)] cleavage site is marked with a downward arrow. (B and C) Northern analysis was done using the same 5'-end-labeled probe a. Unlabeled *pheU* tRNA transcripts terminated with either a 5'-monophosphate (B) or a 5'-triphosphate (C) were incubated without enzyme (lanes 1), or with 150 ng of RNase G (lanes 2 to 5), 150 ng of Rng-219 (lanes 6 to 9), or 30 ng of RNase E (lanes 10 to 13). The products were separated electrophoretically on an 8 % polyacrylamide/7 M urea gel (see *Materials and Methods*). The time of each digestion is shown above lanes. The positions of the full-length substrate (140 residues) and major product are shown in the left margin. The composition of the bands (★) generated by RNase G and Rng-219 was not determined.



(B) p-*pheU* tRNA



(C) ppp-*pheU* tRNA

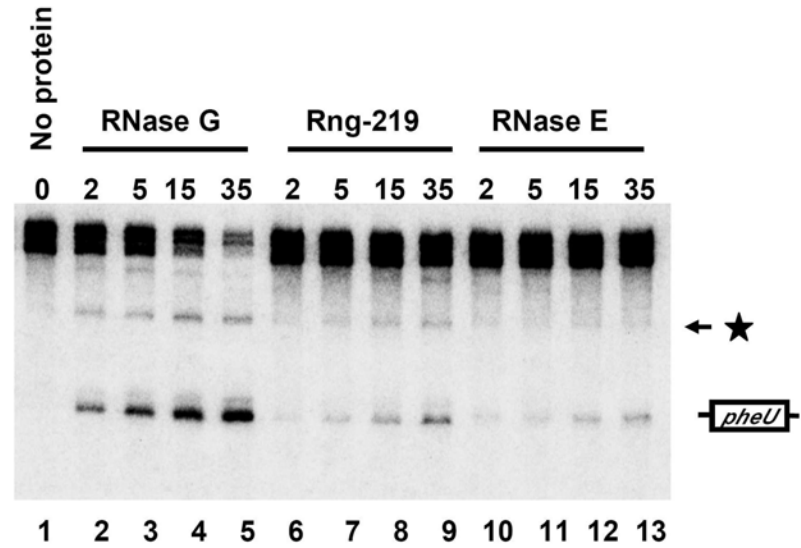


Figure 3.8. *In vitro* analysis of the processing of the *argX hisR leuT proM* polycistronic transcript.

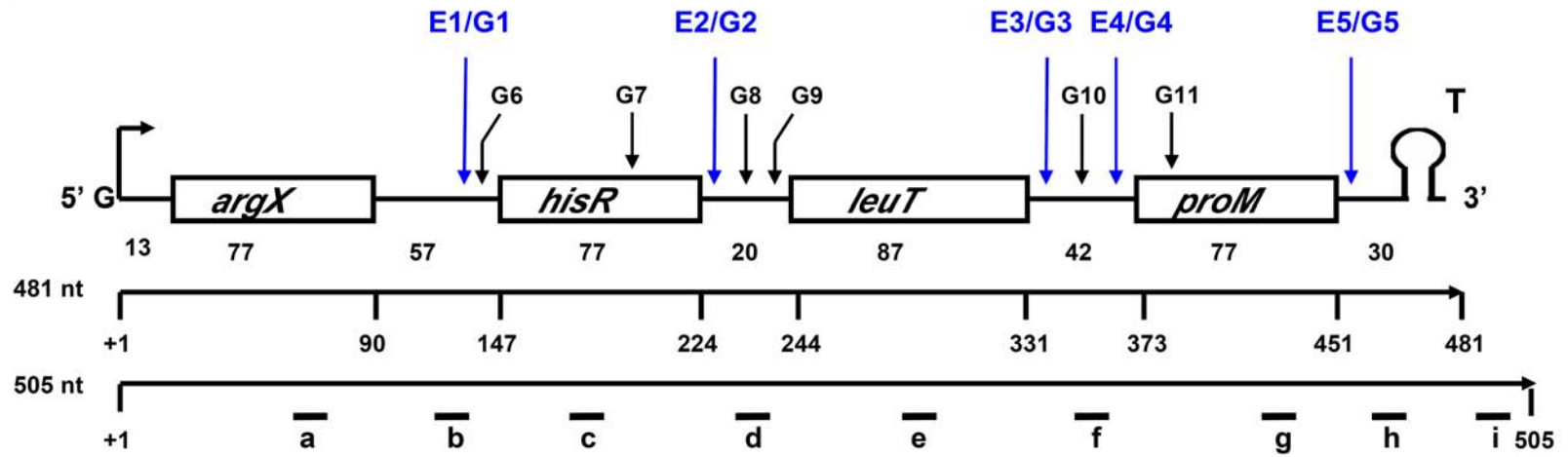
(A) Schematic drawing of the *argX hisR leuT proM* operon DNA template used for *in vitro* transcription. The fragment contains one extra 'G' upstream of the *in vivo* transcription start site as well as 24 extra nt downstream of the Rho independent transcription terminator.

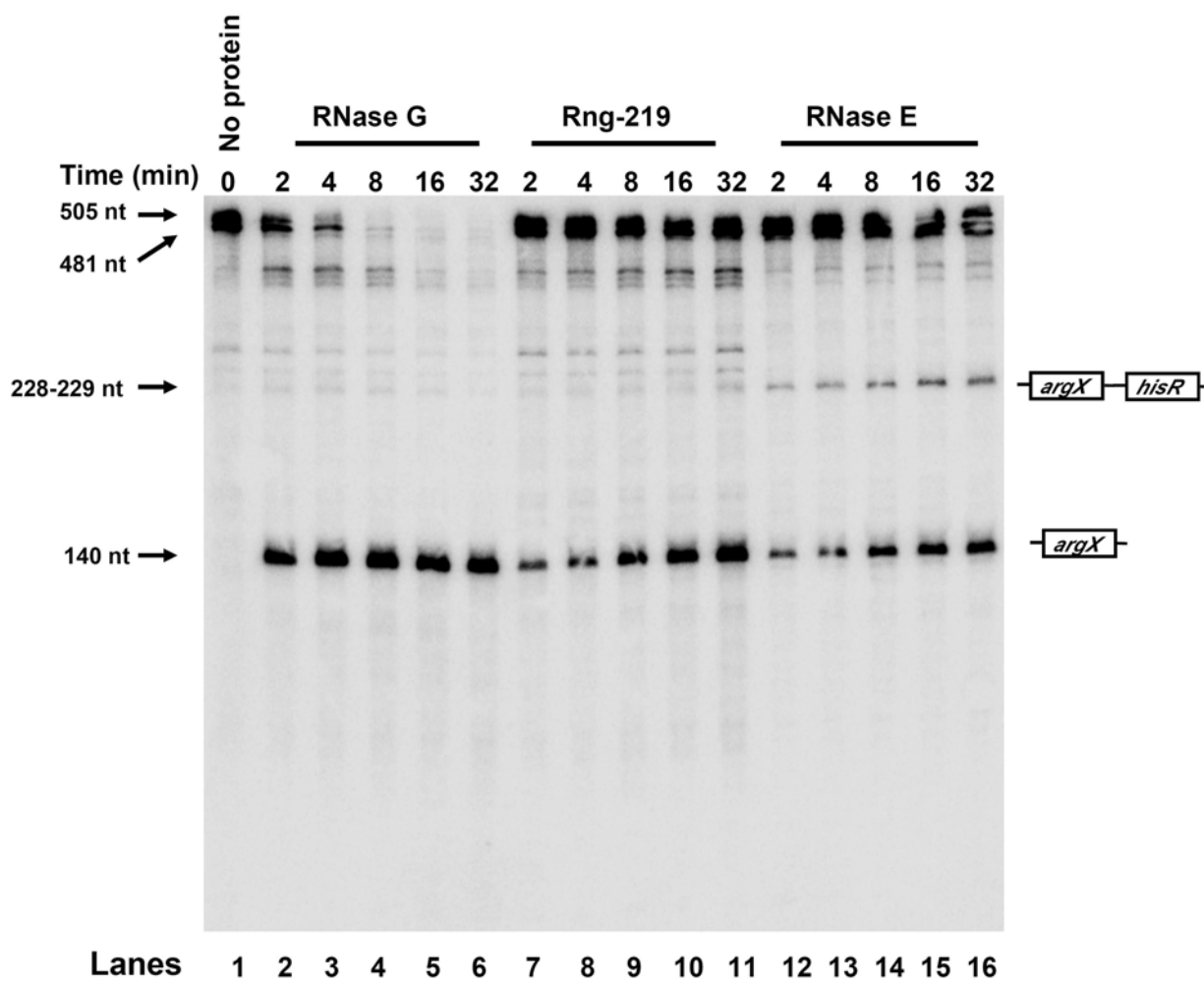
Transcription using this DNA template resulted in two species, a 505 nt run-off transcript and a 481 nt species arising from termination at the encoded Rho independent transcription terminator.

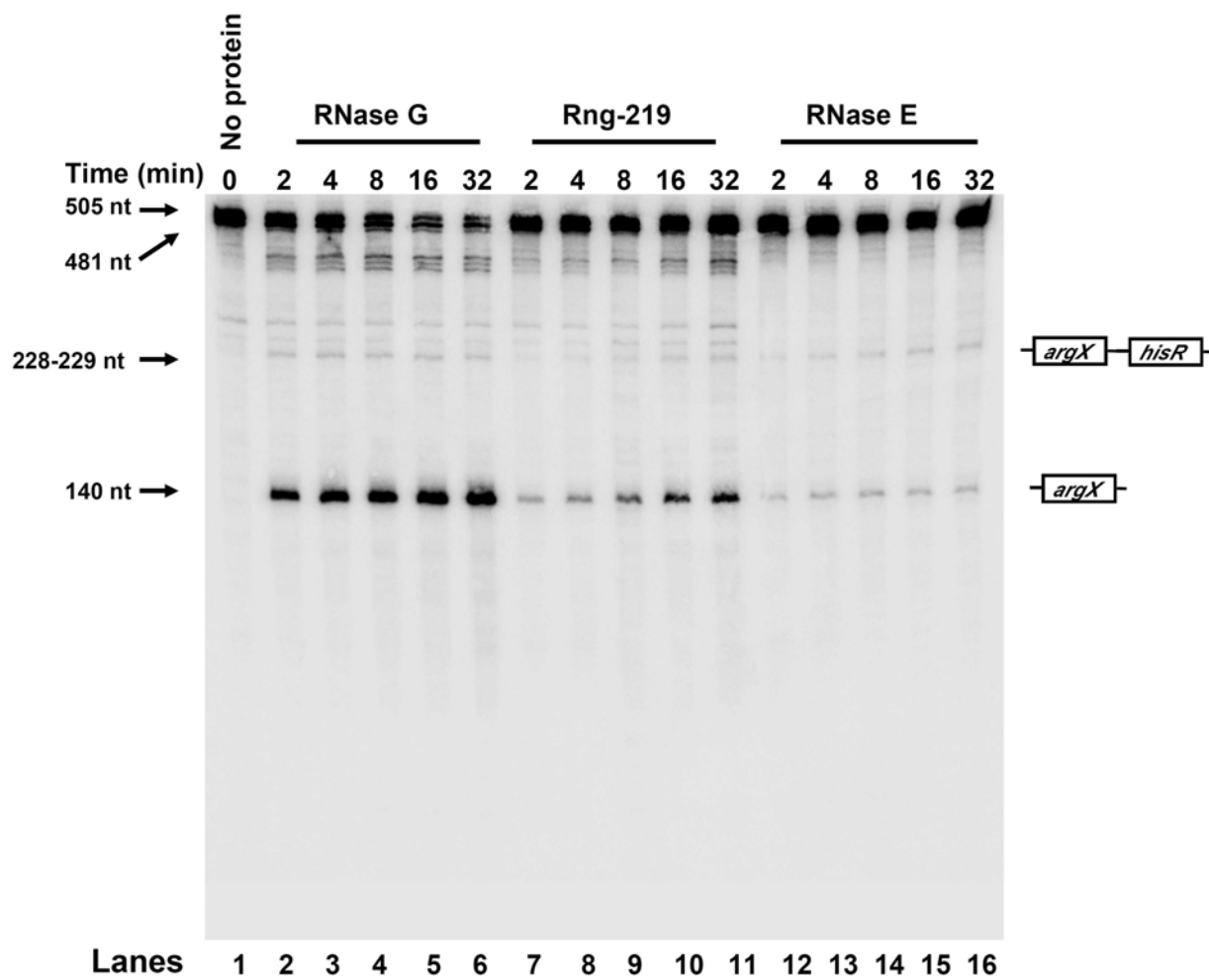
Based on our *in vitro* analysis the overlapping RNase E/G cleavage sites are marked with downward blue arrows. Additional RNase G specific cleavage sites are marked with downward black arrows. The locations of the probes used for the analysis are positioned below the transcript.

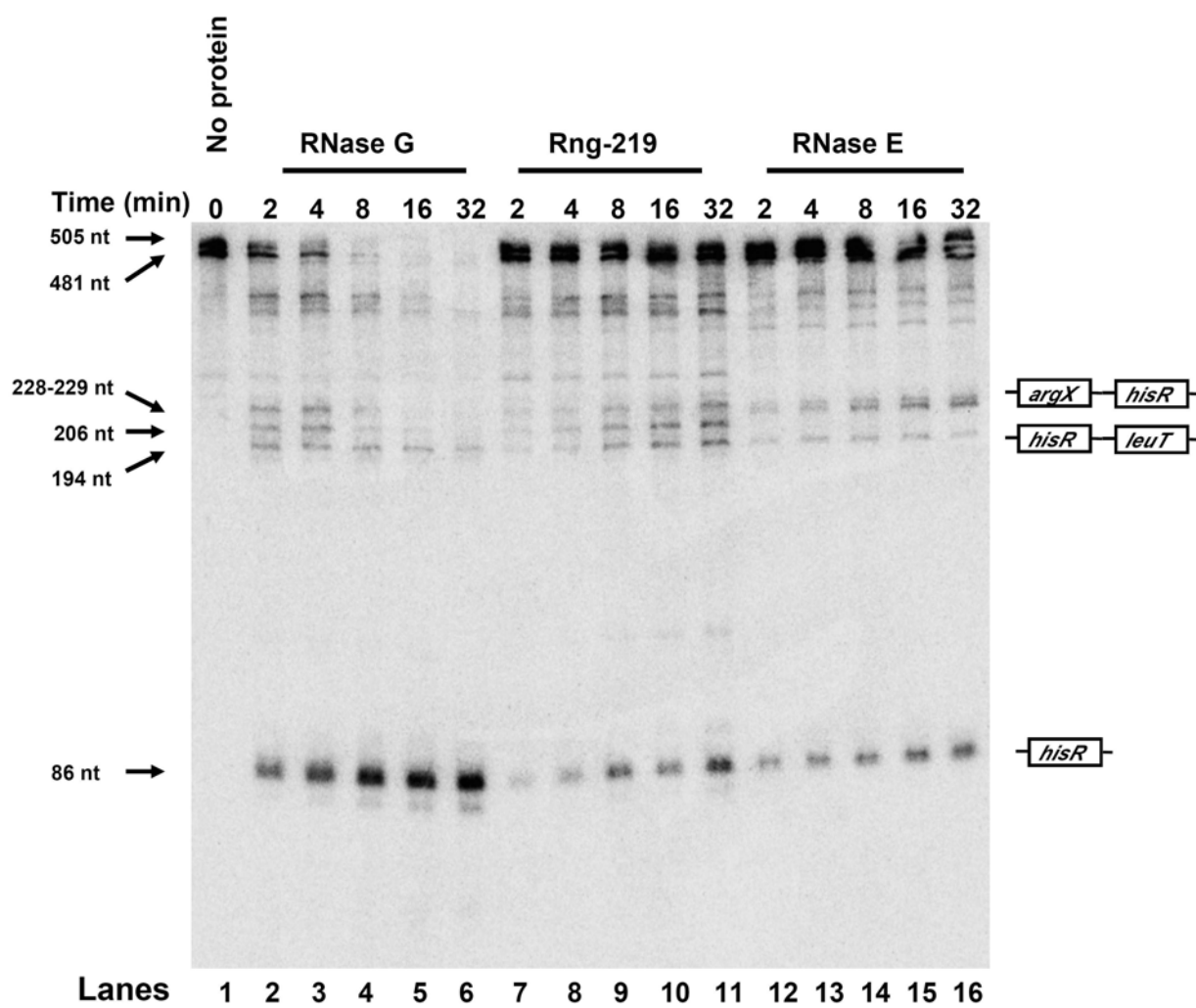
(B - I) The unlabeled *argX hisR leuT proM* polycistronic transcripts containing either a 5'-monophosphate terminus (B, D, F, H) or a 5' triphosphate terminus (C, E, G, I) were incubated without enzyme (lanes 1), with 30 ng of RNase G (lanes 2 to 6), with 30 ng of Rng-219 (lanes 7 to 11), and with 6 ng of RNase E (lanes 12 to 16). The products were separated electrophoretically on a 6 % polyacrylamide/7 M urea gel (see *Materials and Methods*). The two membranes (one for the 5' monophosphate substrate and one for the 5' triphosphate substrate) used for the four Northern blots shown in this figure were sequentially probed by following the recommendations of the manufacturer for membrane stripping. The composition of the major cleavage products are shown in the right margins. The time of digestion is shown above each lane. (B) 5' monophosphate species probed for *argX* (probe a). (C) 5' triphosphate species probed for *argX* (probe a). (D) 5' monophosphate species probed for *hisR* (probe c). (E) 5' triphosphate species probed for *hisR* (probe c). (F) 5' monophosphate species probed for *leuT* (probe e). (G) 5' triphosphate species probed for *leuT* (probe e). (H) 5' monophosphate species probed for *proM* (probe g). (I) 5' triphosphate species probed for *proM* (probe g).

(A)

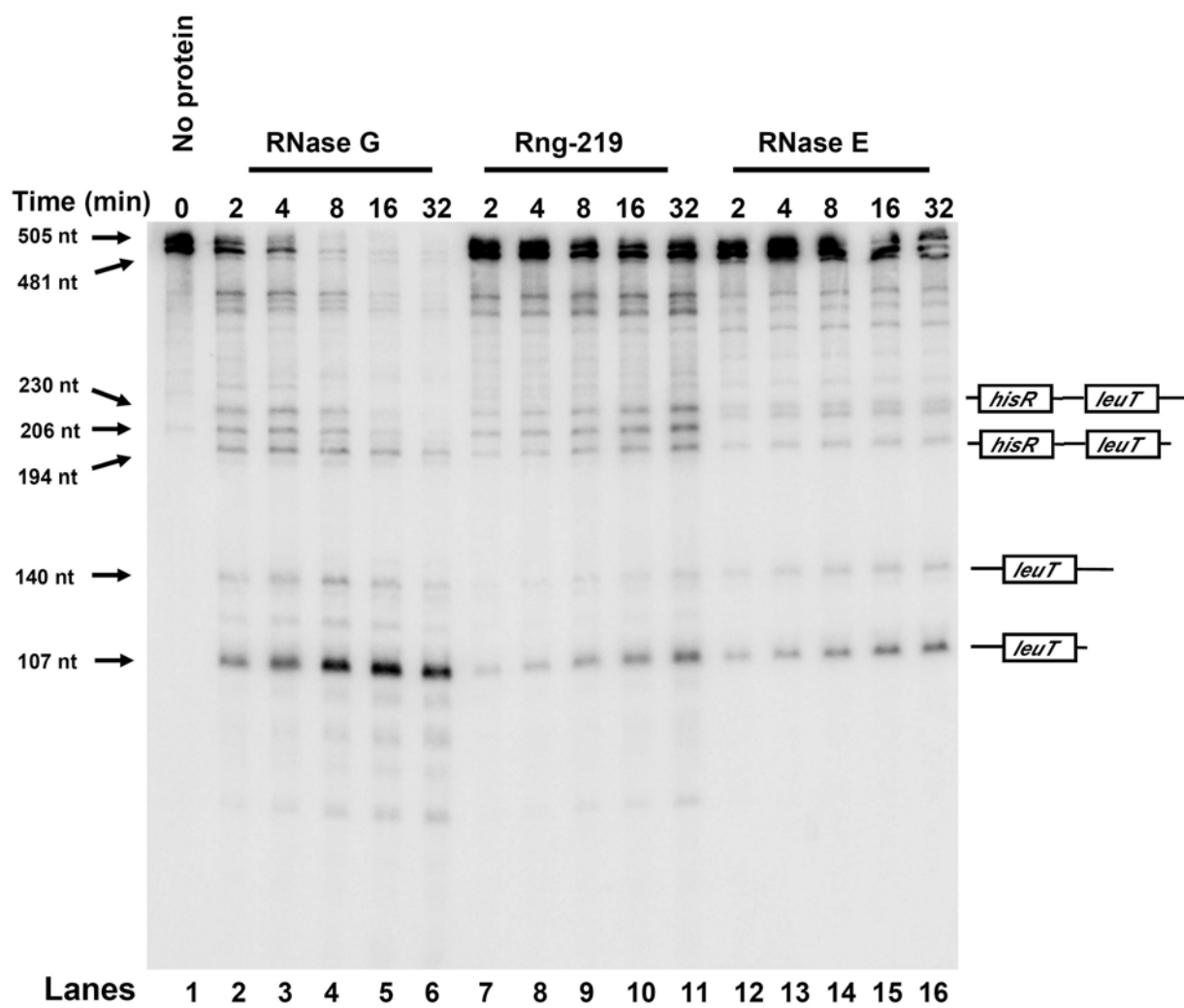


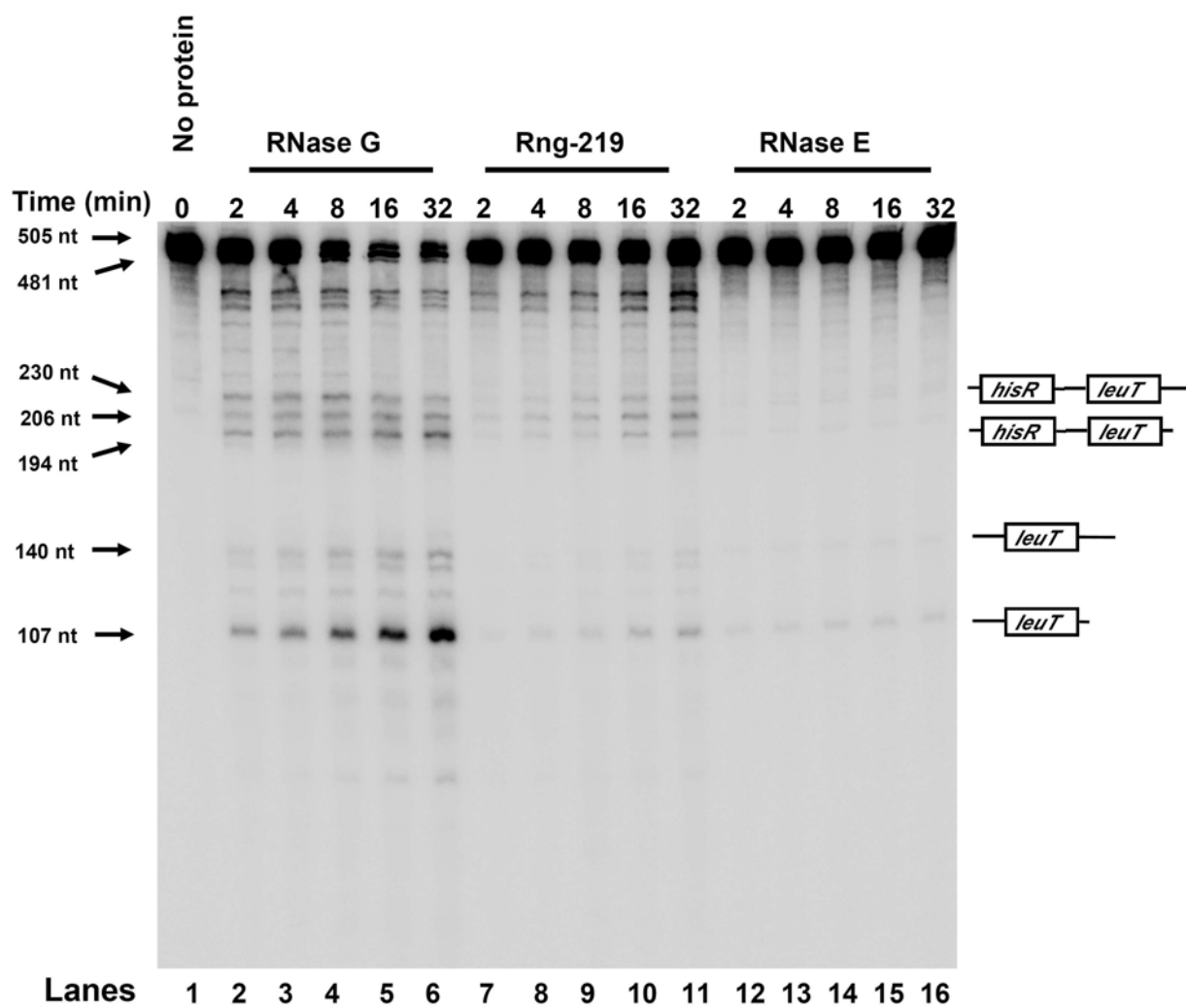
(B) tRNA^{Arg} (5'-monophosphate)

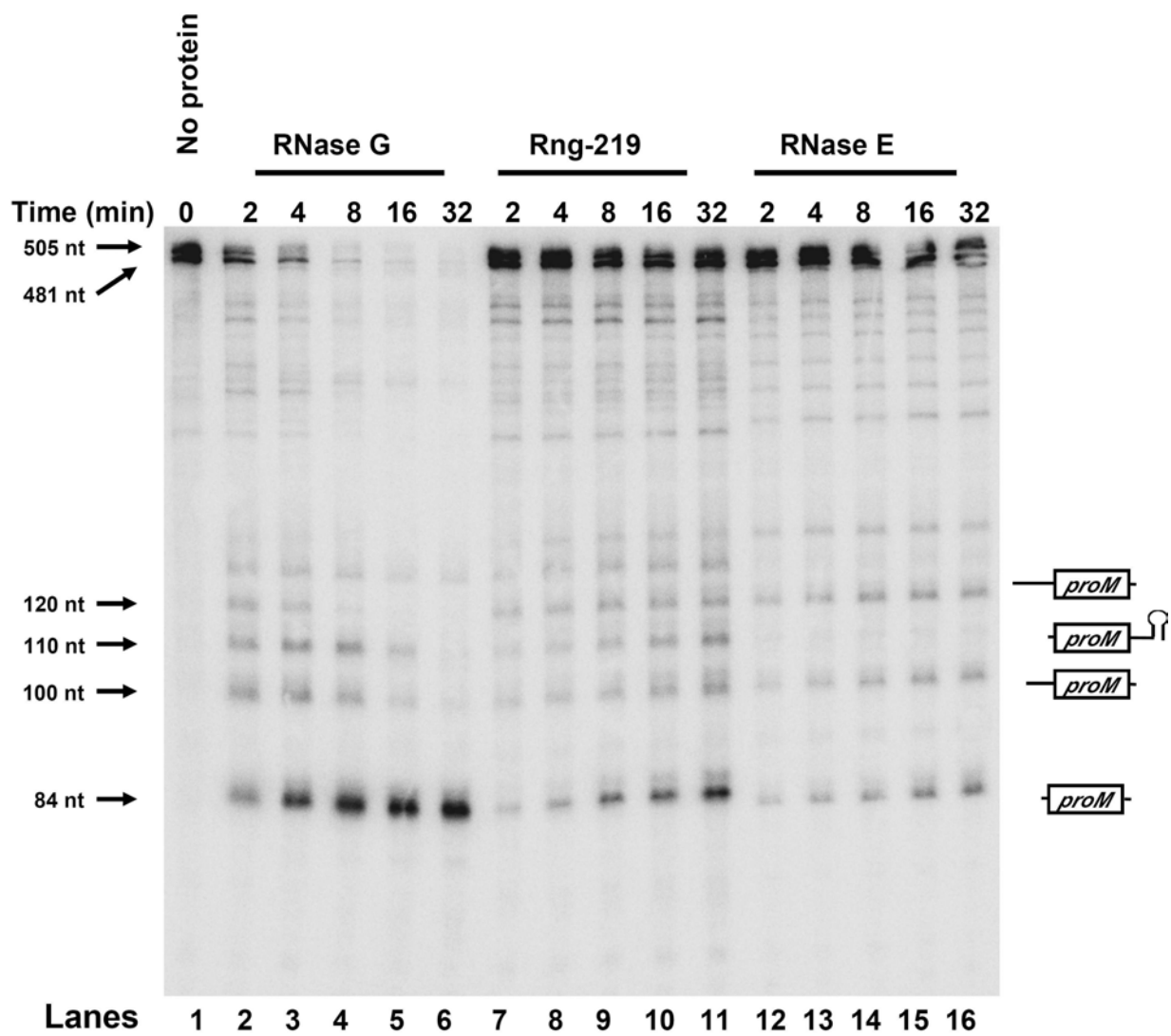
(C) tRNA^{Arg} (5'-triphosphate)

(D) tRNA^{His} (5'-monophosphate)

(F) tRNA^{Leu} (5'-monophosphate)



(G) tRNA^{Leu} (5'-triphosphate)

(H) tRNA^{Pro} (5'-monophosphate)

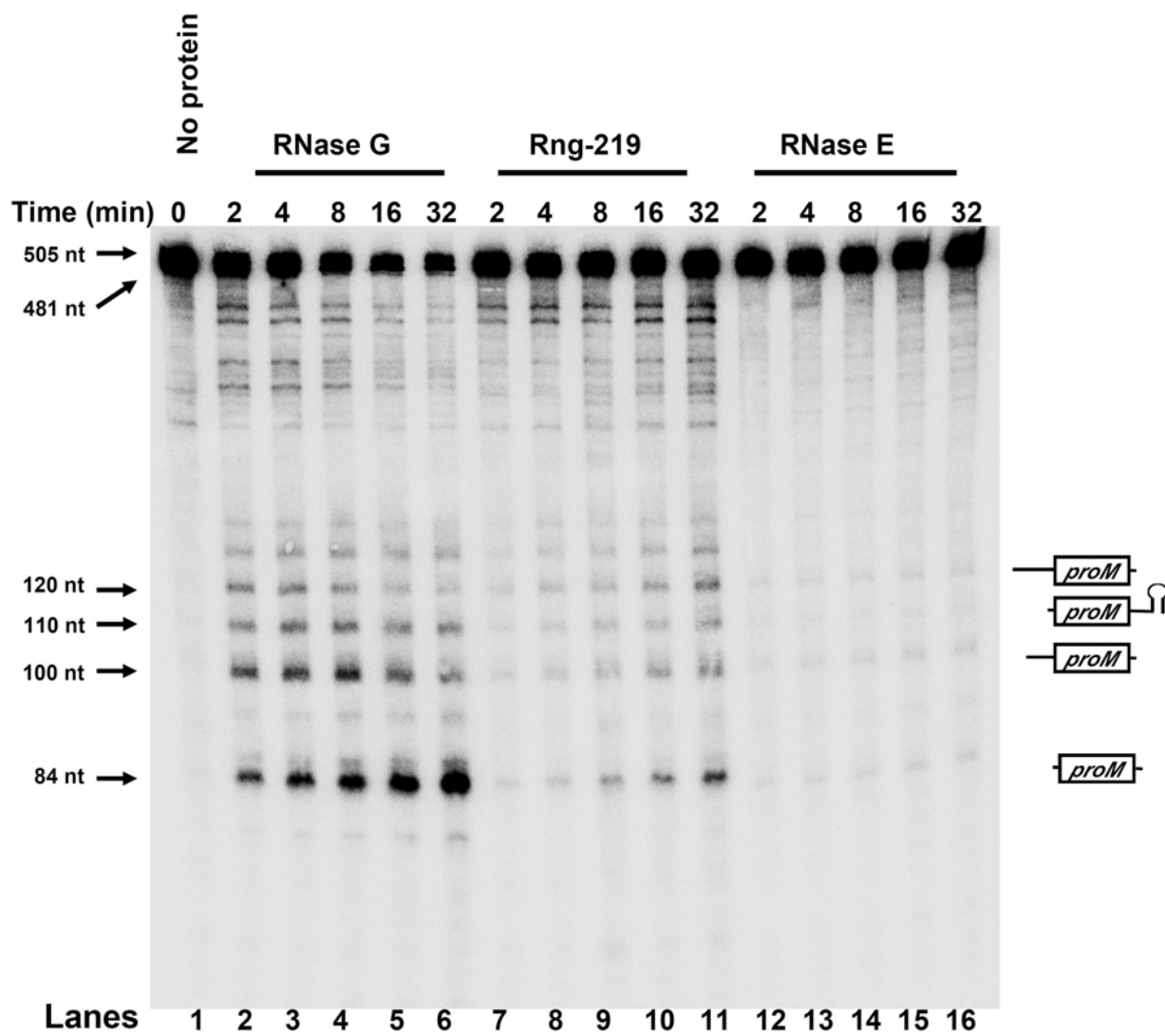
(I) tRNA^{Pro} (5'-triphosphate)

Figure 3.9. Primer extension analysis to map RNase G, Rng-219 and RNase E cleavage sites within the *argX hisR leuT proM* polycistronic transcript.

(A) Schematic diagram of the major RNase G, Rng-219 and RNase E cleavage sites generated within the *argX hisR leuT proM* polycistronic transcript. The 480 nt *argX* operon transcript is identical to that described in Fig. 3.8. Important co-ordinate positions are indicated below the vertical lines. The oligonucleotides used as primers for primer extension analysis are indicated as asterisk capped horizontal lines. Positions of cleavage sites are shown with vertical straight-line arrows (E/G – both RNase G and RNase E) and vertical dashed-line arrows (G – RNase G only). The *in vitro* generated substrate, which was synthesized as described in Fig. 3.8, is shown as a thick black horizontal arrow at the bottom. (B) Results with *hisR* primer. (C) Results with *leuT* primer. An unlabeled *argX hisR leuT proM* polycistronic run-off transcript substrate with a 5'-monophosphate was digested with RNase G (lanes 6 and 7), Rng-219 (lanes 8 and 9) or RNase E (lanes 10 and 11), or without enzyme (lane 5), at 37°C for the times indicated. The reaction products were subsequently used in primer extension reactions as described in *Materials and Methods*. The CTAG sequencing reactions were carried out using the same primers as those used for each reverse transcription (lanes 1 to 4). Arrows indicate 5' termini derived from the time-dependent RNase E and RNase G endonucleolytic cleavages.

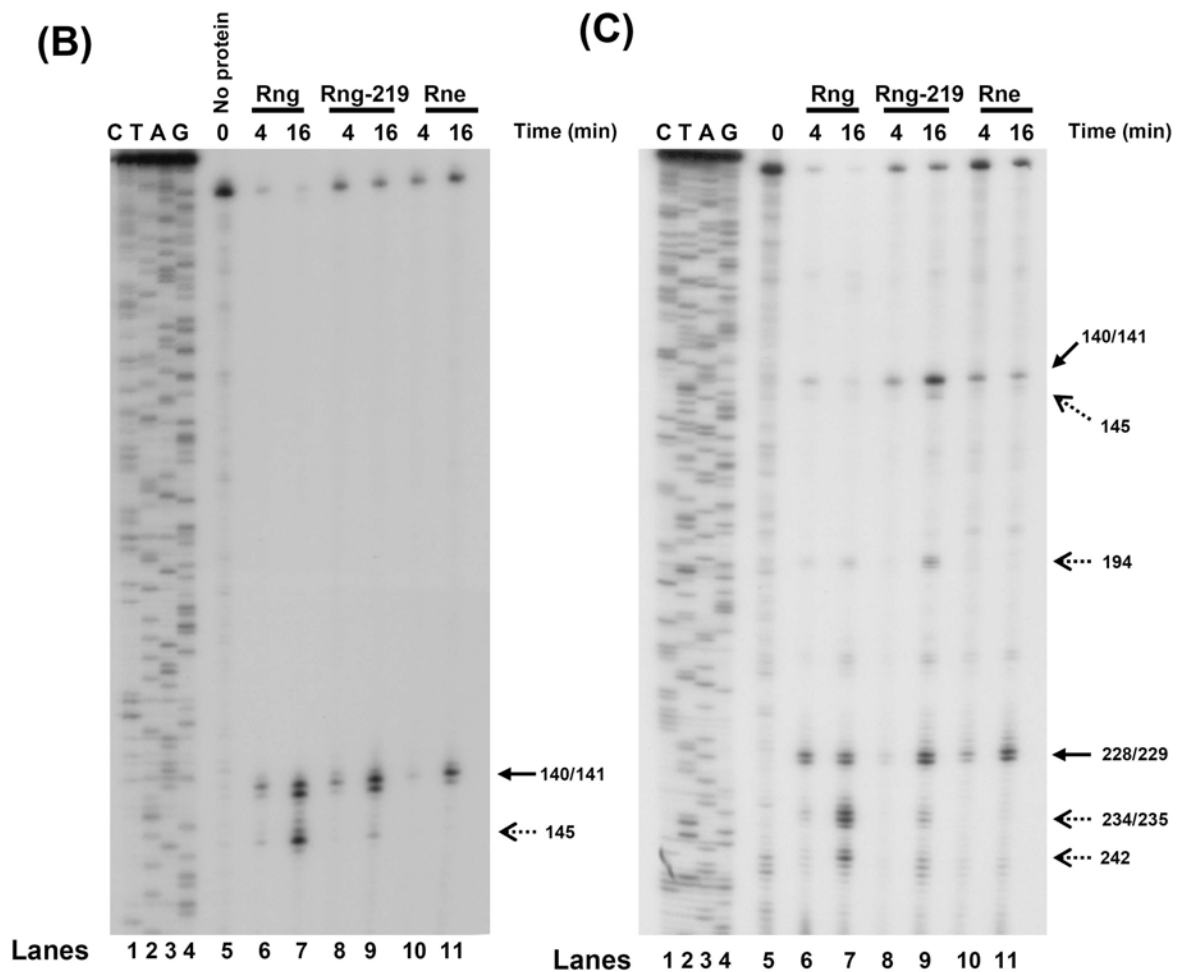
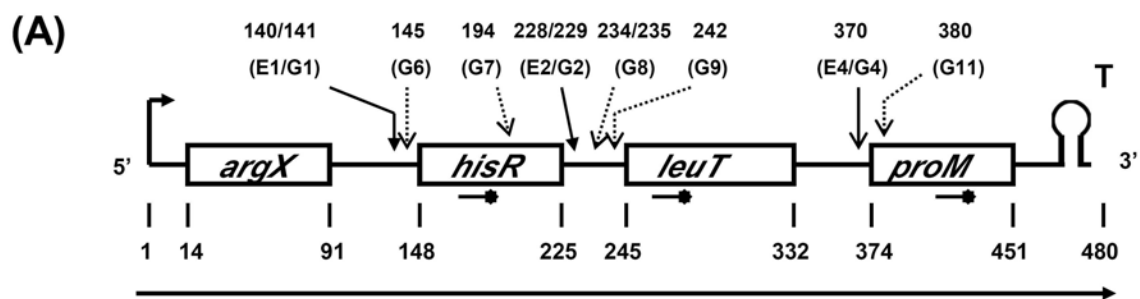
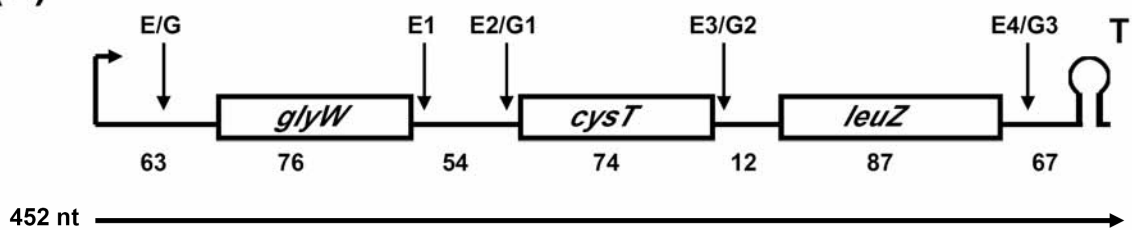


Figure 3.10. *In vitro* analysis of processing of the *glyW cysT leuZ* polycistronic transcript.

(A) Schematic diagram of the *glyW cysT leuZ* polycistronic transcript used for *in vitro* analysis.

The fragment contains one extra 'G' upstream of the *in vivo* transcription start site as well as 19 extra nt downstream of the Rho independent transcription terminator. Transcription of this PCR-generated DNA fragment generated a 452 nt RNA. Based on our *in vitro* experiments including Northern and primer extension analysis the major E/G cleavage sites are marked with downward arrows. It should be noted that RNase G does not cleave immediately downstream of the *glyW* tRNA where there is an RNase E cleavage site. (B) An internally ³²P-labeled 452 nt substrate terminated with a 5'-monophosphate was incubated without enzyme (lanes 1 and 2), with 60 ng of RNase G (lanes 3 and 4), with 60 ng of Rng-219 (lanes 5 and 6), or with 12 ng of RNase E (lanes 7 and 8). The products were separated on a 6% polyacrylamide/7 M urea gel (see *Materials and Methods*). The time of digestion is shown above each lane. The positions of the full length substrate (452 nt), and the major products derived by RNase E and RNase G cleavage activity are shown in the left margin. The compositions of the various processing intermediates, if determined, are indicated in the right margin.

(A)



(B)

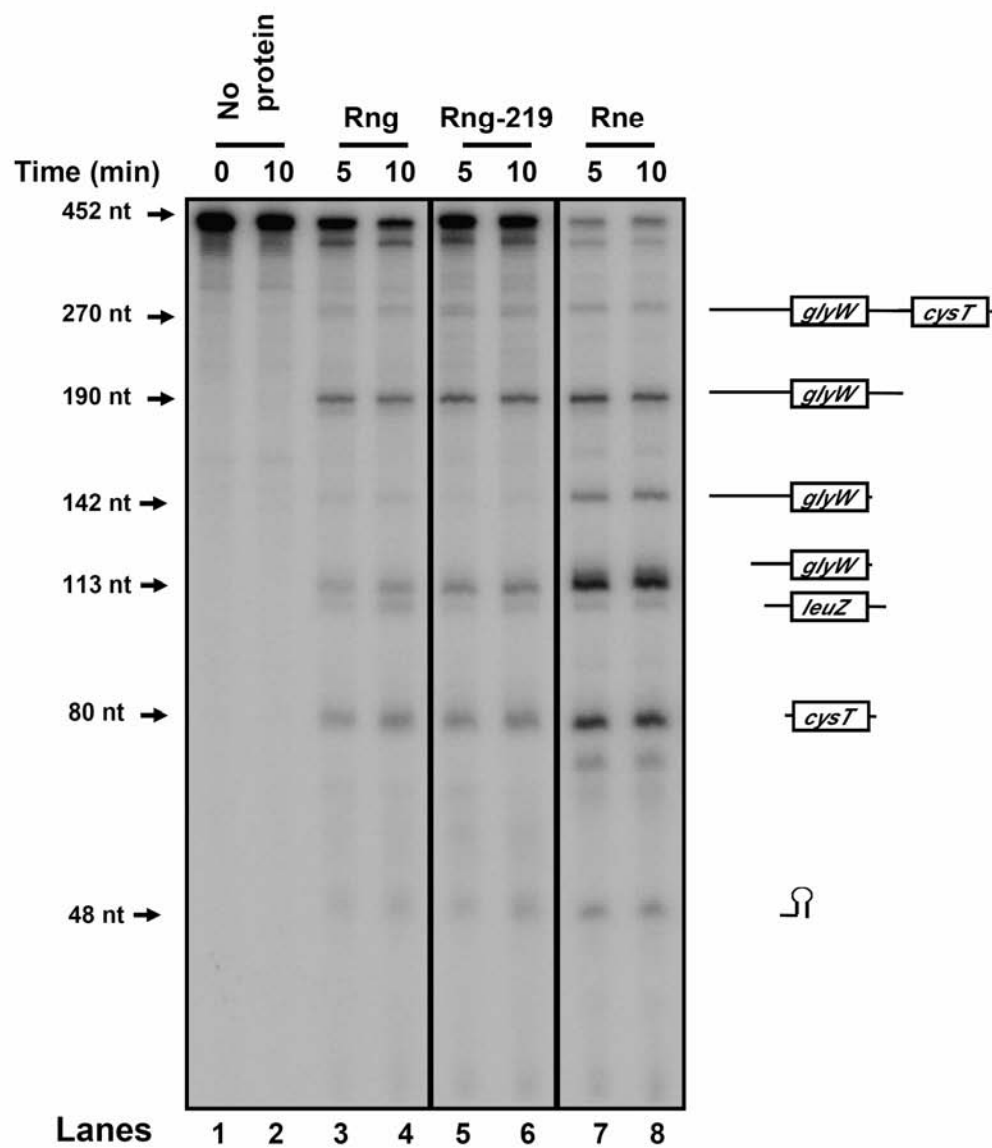
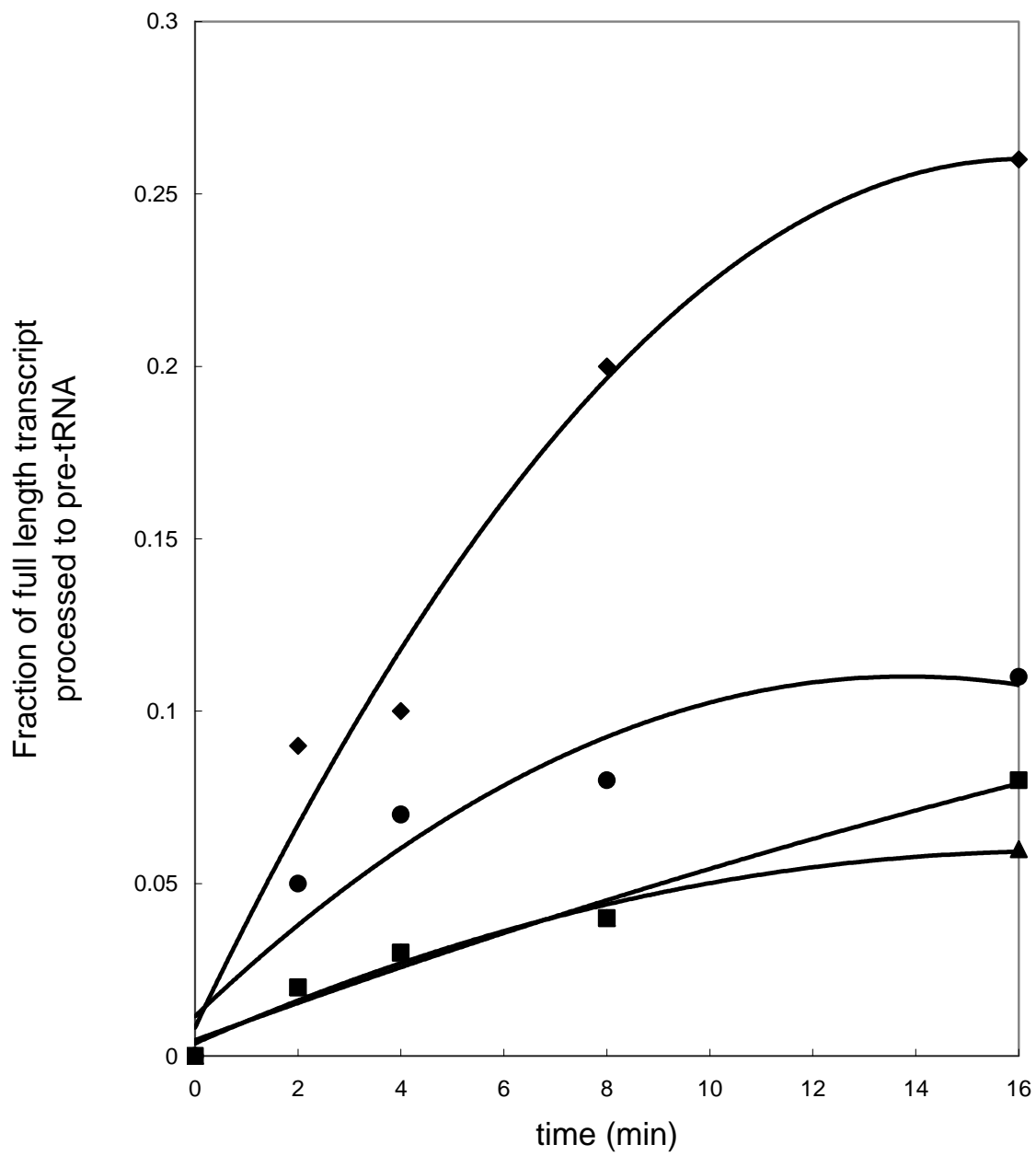
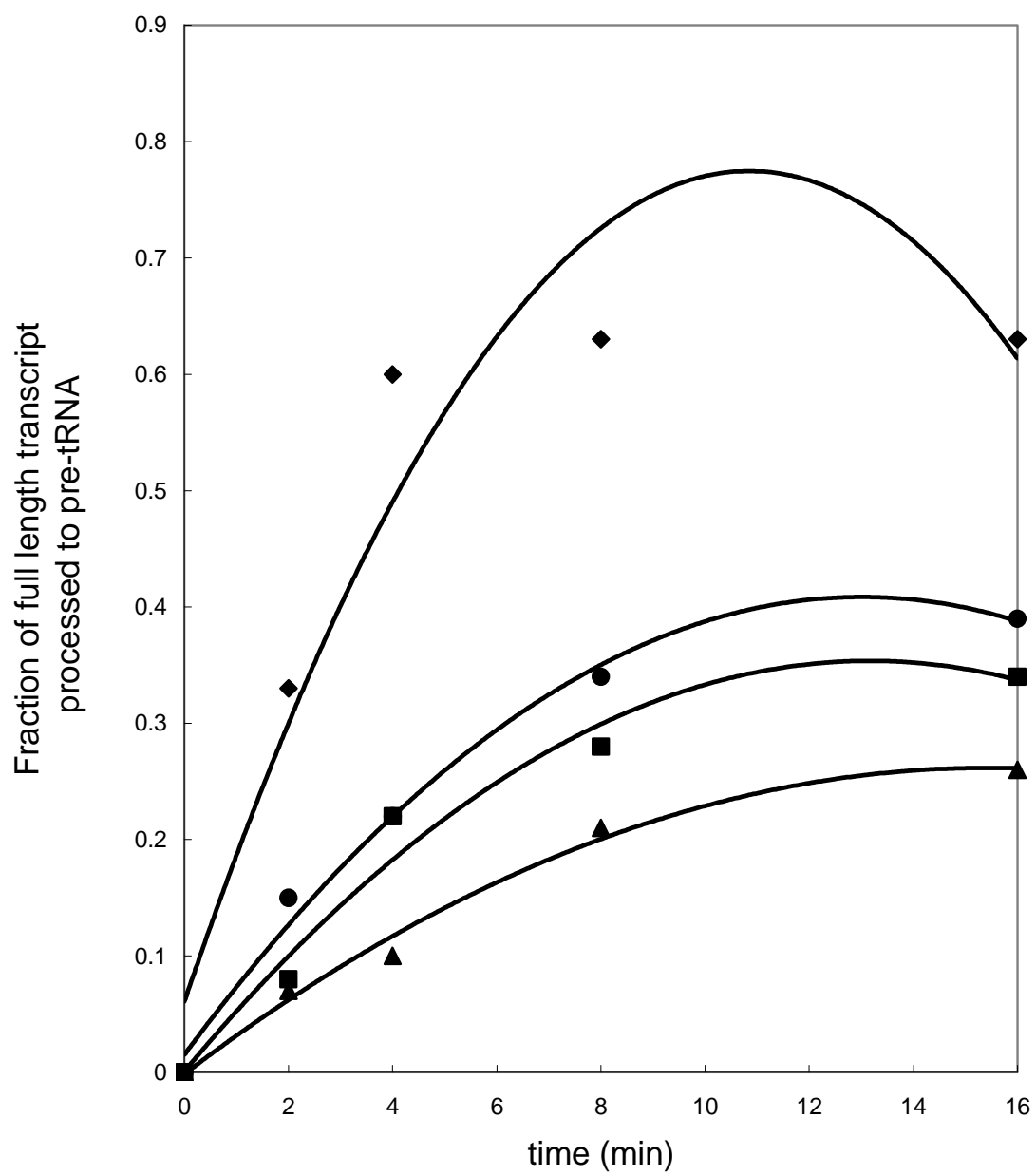


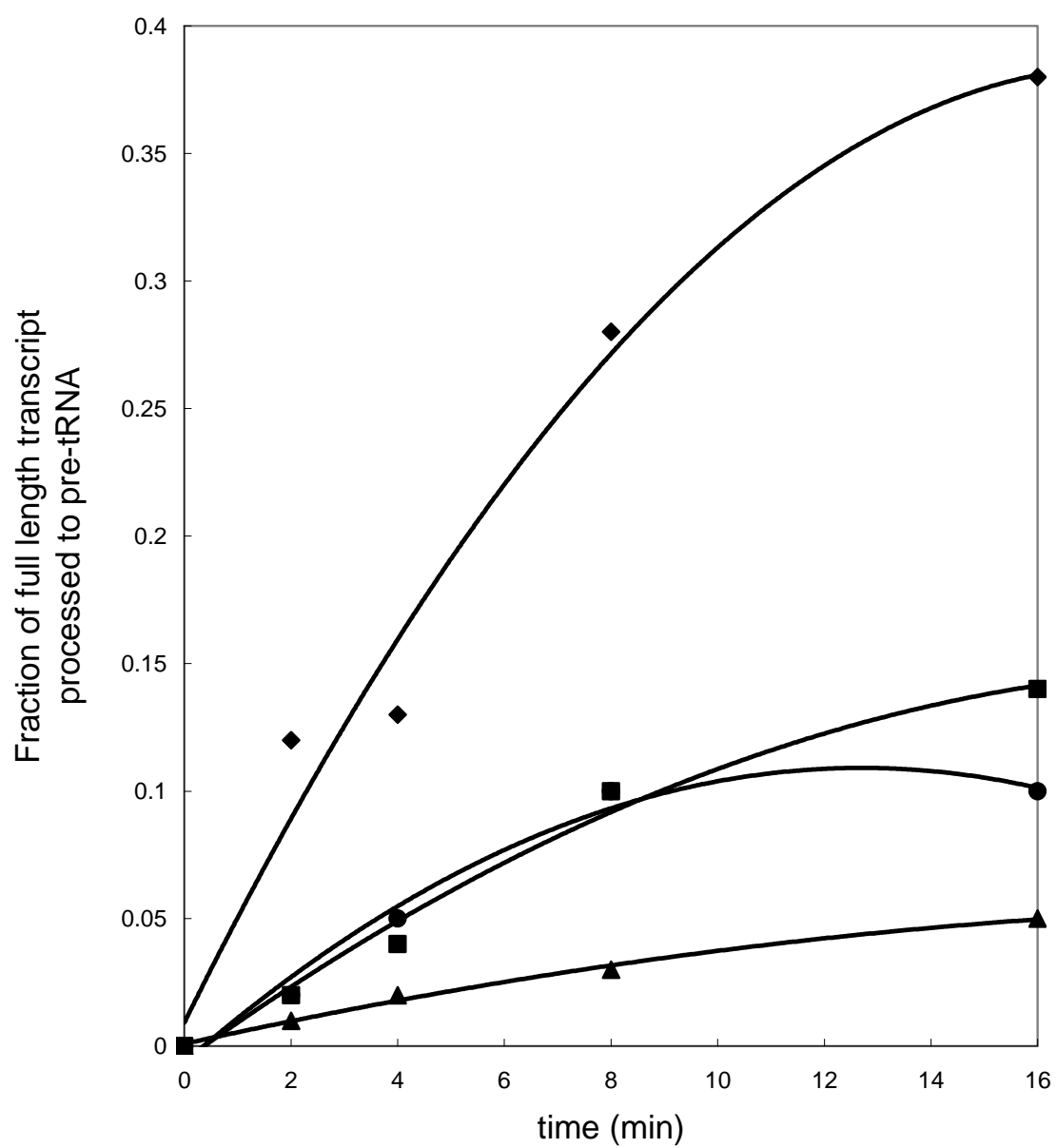
Figure 3.11. Release of pre-tRNAs from *argX* polycistronic transcript.

Data are derived from experiments shown in Fig. 3.8B, 8D, 8F, and 8H using a 5' monophosphate terminated transcript (\diamond ; pre-*argX*, \circ ; pre-*hisR*, Δ ; pre-*leuT*, \square ; pre-*proM*).

(A) RNase E. (B) RNase G. (C) Rng-219.

(A)

(B)

(C)

CHAPTER 4

Conclusion

In addition to the efficiency of transcription and the initiation of translation, mRNA degradation and stable RNA maturation provide additional levels of post-transcriptional regulation in the control of gene expression in *Escherichia coli*. The inherent instability of mRNAs and their wide-range longevity provide prokaryotic organisms with mechanisms to adjust their metabolic processes in response to continuously changing growth conditions. In the case of stable RNAs, rRNAs and tRNAs, there is a direct correlation between growth rate and the efficiency of tRNA and rRNA maturation (Chapter 2, Ow & Kushner, 2002, Ow *et al.*, 2003). Traditionally, these two events have been considered to be distinct processes. However, there exists considerable overlap between the endoribonucleases involved in mRNA degradation and stable RNA maturation (Deutscher, 2006, Kushner, 2007). It is now clear that there are close interrelationships between degradation and maturation of RNA molecules.

The identification and extensive investigation of RNase E, an essential endoribonuclease in *E. coli*, suggests that it plays a central role in mRNA decay (Ono & Kuwano, 1979, Arraiano *et al.*, 1988, Ow *et al.*, 2000), rRNA maturation (Ghora & Apirion, 1978, Li *et al.*, 1999), initiation of tRNA maturation (Li & Deutscher, 2002, Ow & Kushner, 2002), as well as many other aspects of RNA metabolism. These findings have provided important advances in the understanding of RNA metabolism in prokaryotes. *E. coli* encodes a related endoribonuclease, RNase G, that shares a high degree of sequence homology and a number of biochemical properties (McDowall & Cohen, 1996, Jiang *et al.*, 2000, Tock *et al.*, 2000). However, RNase G is dispensable for cell viability and appears to have limited biological functions compared to RNase E.

The results of Chapter 2 have directly addressed the question of whether over-production of either native or extended forms of RNase G (containing either six additional amino acids at its N-terminus or six histidines at its C-terminus) can complement RNase E deficiency in *E. coli*. Our data clearly indicates that neither native nor extended forms of RNase G are

able to complement the loss of RNase E activity under normal physiological conditions. We could get stable complementation of the *rne-1* and *rne* Δ 1018 alleles only through a combination of mutational changes within the *rng* coding sequence and over-expression of the altered RNase G protein to a comparable level as RNase E (Chapter 2). Based on these observations, we conclude that the biological functions of the two enzymes differ not only because of the low abundance of RNase G, but also because of the differences in their intrinsic properties.

The *rng-219* and *rng-248* alleles, which are able to complement the growth defect associated with various RNase E mutants at physiologically relevant protein levels, have provided insights into what features of the two proteins are responsible for differences in their biological functions (Chapter 2). Both the *rng-219* and *rng-248* mutations, comprising single amino acid substitutions at residues 219 and 248 respectively, occurred in the predicted RNase H domain which exhibits the most sequence divergence (only 26.6% identity) and the least apparent 3-dimensional similarity to RNase E. These observations strongly imply that the different substrate specificities and cleavage site selections of RNase E and RNase G are controlled to some extent by their RNase H domains.

In addition, *in vivo* characterization of the altered RNase G proteins (Rng-219 and Rng-248) in the total absence of RNase E (Chapter 2), has allowed us to investigate more critically the distinct physiological roles of RNase E and RNase G in RNA metabolism in *E. coli*. The analysis of tRNA processing efficiency of some tRNAs (tRNA^{His}, tRNA^{Cys}, and tRNA^{Pro}) demonstrates that the initiation of tRNA maturation of the polycistronic transcripts containing these species appears to be absolutely dependent on RNase E under normal physiological conditions (Chapter 2).

While RNase E appears to be the primary enzyme involved in the initiation of mRNA decay (Bernstein *et al.*, 2004), other ribonucleases such as RNase G (Li *et al.*, 1999, Wachi *et*

al., 1999), RNase Z (Perwez & Kushner, 2006), RNase LS (Otsuka & Yonesaki, 2005), RNase III and RNase P (Alifano *et al.*, 1994) can initiate the decay of particular transcripts. The mRNA half-life experiments employing *rneΔ1018/rng-219* and *rneΔ1018/rng-248* double mutant strains allowed us to analyze the complete dependence of degradation initiation of certain transcripts on RNase E. For example, while *rpsO* transcripts were dramatically stabilized in both the double mutant strains and no decay intermediates were observed, suggesting that RNase E was the only ribonuclease initiating its decay (Chapter 2); on the other hand, the stability of *rpsT* transcripts was not significantly affected by the absence of RNase E activity, and also new decay intermediates appeared that were not present in wild type cells. These observations strongly imply that other ribonucleases besides RNase E are able to initiate the decay of *rpsT* transcripts, and the altered RNase G proteins (Rng-219 and Rng-248) cleave these transcripts at different locations than RNase E. The *in vitro* analysis employing purified RNase E, Rng-219 and RNase G proteins has confirmed the different cleavage site selections between RNase E and the two RNase G proteins on *rpsT* transcripts (Chapter 3).

In contrast, there was significant *in vivo* functional overlap between RNase E and RNase G in 9S rRNA and 16S rRNA processing. *rne-1* dependent defects in both rRNA's processing were restored to almost wild type levels by overproduction of either native or altered forms of RNase G at physiologically comparable level of protein. Additionally, in the *rneΔ1018* genetic background, Rng-219 and Rng-248 almost completely substituted for the function of RNase E in the maturation of 9S rRNA and 16S rRNA (Chapter 2, Chung and Kushner, unpublished results).

The *in vitro* assays of purified RNase E, Rng-219 and RNase G proteins employing various full-length RNA substrates (9S rRNA, mRNAs and tRNAs) have provided a number of new insights into the biochemical properties of the three proteins under conditions that resemble the *in vivo* situation (Chapter 3). Both the Rng-219 and RNase G proteins site-specifically

cleaved structured RNAs (9S rRNA and tRNA substrates) at locations identical to those obtained with RNase E. However, the Rng-219 and RNase G proteins also cleaved at additional sites on mRNAs and tRNAs substrates. Interestingly, both RNase G protein derivatives were much more active in the presence of Mn^{2+} than Mg^{2+} .

The altered RNase G protein (Rng-219) clearly acts on substrates differently than wild type RNase G (Chapter 3). The single amino acid substitution within the predicted RNase H domain in RNase G caused a reduction in the non-specific cleavage activities of RNase G so that it cleaved RNA molecules more like RNase E, and may remove the toxicity of RNase G (Okada *et al.*, 1994). This conclusion is supported by the observations that the RNase G protein cleaves the region located within tRNA^{His}, tRNA^{Leu} and tRNA^{Pro} coding sequences, and the cleavage products containing the 5S rRNA were less stable in the RNase G *in vitro* reaction preparation than the Rng-219 preparation (Chapter 3). In addition, the cleavage profiles of the *cspA* transcript in the RNase G cleavage assay suggest another possible explanation. RNase G may completely degrade some transcripts which encode essential proteins that are required to support cell viability and/or degrade one of the many small regulatory RNAs resulting in inhibition of an essential pathway.

Both RNase E and RNase G have been shown to be 5'-end-dependent endoribonucleases (Jiang *et al.*, 2000, Tock *et al.*, 2000) and the residues that make contact with the 5' end of substrates are conserved between two enzymes (Callaghan *et al.*, 2005, Jourdan & McDowall, 2008). Recently, the crystallographic structure of RNase E revealed that the discrimination between 5'-monophosphate and 5'-triphosphate terminus of a substrate is based on the size of the binding pocket and the net charge of the 5' terminal groups. Although, both RNase E and RNase G proteins exhibit a propensity to cleave substrates with a 5' monophosphate over 5' triphosphate ones, the cleavage activity on mRNAs and tRNAs of RNase E is 2–8 times more affected by the 5' phosphorylation status than RNase G. These

data suggest that the size of the binding pocket and/or the key residues associated in interactions with 5' end of substrates of RNase G is actually different from RNase E.

Another hypothesis is that RNase G is able to cleave the RNA molecules much more efficiently by 'internal entry pathway' mechanism (Joyce & Dreyfus, 1998, Baker & Mackie, 2003). The cleavage site of *cspA* mRNA is located at a significant distance from the 5' end and it has a protective 5' stem-loop structure that might antagonize the binding ability of RNase E and RNase G (Hankins *et al.*, 2007). Thus the cleavage on *cspA* mRNA substrate would constitute an example of the internal entry pathway mechanism by RNase E and RNase G. The complete degradation of *cspA* transcript in RNase G cleavage assay (Chapter 3) strongly implies a greater proficiency of RNase G in cleaving the substrates without interacting with their 5' end than RNase E. These results could explain the broader sequence specificity and distributive mode of cleavage action of RNase G as compared to RNase E (Feng *et al.*, 2002).

An important question that still remains is how the subtle changes in the predicted RNase H domain directly affect the biochemical activity of RNase G. Unfortunately, the use of molecular modeling (Chapter 2) was not sufficient to accurately predict the nature of conformational change in Rng-219 and Rng-248. In principle, the changes in biochemical properties of altered RNase G proteins could be a consequence of differences in initial binding with RNA substrates and/or in catalytic activation of the protein. These two possible explanations can be distinguished by comparing the Michaelis–Menten kinetic parameters K_{cat} and K_m between wild type and altered RNase G proteins. However, the crystallization of RNase G, Rng-219 and/or Rng-248 would be invaluable. Obtaining the crystal structure of these proteins will not only help in addressing this question but also provide clues to better understanding the features responsible for the observed differences in the physiological properties and biochemical activities between RNase E and RNase G.

Finally, the construction of *rne*Δ1018/*rng-219* and *rne*Δ1018/*rng-248* double mutant strains would be able to provide a useful means to achieve further comprehensive understanding of the important features of RNase E by employing a recently developed high density tiling microarray, which can analyze the gene expression profile on a transcriptome scale. For example, we could identify tRNA species that are highly dependent on RNase E as well as those independent of RNase E and new RNA substrates cleaved by RNase E, and investigate critically the global effect of inactivation of RNase E in RNA metabolism in *E. coli*. Such microarray analysis is currently under investigation (Mark B. Stead, Sarah Marshburn, and Sidney R. Kushner).

REFERENCES

- Alifano, P., F. Rivellini, C. Piscitelli, C. M. Arraiano, C. B. Bruni & M. S. Carlomagno, (1994) Ribonuclease E provides substrates for ribonuclease P-dependent processing of a polycistronic mRNA. *Genes Dev.* **8**: 3021-3031.
- Arraiano, C. M., S. D. Yancey & S. R. Kushner, (1988) Stabilization of discrete mRNA breakdown products in *ams pnp rnb* multiple mutants of *Escherichia coli* K-12. *J. Bacteriol.* **170**: 4625-4633.
- Baker, K. E. & G. A. Mackie, (2003) Ectopic RNase E sites promote bypass of 5'-end-dependent mRNA decay in *Escherichia coli*. *Mol. Microbiol.* **47**: 75-88.
- Bernstein, J. A., P.-H. Lin, S. N. Cohen & S. Lin-Chao, (2004) Global analysis of *Escherichia coli* RNA degradosome function using DNA microarrays. *Proc. Natl. Acad. Sci. USA* **101**: 2748-2763.
- Callaghan, A. J., M. J. Marcaida, J. A. Stead, K. J. McDowall, W. G. Scott & B. F. Luisi, (2005) Structure of *Escherichia coli* RNase E catalytic domain and implications for RNA turnover. *Nature* **437**: 1187-1191.

- Deutscher, M. P., (2006) Degradation of RNA in bacteria: comparison of mRNA and stable RNA. *Nucleic Acids Res.* **34**: 659-666.
- Feng, Y., T. A. Vickers & S. N. Cohen, (2002) The catalytic domain of RNase E shows inherent 3' to 5' directionality in cleavage site selection. *Proc. Natl. Acad. Sci. USA* **99**: 14746-14751.
- Ghora, B. K. & D. Apirion, (1978) Structural analysis and *in vitro* processing to p5' rRNA of a 9S RNA molecule isolated from an *rne* mutant of *E. coli*. *Cell* **15**: 1055-1066.
- Hankins, J. S., C. Zappavigna, A. Prud'homme-Genereux & G. A. Mackie, (2007) Role of RNA Structure and susceptibility to RNase E in regulation of a cold shock mRNA, *cspA* mRNA. *J. Bacteriol.* **189**: 4353-5358.
- Jiang, X., A. Diwa & J. G. Belasco, (2000) Regions of RNase E important for 5'-end-dependent RNA cleavage and autoregulated synthesis. *J. Bacteriol.* **182**: 2468-2475.
- Jourdan, S. S. & K. J. McDowall, (2008) Sensing of 5' monophosphate by *Escherichia coli* RNase G can significantly enhance association with RNA and simulate the decay of functional mRNA transcripts *in vivo*. *Mol. Microbiol.* **67**: 102-115.
- Joyce, S. A. & M. Dreyfus, (1998) In the absence of translation, RNase E can bypass 5' mRNA stabilizers in *Escherichia coli*. *J. Mol. Biol.* **282**: 241-254.
- Kushner, S. R., (2007) Messenger RNA decay. In: *Escherichia coli* and *Salmonella*: cellular and molecular biology. A. Böck, R. Curtis III., C. A. Gross, J. B. Kaper, F. C. Neidhardt, T. Nyström, K. E. Rudd & S. C. L. (eds). Washington, DC: American Society for Microbiology Press, pp. <http://www.ecosal.org>.
- Li, Z. & M. P. Deutscher, (2002) RNase E plays an essential role in the maturation of *Escherichia coli* tRNA precursors. *RNA* **8**: 97-109.
- Li, Z., S. Pandit & M. P. Deutscher, (1999) RNase G (CafA protein) and RNase E are both required for the 5' maturation of 16S ribosomal RNA. *EMBO J.* **18**: 2878-2885.

- McDowall, K. J. & S. N. Cohen, (1996) The N-terminal domain of the *rne* gene product has RNase E activity and is non-overlapping with the arginine-rich RNA-binding motif. *J. Mol. Biol.* **255**: 349-355.
- Okada, Y., M. Wachi, A. Hirata, K. Suzuki, K. Nagai & M. Matsushashi, (1994) Cytoplasmic axial filaments in *Escherichia coli* cells: possible function in the mechanism of chromosome segregation and cell division. *J. Bacteriol.* **176**: 917-922.
- Ono, M. & M. Kuwano, (1979) A conditional lethal mutation in an *Escherichia coli* strain with a longer chemical lifetime of mRNA. *J. Mol. Biol.* **129**: 343-357.
- Otsuka, Y. & T. Yonesaki, (2005) A novel endoribonuclease, RNase LS, in *Escherichia coli*. *Genetics* **169**: 13-20.
- Ow, M. C. & S. R. Kushner, (2002) Initiation of tRNA maturation by RNase E is essential for cell viability in *Escherichia coli*. *Genes Dev.* **16**: 1102-1115.
- Ow, M. C., Q. Liu & S. R. Kushner, (2000) Analysis of mRNA decay and rRNA processing in *Escherichia coli* in the absence of RNase E-based degradosome assembly. *Mol. Microbiol.* **38**: 854-866.
- Ow, M. C., T. Perwez & S. R. Kushner, (2003) RNase G of *Escherichia coli* exhibits only limited functional overlap with its essential homologue, RNase E. *Mol. Microbiol.* **49**: 607-622.
- Perwez, T. & S. R. Kushner, (2006) RNase Z in *Escherichia coli* plays a significant role in mRNA decay. *Mol. Microbiol.* **60**: 723-737.
- Tock, M. R., A. P. Walsh, G. Carroll & K. J. McDowall, (2000) The CafA protein required for the 5'-maturation of 16 S rRNA is a 5'- end-dependent ribonuclease that has context-dependent broad sequence specificity. *J. Biol. Chem.* **275**: 8726-8732.
- Wachi, M., G. Umitsuki, M. Shimizu, A. Takada & K. Nagai, (1999) *Escherichia coli* *cafA* gene encodes a novel RNase, designated as RNase G, involved in processing of the 5' end of 16S rRNA. *Biochem. Biophys. Res. Comm.* **259**: 483-488.

APPENDIX A

Single amino acid changes in the predicted RNase H domain of *E. coli*

RNase G lead to complementation of RNase E deletion mutants¹

¹ Dae-hwan Chung, Zhao Min, Bi-Cheng Wang, and Sidney R. Kushner. Submitted to *Nucleic Acids Research* as a Supplementary Information, 06/02/2008

MATERIALS AND METHODS

Plasmid constructions

The plasmids described below were generated using overlapping PCR techniques and the high fidelity *Pfu* DNA polymerase (Stratagene). For the construction of pDHK11 (Fig. 2.1A), a 2.2 kb fusion DNA fragment was synthesized that contained the regulatory region, ribosome binding site, and ATG start codon of *rne* along with the *rng*⁺ sequence that included 15 bp encoding an additional five amino acids (RKGIN) upstream of the native RNase G translation start codon (1). The ATG from *rne* replaced the GTG from *rng* such that a total of six extra amino acids were synthesized at the amino terminus of the RNase G protein derived from pDHK11. First, an *rne* gene fragment (640 bp) was amplified by PCR using the primers RNE-UP and RNE-OE1 and pQLK26 plasmid DNA (2) as template. In addition, an *rng* gene fragment (1579 bp) was amplified by PCR using the primers RNG-OE1 and RNG-antisense and pUGK24 plasmid DNA (3) as template. The RNE-UP and RNG-antisense primers were engineered to contain *Eco*RI and *Xba*I sites, respectively. Subsequently, overlap extension PCR with primers RNE-OE1 and RNG-OE1 was used to generate a 2.2 kb fusion DNA fragment containing the *rne* gene fragment (640 bp) and *rng* gene fragments (1579 bp). The amplified fusion DNA fragment was cloned into pWSK129 (Wang and Kushner, 1991), which had been digested with *Eco*RI and *Xba*I, to generate pDHK11.

Plasmid pDHK23 (encoding the native form of RNase G, Fig. 2.1A) is identical to pDHK11 except for the GTG (putative upstream start codon derived from *rng*) was changed to CTG to prevent translation initiation from this location and a canonical ribosome binding site (AGGAGG) was inserted seven nt upstream of the ATG start codon to produce the native form of RNase G (Fig. 2.1A). To make these changes, a 658 bp *rne* DNA fragment was amplified by PCR using the primers RNE-UP and RNE-upstream and pQLK26 plasmid DNA as template

along with a *rng* gene fragment (1561 bp) that was amplified by using the primers RNG-RBS (and RNG-antisense and pUGK24 plasmid DNA as template. The RNE-upstream and RNG-RBS primer sequences were used for overlapping extension PCR to generate a 2.2 kb fusion DNA fragment that was subsequently cloned into pWKS129 as described for pDHK11.

To generate pDHK31, a 2.2 kb *EcoRI/NotI* DNA fragment containing the complete *rne-rng* fusion from pDHK23 was cloned into the single copy vector pMOK40 (4) that had been digested with *EcoRI* and *NotI*.

pDHK29 (*rng-248 Sm^r/Sp^r*) and pDHK30 (*rng-219 Sm^r/Sp^r*) were made by cloning the 2.2 kb *EcoRI/NotI* DNA fragments from pDHK26 and pDHK28, respectively, into the *EcoRI/NotI* sites of pMOK40 (4). Plasmids pDHK29, pDHK30 and pDHK31 all contained the single-copy mini-F origin of DNA replication.

Plasmid pDHK38 [containing two RNase G fragments, one from the N-terminus to amino acid 213 (including the S1 and 5' sensor regions) and one including the C-terminal *rng* coding sequence for amino acids 281-488 (DNase I domain and Zn-link) along with the *rne* coding sequences for amino acids 213-281 (RNase H domain)] was constructed by employing a two-step overlap extension PCR procedure. The regulatory region for this chimeric construct was derived from RNase E as described for pDHK23. To generate the N-terminal 1.5 kb DNA fragment containing *rne/rng* sequences (1.3 kb) and the 206 bp from *rne*, a 1.3 kb *rne/rng* DNA fragment was amplified using primers RNE-UP and RNG-1260 down and plasmid pDHK23 as a template. In addition, a 206 bp *rne* DNA fragment was amplified using primers RNE-1280up and RNE-1486down and plasmid pQLK26 (2) as a template. Overlap extension PCR was then used to generate an N-terminal fragment of 1.5 kb. The C-terminal 715 bp *rng* fragment was amplified using the prime RNG1486up and RNG-antisense along with pUGK24 as the template. The second overlap extension PCR was performed to generate a 2.2 kb fusion DNA fragment

containing the 1.5 kb *rne/rng/rne* DNA fragment and the downstream 715 bp *rng* fragment. The amplified chimeric *rne/rng* gene was cloned into pWSK129 (5) as described for pDHK11.

Plasmid pDHK39 [containing the regulatory region and first 281 amino acids of RNase E (S1, 5' sensor and RNase H subdomains) fused to the *rng* coding sequence for amino acids 282-488] was constructed by first amplifying a 1.5 kb *rne* DNA fragment using primers RNE-UP and RNE-1486down and pQLK26 plasmid DNA as a template. In addition a 715 bp *rng* DNA fragment was amplified using primer RNG-1486up and RNG-antisense and pUGK24 plasmid DNA as template. The RNE-1486down and RNA-1486up primers were used for the overlap PCR reaction. The fusion fragment was cloned into pWSK129 as described for pDHK11.

Plasmid pDHK40 [containing the regulatory region of RNase E, the first 280 amino acids of RNase G (S1, 5' sensor and RNase H subdomains) along with amino acids 281-418 from RNase E (DNase I subdomain and Zn-link)] was constructed by first amplifying a 1.5 kb *rne/rng* DNA fragment using primers RNE-UP and RNG+278down and pDHK23 plasmid DNA as a template. In addition, a 450 bp *rne* DNA fragment was amplified using primers RNE+279up and RNE+417down and pMOK21 (*rne* Δ 645) plasmid DNA (3) as a template. The RNE+417down primer contained a *Xba*I site. The fusion fragment, generated using the RNG+278down and RNE+279up primer sequences, was subsequently cloned into pWSK129 as described for pDHK11.

All the plasmid constructions were verified using a combination of DNA sequencing and western blot analysis. Western blot analysis of RNase E/G Chimeric proteins 1 and 3 employed a polyclonal anti-RNase G antibody that was kindly provided by G. Mackie (1). RNase E/G Chimeric protein 2 was detected using a MAP antibody raised against the first 20 amino acids of RNase E (2). To determine if the RNase G proteins were biologically active, steady-state RNA was isolated from independent transformants in an *rng::cat* genetic background (SK2538) and

the presence or absence of the 16.3S rRNA precursor was determined as described by Wachi *et al.* (6).

Site-directed mutagenesis

Overlapping PCR was used to individually introduce the two different single nucleotide changes in pDHK23. The G → T transversion at the first base-pair of the codon encoding aa 219 and the G → A transition at the first base-pair of aa 248 resulted in plasmids pDHK32 and pDHK33, respectively. Plasmids pDHK34 (*rng*-219 Km^r) and pDHK35 (*rng*-248 Km^r) were constructed to determine the effect of the two independent single amino acid substitutions on RNase G when the proteins were synthesized from the native *rng* regulatory region instead of from *rne* promoters. In this case, the experiment was identical to that described above for pDHK32 and pDHK33, except that pUGK24 (*rng*⁺ Km^r) (3) plasmid DNA was used as a template. Specific experimental details are available upon request. The presence of the predicted point mutations in the four plasmids was confirmed by manual plasmid DNA sequencing using *fmol*[®] DNA Cycle Sequencing System Kit (Promega) as instructed by the manufacturer.

REFERENCES

1. Briant, D.J., Hankins, J.S., Cook, M.A. and Mackie, G.A. (2003) The quaternary structure of RNase G from *Escherichia coli*. *Mol. Microbiol.*, **50**, 1381-1390.
2. Ow, M.C., Liu, Q. and Kushner, S.R. (2000) Analysis of mRNA decay and rRNA processing in *Escherichia coli* in the absence of RNase E-based degradosome assembly. *Mol. Microbiol.*, **38**, 854-866.

3. Ow, M.C., Perwez, T. and Kushner, S.R. (2003) RNase G of *Escherichia coli* exhibits only limited functional overlap with its essential homologue, RNase E. *Mol. Microbiol.*, **49**, 607-622.
4. Ow, M.C. and Kushner, S.R. (2002) Initiation of tRNA maturation by RNase E is essential for cell viability in *Escherichia coli*. *Genes Dev.*, **16**, 1102-1115.
5. Wang, R.F. and Kushner, S.R. (1991) Construction of versatile low-copy-number vectors for cloning, sequencing and expression in *Escherichia coli*. *Gene*, **100**, 195-199.
6. Wachi, M., Umitsuki, G., Shimizu, M., Takada, A. and Nagai, K. (1999) *Escherichia coli* *cafA* gene encodes a novel RNase, designated as RNase G, involved in processing of the 5' end of 16S rRNA. *Biochem. Biophys. Res. Comm.*, **259**, 483-488.
7. Callaghan, A.J., Marcaida, M.J., Stead, J.A., McDowall, K.J., Scott, W.G. and Luisi, B.F. (2005) Structure of *Escherichia coli* RNase E catalytic domain and implications for RNA turnover. *Nature*, **437**, 1187-1191.
8. Ow, M.C., Liu, Q., Mohanty, B.K., Andrew, M.E., Maples, V.F. and Kushner, S.R. (2002) RNase E levels in *Escherichia coli* are controlled by a complex regulatory system that involves transcription of the *rne* gene from three promoters. *Mol. Microbiol.*, **43**, 159-171.

Table A1.1. Processed fractions for tRNA maturation experiments¹

A. Alleles present in single copy

30°C					
	<i>rne</i> ⁺	<i>rne-1</i>	<i>rne</i> Δ645	<i>rng-219</i>	<i>rng-248</i>
tRNA ^{His}	0.57 ± 0.11	0.40 ± 0.1	0.53 ± 0.13	0.05 ± 0.01	0.05 ± 0.0
tRNA ^{Pro}	0.70 ± 0.13	0.59 ± 0.14	0.69 ± 0.12	0.12 ± 0.03	0.11 ± 0.02
tRNA ^{Asn}	0.95 ± 0.03	0.91 ± 0.02	0.96 ± 0.01	0.40 ± 0.05	0.42 ± 0.04
tRNA ^{Cys}	0.59 ± 0.12	0.44 ± 0.11	0.54 ± 0.10	0.11 ± 0.02	0.13 ± 0.01
44°C					
	<i>rne</i> ⁺	<i>rne-1</i>	<i>rne</i> Δ645	<i>rng-219</i>	<i>rng-248</i>
tRNA ^{His}	0.64 ± 0.09	0.11 ± 0.1	0.43 ± 0.08	0.10 ± 0.0	0.11 ± 0.01
tRNA ^{Pro}	0.74 ± 0.11	0.15 ± 0.02	0.54 ± 0.14	0.15 ± 0.03	0.15 ± 0.06
tRNA ^{Asn}	0.96 ± 0.02	0.64 ± 0.02	0.96 ± 0.03	0.53 ± 0.03	0.53 ± 0.06
tRNA ^{Cys}	0.64 ± 0.08	0.29 ± 0.03	0.59 ± 0.04	0.19 ± 0.03	0.23 ± 0.02

B. Alleles present in 6-8 copies

30°C					
	<i>rne</i> ⁺	<i>rne-1</i>	<i>rne</i> Δ645	<i>rng-219</i>	<i>rng-248</i>
tRNA ^{His}	0.65 ± 0.05	0.61 ± 0.12	0.48 ± 0.03	0.10 ± 0.01	0.11 ± 0.02
tRNA ^{Pro}	0.73 ± 0.03	0.74 ± 0.02	0.64 ± 0.09	0.15 ± 0.03	0.21 ± 0.05
tRNA ^{Asn}	0.97 ± 0.02	0.96 ± 0.02	0.97 ± 0.03	0.40 ± 0.03	0.46 ± 0.04
tRNA ^{Cys}	0.81 ± 0.11	0.74 ± 0.09	0.66 ± 0.04	0.19 ± 0.02	0.16 ± 0.01
44°C					
	<i>rne</i> ⁺	<i>rne-1</i>	<i>rne</i> Δ645	<i>rng-219</i>	<i>rng-248</i>
tRNA ^{His}	0.74 ± 0.06	0.28 ± 0.03	0.43 ± 0.03	0.16 ± 0.01	0.18 ± 0.02
tRNA ^{Pro}	0.70 ± 0.05	0.23 ± 0.06	0.60 ± 0.03	0.21 ± 0.02	0.29 ± 0.03
tRNA ^{Asn}	0.98 ± 0.03	0.90 ± 0.03	0.97 ± 0.04	0.64 ± 0.07	0.58 ± 0.06
tRNA ^{Cys}	0.71 ± 0.09	0.56 ± 0.12	0.59 ± 0.11	0.20 ± 0.03	0.20 ± 0.04

¹Represents the average and the standard deviations from the mean of either three or four independent determinations for each condition listed. Processed fraction is as described in Figures 2.6 and A1.4.

Table A1.2. Oligonucleotides used for Northern analysis and automatic sequencing.

Primer	Sequence (5'→ 3')
PB5S	CGCTACGGCGTTTCACTTCT
asn	GACTCGAACCAGTGACATAC
cysT	ACGGATTTGCAATCCGCTAC
hisR	CCCACGACAACCTGGAATCAC
proM	CGGCGAGAGAGGATTCGAAC
pWSK 29-F	CGCGCGTAATACGACTCACT
pWSK 29-R	CGCGCAATTAACCCTCACTA
rne +456	CGCTGTTTTTCCGCATGAA
rng +440	CGACATCTCGGAACTGGTT
rng +874	GCCTGACTTACGAAGCGTT
rng +1322	GGTGGAGATGACGCGTAAA
rne (B) +549	CCTCGTGTCTAGTCGCGT
rng(B) +551	GCGAGAAGGGAGCGTGATA
rng(B) +942	GCTCCAGCTTGCTTGTCAT
rng(B) +1391	GCAGGTTGGGCATTTCGTTA'

Figure A1.1. Stereo views of the crystal structure of the catalytic domain of *E. coli* RNase E and the predicted structure of its homologue RNase G. (A) The three dimensional ribbon structure of the catalytic domain of RNase E is based on the coordinates published by Callaghan *et al.* (7). (B) The predicted structure of *E. coli* RNase G bound to RNA as described in Materials and Methods. The RNA is shown in stick representation. Figures are prepared in PyMOL. The S1, 5' sensor, RNase H and DNase I subdomains are indicated as well as the approximate locations of the *rng-219* and *rng-248* alleles.

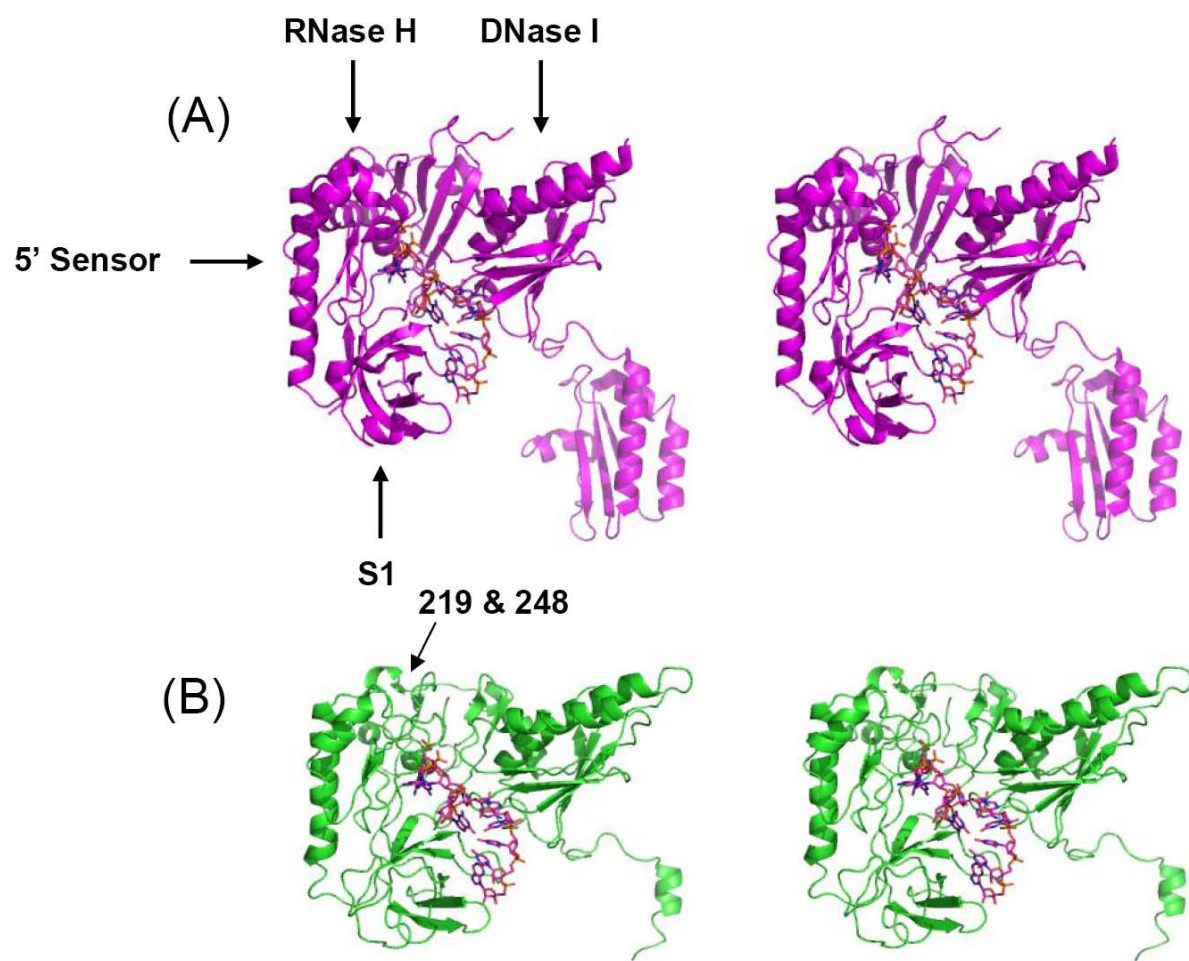


Figure A1.2. Expanded view of the RNase H subdomain of the RNase E, RNase G, Rng-219 and Rng-248 proteins. The structures were prepared as described in Experimental Procedures and are viewed in PyMOL. The adjacent 5' sensor and DNase I subdomains are indicated. (A) Top view. (B) Bottom view. Cyan, RNase E; yellow, model of RNase G; green, model of Rng-219; and magenta, model of Rng-248.

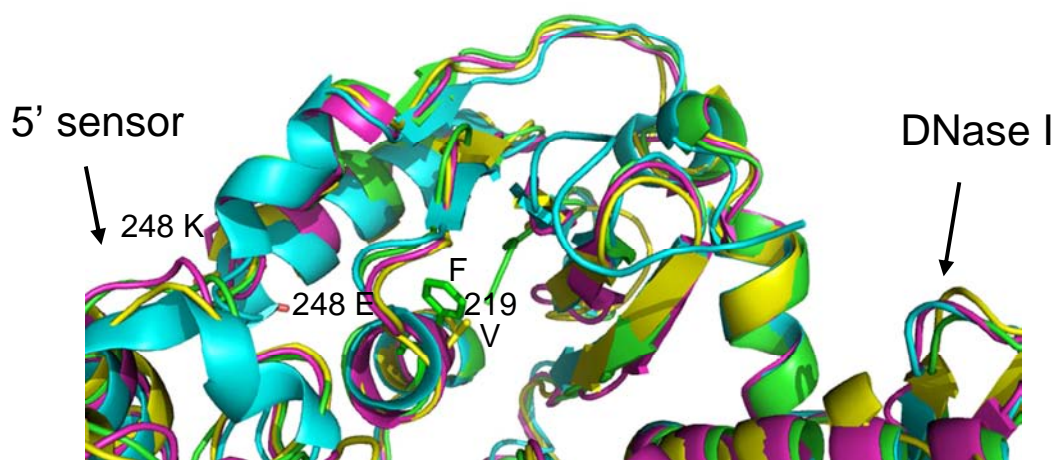
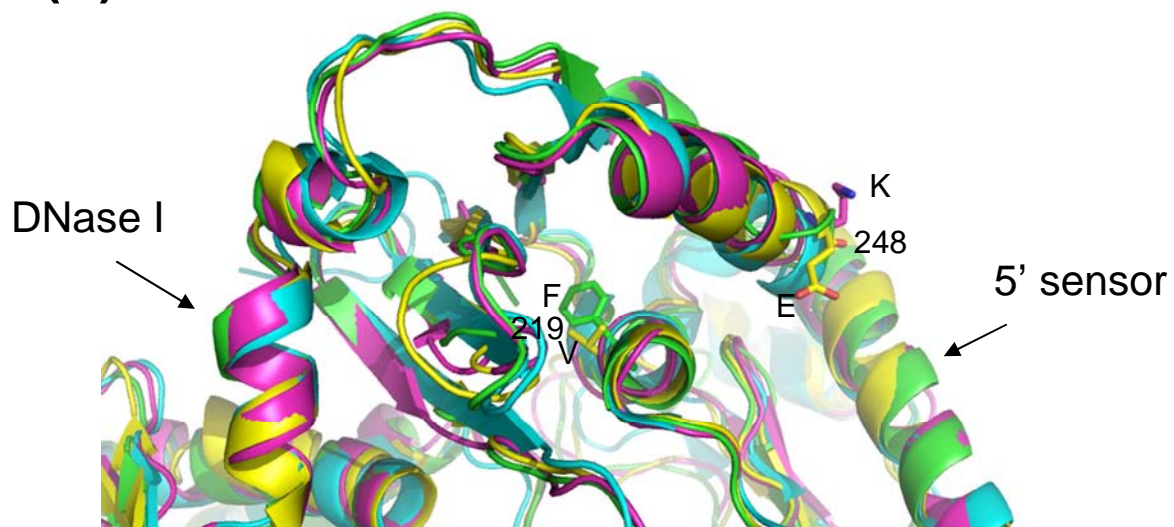
(A)**(B)**

Figure A1.3. Analysis of 9S rRNA processing. Equivalent amounts (5 μ g) of total steady-state RNA extracted from cultures that had either been grown at 30°C or had been shifted to 44°C for 120 min, as described in Materials and Methods, were separated in a 6% polyacrylamide/7 M urea gel, and electroblotted onto a Biotrans⁺ membrane. The membrane was probed with ³²P-end-labeled oligonucleotide complementary to the mature 5S rRNA [PB5S (48)]. The leftward arrows indicate the mature 5S rRNA. (A) *rne* and *rng* alleles present in 6-8 copies/cell. SK9714 (*rne*⁺), SK9937 (*rne-1*), SK9987 (*rne* Δ 645), SK3541 (*rng-248*), and SK3543 (*rng-219*). (B) *rne* and *rng* alleles present in single copy/cell. SK10143 (*rne*⁺), SK10144 (*rne-1*), SK2685 (*rne* Δ 645), SK3563 (*rng-248*), and SK3564 (*rng-219*). PF denotes the processed fraction, which is defined as the amount of mature 5S rRNA divided by the total amount of the 5S rRNA (processed and unprocessed).

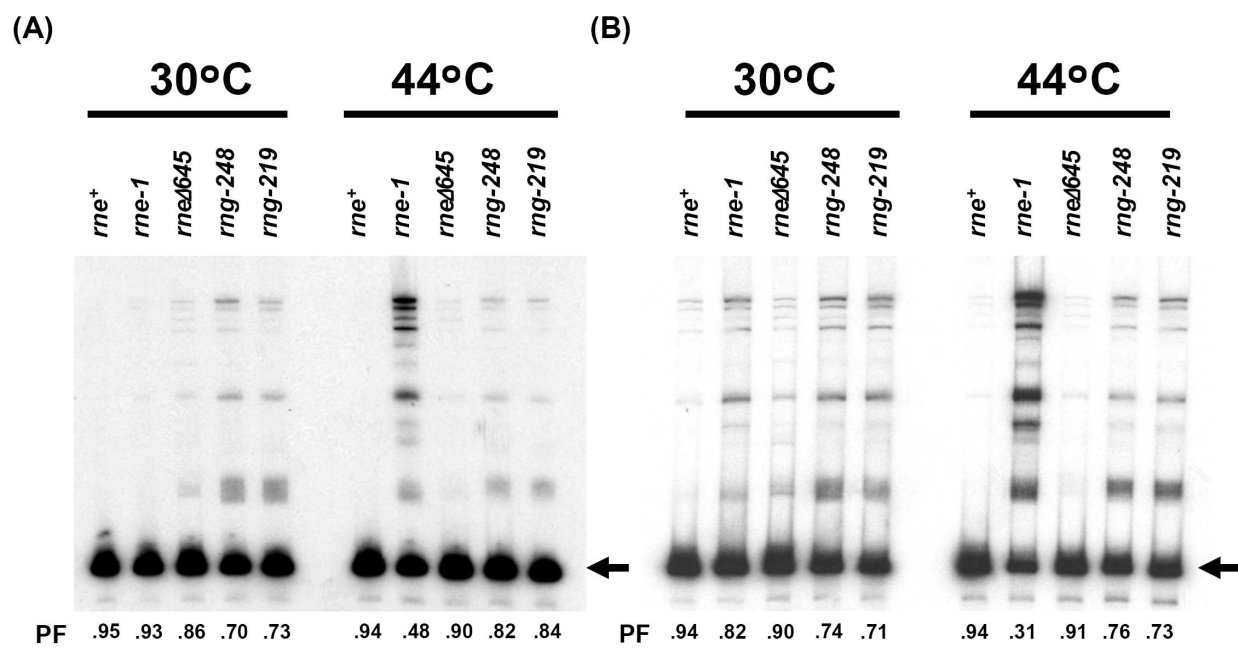


Figure A1.4. tRNA maturation in strains carrying the *rng-248* and *rng-219* alleles in 6-8 copies/cell. Steady-state RNA (5 μ g/lane) isolated from cultures grown at 30°C or after being shifted to 44°C for 120 min were separated in a 6% polyacrylamide/7M urea gel and electroblotted to a Biotrans⁺ membrane. Oligonucleotides specific for each of the tRNAs were used as probes. PF denotes the processed fraction as defined in Fig. A1.3. Arrows in the right margin indicate the position of each mature tRNA.

